

ABSTRACT

Title of Dissertation: Comparison of toxicogenomic effects of sodium hypochlorite, hydrogen peroxide, and peracetic acid on *Pseudomonas aeruginosa*

Degree Candidate: David Andrew Small

Degree and year: Doctor of Philosophy, 2007

Dissertation directed by: Professor William E. Bentley
Department of Chemical Engineering

Oxidative compounds are routinely used as disinfectants on pathogenic bacteria such as *Pseudomonas aeruginosa*. Previous studies have not been able to reveal the mechanisms by which sodium hypochlorite, hydrogen peroxide, or peracetic acid result in antimicrobial activity. However, determining the transcriptional responses of the entire genome to these oxidative stressors may lead to a better understanding the mechanisms by which these antimicrobial compounds kill. The goal of this study is to determine the global gene expression changes in *P. aeruginosa* after exposure to a sub-lethal dose of oxidative stress disinfectants (sodium hypochlorite, peracetic acid, and hydrogen peroxide) by means of Affymetrix *Pseudomonas* GeneChip arrays; to hypothesize some mechanisms for further study; and to develop predictive technologies that could be used to monitor toxicogenomic responses based on microarray research.

This is the first simultaneous comparison of microarray data on the *P. aeruginosa* genome after treatment with sodium hypochlorite, peracetic acid, or hydrogen peroxide to elucidate the mode of action by which these oxidative stressors kill through a genomics perspective. A 20 min exposure time to 4.4 mM sodium hypochlorite, 1 mM hydrogen

peroxide, and 0.5 mM peracetic acid sufficiently inhibited cellular growth of *P. aeruginosa* without resulting in significant cell death allowing for the proper extraction of RNA to be assayed on the microarray. These concentrations and the 20 min exposure time were confirmed using viability testing that included culture plating, cell flow cytometry, and bioluminescence (adenosine triphosphate, ATP) measurements. The microarray data was analyzed using statistical techniques that included scatter plots, analysis of variance (ANOVA), hierarchical clustering, metabolic pathway analysis, and principal component analysis (PCA).

The ANOVA and successive metabolic pathway analysis and PCA suggested that the mechanism of action for all of the oxidative stressors was different, except for the increase in cellular protection mechanisms. Sodium hypochlorite exposure resulted in more gene expression changes (upregulation and downregulation) than either peracetic acid exposure or hydrogen peroxide exposure. Sodium hypochlorite exposure revealed a downregulation of oxidative phosphorylation and electron transport genes and the upregulation of organic sulfur transport and metabolism genes. Peracetic acid exposure resulted in an upregulation of glycerol metabolism genes. Hydrogen peroxide exposure resulted in an upregulation of the pyocin synthesis genes. The resulting global transcription profile of the oxidative stressors in this comparison can help identify similarly activated genes and differentially expressed genes on a genome-wide scale to help researchers better understand the mechanisms by which oxidative disinfectants kill bacterial pathogens, such as *P. aeruginosa*.

**COMPARISON OF TOXICOGENOMIC EFFECTS OF SODIUM
HYPOCHLORITE, HYDROGEN PEROXIDE, AND
PERACETIC ACID ON *PSEUDOMONAS AERUGINOSA***

by

David Andrew Small

Dissertation submitted to the Faculty of the Graduate School of the
University of Maryland, College Park in partial fulfillment
of the requirements for the degree of
Doctor of Philosophy
2007

Advisory Committee:

Professor William E. Bentley, Chair/Advisor
Freshteh Toghrol, Co-Advisor
Professor John Fisher
Professor Daniel Stein
Professor William A. Weigand
Professor Nam Wang

©Copyright by

David Andrew Small

2007

DEDICATIONS

I would like to dedicate this dissertation to my family: my mother, Lea; my father, Arnold; my brothers, Jason and Scott; my grandmother, Sophie; and particularly, my wife, Jennifer for their love, encouragement, and support in all of my endeavors.

ACKNOWLEDGEMENTS

I would like to thank Dr. Wook Chang at the University of Maryland Biotechnology Institute and Dr. Freshteh Toghol, Senior Science Advisor and Director of the Microarray Research Laboratory (MARL) at the Environmental Protection Agency (EPA) for their thoughtful insight, assistance, and friendship throughout this project. I would like to acknowledge my advisor, Dr. William E. Bentley, Director of the Bioengineering Program at the University of Maryland, for his support, guidance, and encouragement during my studies here at the University of Maryland, College Park.

Although the research described in this dissertation has been funded wholly by the United States Environmental Protection Agency (Grant No. T-83100801-0, IPA No. HQ-514-04-06, and HQ-515-04-06), it has not been subjected to the Agency's peer and administrative review and therefore may not necessarily reflect the views of the EPA; nor does the mention of trade names or commercial products constitute endorsement or recommendation of use.

I would also like to thank Esther Volper from the laboratory of Dr. E. Peter Greenberg at the University of Iowa for kindly providing the *Pseudomonas aeruginosa* PA01 strain.

TABLE OF CONTENTS

LIST OF TABLES	viii
LIST OF FIGURES	x
LIST OF ABBREVIATIONS.....	xiii
Chapter 1: Introduction	2
1.1. Overview	2
1.2. Objectives	3
1.3. Hypothesis.....	3
1.4. Experimental plan	4
1.5. Experimental design.....	5
1.6. <i>Pseudomonas aeruginosa</i>	9
1.7. Disinfectants	10
1.7.1. History.....	10
1.7.2. Differences between disinfectants, sterilants, antiseptics, and biocides	11
1.7.3. Mode of action (mechanism of action)	12
1.7.4. Sodium hypochlorite	15
1.7.5. Hydrogen peroxide.....	16
1.7.6. Peracetic acid	17
1.8. Overview of methods used.....	18
1.8.1. Plate counting for cell viability.....	18
1.8.2. Cell flow cytometry for cell viability.....	18
1.8.3. Adenosine triphosphate (ATP) quantitation for cell viability.....	21

1.9.	Gene expression measurement.....	22
1.9.1.	DNA microarray (Affymetrix GeneChip)	22
1.9.2.	Real-time quantitative polymerization chain reaction	24
1.10.	Statistical analysis of microarray data	27
1.10.1.	Scatter plots.....	27
1.10.2.	Analysis of variance (ANOVA).....	28
1.11.	Further analysis of microarray data	31
1.11.1.	Metabolic pathway analysis.....	31
1.11.2.	Hierarchical clustering.....	33
1.11.3.	Principal component analysis (PCA).....	40
Chapter 2: Methods and Materials.....		45
2.1.	Bacterial strains and growth conditions.....	45
2.2.	Viability verification.....	46
2.2.1.	Culture plating	47
2.2.2.	Cell flow cytometry	47
2.2.3.	Relative adenosine triphosphate (ATP) quantitation	48
2.3.	<i>P. aeruginosa</i> RNA isolation.....	49
2.4.	cDNA synthesis and labeling.....	50
2.5.	Hybridization and scanning	51
2.6.	Data analysis	51
2.7.	Real-time polymerization chain reaction (PCR) validation.....	52
Chapter 3: Results.....		54
3.1.	<i>P. aeruginosa</i> shaker flask studies.....	54

3.2.	<i>P. aeruginosa</i> viability studies.....	56
3.2.1.	Plating.....	56
3.2.2.	Cell flow cytometry.....	58
3.2.3.	Relative adenosine triphosphate (ATP) quantitation.....	61
3.3.	Ribonucleic acid (RNA) quality control.....	62
3.4.	GeneChip metrics.....	65
3.5.	Scatter plots.....	68
3.6.	Real-time polymerization chain reaction (PCR) validation.....	70
3.7.	Comparison of <i>P. aeruginosa</i> transcriptome changes in response to the oxidative stressors: sodium hypochlorite, hydrogen peracetic acid, and hydrogen peroxide.....	72
3.8.	Functional classifications analysis.....	76
3.9.	Metabolic pathway analysis.....	81
3.10.	Hierarchical clustering.....	84
3.11.	Principal component analysis (PCA).....	91
Chapter 4: Discussion.....		92
4.1.	Overview.....	92
4.2.	Functional classification analysis.....	93
4.3.	Adaptive/protective processes.....	93
4.4.	Oxidative phosphorylation and electron transport.....	95
4.5.	Entner-Doudoroff (ED) pathway and Embden-Meyerhof-Parnas (EMP) pathway analysis.....	98
4.6.	Organic sulfur ATP Binding Cassettes (ABC).....	101

4.7.	Iron regulation.....	106
4.8.	Pyocin genes	107
4.9.	Hierarchical clustering.....	110
4.10.	Principal component analysis (PCA) on conditions	112
Chapter 5: Conclusions.....		115
5.1.	Overview.....	115
5.2.	Oxidative stressor comparison.....	115
5.3.	Cell viability.....	116
5.4.	Eukaryotic implications	117
5.5.	Future directions	118
5.5.1.	Disinfectant time-course studies	118
5.5.2.	Sodium hypochlorite and organic sulfur compounds	119
5.5.2.1.	Real-time PCR studies after sodium hypochlorite exposure	119
5.5.2.2.	Media studies after sodium hypochlorite exposure	119
5.5.3.	Signature genes in different bacteria.....	121
5.6.	Further applications of this study.....	121
REFERENCES		123

LIST OF TABLES

Table 1: Specific definition of antimicrobials	12
Table 2: Antibacterial responses after biocide exposure	13
Table 3: Biocidal potential targets	14
Table 4: Mode of Action for Various Disinfectants	15
Table 5: Functional Classification of <i>P. aeruginosa</i> Genes	33
Table 6: Distance matrix for hierarchical clustering example	37
Table 7: Primer sequences for real-time PCR validation.....	53
Table 8: Summary of plating data for <i>P. aeruginosa</i> cell viability	58
Table 9: Summary of Bioanalyzer 2100 and Spectrophotometer RNA quality data.....	65
Table 10: Summary of <i>P. aeruginosa</i> GeneChip metrics	67
Table 11: Summary of real-time PCR data compared to microarray data.....	72
Table 12: Venn diagram data for various statistically significant fold changes of upregulated or downregulated genes between sodium hypchlorite, peracetic acid, and hydrogen peroxide.....	75
Table 13: Venn diagram data for functional classifications of statistically significant ≥ 2 -fold genes upregulated between sodium hypchlorite, peracetic acid, and hydrogen peroxide.....	79
Table 14: Venn diagram data for functional classifications of statistically significant ≥ 2 -fold genes downregulated between sodium hypchlorite, peracetic acid, and hydrogen peroxide.....	80

Table 15: Comparison of cellular protective mechanism-related gene expression for sodium hypochlorite, peracetic acid, and hydrogen peroxide exposed <i>P. aeruginosa</i>	95
Table 16: Comparison of genes related to oxidative phosphorylation for sodium hypochlorite, peracetic acid, and hydrogen peroxide exposed <i>P. aeruginosa</i>	97
Table 17: Comparison of Entner-Doudoroff (ED) pathway and Embden-Meyerhof-Parnas (EMP) pathway gene expression for sodium hypochlorite, peracetic acid, and hydrogen peroxide exposed <i>P. aeruginosa</i>	100
Table 18: Comparison of organic sulfur transport gene expression for sodium hypochlorite, peracetic acid, and hydrogen peroxide exposed <i>P. aeruginosa</i>	105
Table 19: Comparison of iron regulation-related gene expression for sodium hypochlorite, peracetic acid, and hydrogen peroxide exposed <i>P. aeruginosa</i>	107
Table 20: Comparison of pyocin system-related gene expression for sodium hypochlorite, peracetic acid, and hydrogen peroxide exposed <i>P. aeruginosa</i>	108
Table 21: Comparison of the five extreme upregulated and downregulated gene expression for sodium hypochlorite, peracetic acid, and hydrogen peroxide exposed <i>P. aeruginosa</i>	114

LIST OF FIGURES

Figure 1: Basic microarray experimental design schemes.....	6
Figure 2: Microarray experimental scheme to compare the effect of oxidative disinfectants on <i>P. aeruginosa</i>	8
Figure 3: Picture of <i>P. aeruginosa</i>	10
Figure 4: SYTO 9 and propidium iodide (PI) dye viability staining	20
Figure 5: The luciferase reaction for adenosine triphosphate (ATP) quantitation.....	21
Figure 6: Photolithographic and combinatorial method to construct DNA microarrays.	22
Figure 7: Affymetrix GeneChip system.....	24
Figure 8: Real-time polymerization chain reaction (PCR)	26
Figure 9: Scatter plot of microarray data.	28
Figure 10: Dendrogram of distance matrix for the hierarchical clustering example	38
Figure 11: Dendrogram (heat map) illustrating the clustering of microarray data	39
Figure 12: Principal component analysis (PCA) plots.....	44
Figure 13: RNA isolation and purification	50
Figure 14: <i>P. aeruginosa</i> cell growth after addition of sodium hypochlorite.....	55
Figure 15: <i>P. aeruginosa</i> plating viability after addition of sodium hypochlorite	57
Figure 16: Live/Dead <i>BacLight</i> Bacterial Viability and 2100 Bioanalyzer results with plating confirmation of <i>P. aeruginosa</i>	59
Figure 17: Sodium hypochlorite-exposed cell flow cytometry results	60
Figure 18: Bioluminescence (relative energy, ATP) results	62
Figure 19: Bioanalyzer 2100 RNA electrograms.....	64

Figure 20: Present, marginal, and absent calls from <i>p</i> -values	66
Figure 21: Scatter plots of treatment gene expression data	69
Figure 22: Real-time PCR data	71
Figure 23: Sodium hypochlorite, peracetic acid, and hydrogen peroxide Venn diagram	74
Figure 24: Functional classification of the number of genes with statistically significant increased mRNA levels.....	77
Figure 25: Functional classification of the number of genes with statistically significant decreased mRNA levels	78
Figure 26: Oxidative phosphorylation and electron transport pathways	82
Figure 27: Entner-Doudoroff (ED) and Embden-Meyerhof-Parnas (EMP) pathways.....	83
Figure 28: Hierarchical clustering of 1-way ANOVA genes.....	85
Figure 29: Hierarchical clustering of “carbon compound catabolism” functional class genes	86
Figure 30: Hierarchical clustering of “energy metabolism” functional class genes.....	87
Figure 31: Hierarchical clustering of the “membrane proteins” functional class genes...88	
Figure 32: Hierarchical clustering of the “related to phage, transposon, or plasmid” functional class genes	89
Figure 33: Hierarchical clustering of the “transport of small molecules” functional class genes.....	90
Figure 34: Principal component analysis (PCA) scatter plot of principal component 1 vs. principal component 2.....	91
Figure 35: ATP-Binding Cassette	104

Figure 36: Production of pyocin110

LIST OF ABBREVIATIONS

3'	three prime region
3-D	three dimensional
5'	five prime region
·OH	hydroxyl radical
-OH	hydroxyl group
°C	degrees centigrade
α_1	<i>alpha 1</i>
α_2	<i>alpha 2</i>
$\Delta\Delta C_T$	<i>delta delta C_T</i>
τ	<i>tau</i>
A	adenine
A_{260}	absorbance at 260 nm
A_{280}	absorbance at 280 nm
A_{320}	absorbance at 320 nm
<i>B. subtilis</i>	<i>Bacillus subtilis</i>
ABC	ATP binding cassette
ANOVA	analysis of variance
AMP	adenosine monophosphate

ATP	adenosine triphosphate
BHA	butylated hydroxyanisole
BHT	butylated hydroxytoluene
C	cytosine
cDNA	complimentary DNA
CFU	colony forming unit
CF	Cystic Fibrosis
CH ₃ CO ₃ H	peracetic acid
CHG	chlorohexidine gluconate
Cl ⁻	chloride ion
Cl ₂	molecular chlorine
CO ₂	carbon dioxide
cRNA	complimentary RNA
C _T	threshold cycle
DI	deionized
DMT	4, 4'-dimethoxytrityl
DNA	deoxyribonucleic acid
dsRNA	double-stranded RNA
<i>E. coli</i>	<i>Escherichia coli</i>
ED	Entner-Doudoroff
EMP	Embden-Meyerhof-Parnas
EPA	Environmental Protection Agency
G	guanine

g	gram
GCOS	GeneChip Operating Software
GenMAPP	Gene Microarray Pathway Profiler
GO	Gene Ontology
H ₂ O	water
H ₂ O ₂	hydrogen peroxide
HOCl	hypochlorous acid
hr	hours
KEGG	Kyoto Encyclopedia of Genes and Genomes
L	liter
LB	Luria-Bertani
LPS	lipopolysaccharide
MARL	Microarray Research Laboratory
<i>M. bovis</i>	<i>Mycobacterium bovis</i>
min	minute
mg	milligram
mL	milliliter
MM	mismatch
mM	millimolar
MPO	myeloperoxidase
mRNA	messenger RNA
MS	Microsoft
msec	millisecond

Na ⁺	sodium ion
NADH	nicotinamide adenine dinucleotide reduced form
NaOCl	sodium hypochlorite
NaOH	sodium hydroxide
ng	nanogram
nm	nanometer
O ₂	molecular oxygen
OCl ⁻	hypochlorite ion
OD ₆₀₀	optical density at 600 nm
PCA	principal component analysis
PCR	polymerase chain reaction
PI	propidium iodide
<i>P. aeruginosa</i>	<i>Pseudomonas aeruginosa</i>
PP _i	pyrophosphate
<i>PM</i>	perfect match
PseudoCAP	<i>P. aeruginosa</i> Community Annotation Project
QT	quality threshold
R	Discrimination score
R ²	coefficient of determination
rcf	relative centrifugal force
RFU	relative fluorescence unit
RLU	relative luminescence unit
ROS	reactive oxygen species

RNA	ribonucleic acid
rpm	revolutions per minute
rRNA	ribosomal RNA
RT-PCR	reverse transcription-polymerase chain reaction
<i>S. aureus</i>	<i>Staphylococcus aureus</i>
T	thymine
t	time
TCA	Tri Carboxylic Acid
U	unit
UV	ultra violet
μg	microgram
μL	microliter

Chapter 1: Introduction

1.1. Overview

Bacterial pathogens (*Mycobacterium bovis*, *Staphylococcus aureus*, *Pseudomonas aeruginosa*, etc.) are present in hospital environments and can lead to severe and lethal infections. Each year 2,000,000 people are infected by bacterial pathogens, and of these approximately 90,000 die. The annual cost of these infections is estimated to be \$4.5 billion. *P. aeruginosa* was selected because this is one of the pathogens that poses the greatest risk in hospital environments.

The precise mechanisms by which sodium hypochlorite, peracetic acid, and hydrogen peroxide kill *P. aeruginosa* remains to be clarified (Fukuzaki, 2006; Rutala, 1996). Recent advances in the field of genomics such as whole-genome microarrays may assist in overcoming this problem by enabling simultaneous multiple gene analysis. Additionally, the outcomes can be used to explain the mechanisms that may be involved in disinfectant activity. For instance, transcriptome analyses with antimicrobials recently identified genes related to protective mechanisms in *E. coli*, *P. aeruginosa*, *S. aureus*, and yeast (W. Chang, Small, Toghrol, & Bentley, 2005a, 2005b; Wook Chang, Small, Toghrol, & Bentley, 2006; Kitagawa, Takahashi, Momose, & Iwahashi, 2002; Palma, Worgall, & Quadri, 2003; Salunkhe et al., 2002; Zheng et al., 2001).

This research will focus on genome-wide changes in *P. aeruginosa* after exposure to sodium hypochlorite, hydrogen peroxide, and peracetic acid. DNA microarrays (Affymetrix *Pseudomonas* GeneChip arrays) will be employed to study sodium hypochlorite-driven gene regulation and cellular responses. This study is the first microarray analysis of global gene expression of organisms exposed to sodium hypochlorite, peracetic acid, and hydrogen peroxide. Consequently, the results may facilitate further clarification of the mechanisms involved in the toxicity of these oxidative stressors. Specifically, the results may help reveal the modes of action by which the antimicrobials kills the cell.

1.2. Objectives

The objectives of this project were to determine the following: (1) What genes, proteins (enzymes), and ultimately metabolic pathways are affected in *P. aeruginosa* as a result of oxidative disinfectant exposure? (2) What are the potential modes of action by which oxidative stress disinfectants (sodium hypochlorite, hydrogen peroxide, peracetic acid) kill *P. aeruginosa*? (3) Are these modes of action similar? If not, what are the differences?

1.3. Hypothesis

Although routinely used in disinfection and sterilization applications, the mode(s) of action by which oxidative stressors, such as sodium hypochlorite, hydrogen peroxide, and peracetic acid has not yet been completely explained despite much research. Sodium hypochlorite dissociates to form the hypochlorous acid

(HOCl) depending upon the pH of the solution (Baker, 1959). The HOCl is thought to be the molecule responsible for sodium hypochlorite's bactericidal action, since the hypochlorite ion (OCl⁻) possess only about 1.25% of the germicidal properties of HOCl at 2 to 5°C and at various pH levels (Fair, Morris, & Chang, 1948; Morris, 1966). The hydroxyl radical ($\cdot\text{OH}$) is believed to be the strongest oxidant known, and it is by this moiety that hydrogen peroxide delivers antimicrobial activity (Fridovich, 1975, 1978). Peracetic acid is thought to kill bacterial cells either through the hydroxyl radical or other organic radicals formed from peracetic acid (e.g. $\text{CH}_3\text{COO}\cdot$ or $\text{CH}_3\text{CO}\cdot$) (Marquis, Rutherford, Faraci, & Shin, 1995; Shin *et al.*, 1994). Although the modes of action of sodium hypochlorite, peracetic acid, and hydrogen peroxide have not yet been fully explained, the possibility still exists that there is a prototypical or fundamental response by the cell to oxidative stress. This hypothesis was tested by comparing transcriptome responses of sodium hypochlorite, hydrogen peroxide, and peracetic acid on *P. aeruginosa*.

1.4. Experimental plan

The experimental plan was as follows:

- 1) Determine an exposure time and a concentration of sodium hypochlorite, peracetic acid, and hydrogen peroxide that reduces *P. aeruginosa* growth as determined by optical density (OD₆₀₀).
- 2) Confirm the growth data with viability studies (culture plating, cell flow cytometry, and bioluminescence).

- 3) Identify the affected genes using the *P. aeruginosa* GeneChip microarrays.
- 4) Validate the microarray data using real-time polymerase chain reaction (PCR) data.
- 5) Determine if the data supports the hypothesis and compare and contrast the gene expression results.

1.5. Experimental design

The experimental design strongly influences the information that can be ascertained from a microarray experiment. Consequently, design elements affect all microarray experiments, particularly two color hybridizations (Hayes & Bradfield, 2005). The use of a one color system (Affymetrix GeneChip) alleviates many of these hybridization concerns since only one sample of cDNA is hybridized for each array. When using a one or two color hybridization array, there are three basic design schemes as follows: direct, reference, or loop design (Churchill, 2002; Kerr, 2003; Yang & Speed, 2002). The direct design compares a control with an experimental sample for each paired sample set. This method is most often used with two color hybridizations. The reference design compares a set of experimental samples to a common reference sample. A loop design compares a successive set of experimental samples to an initial control.

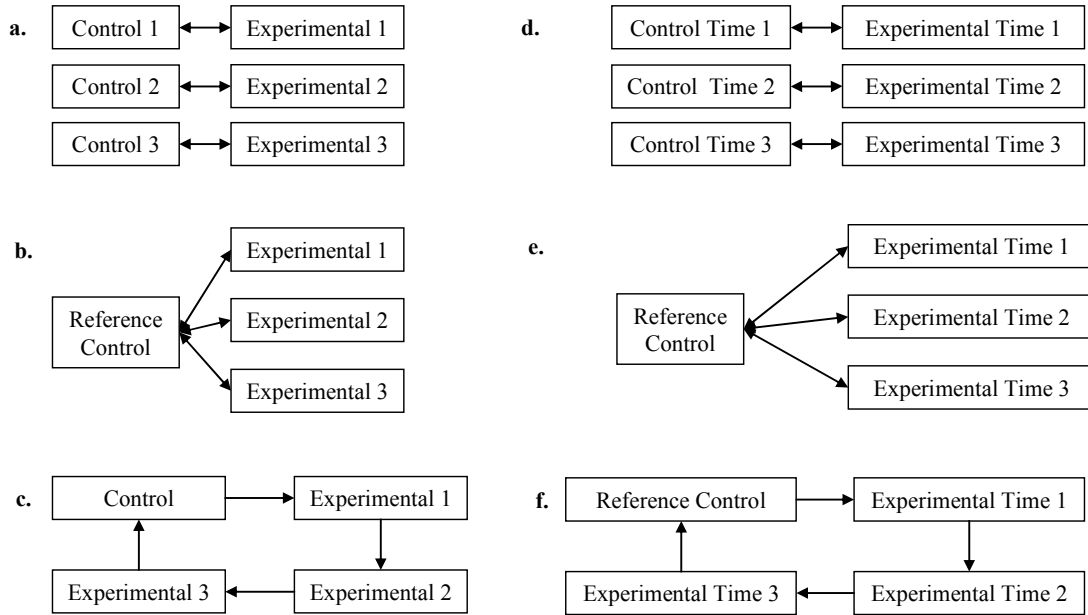


Figure 1: Basic microarray experimental design schemes.

The three basic microarray experimental design schemes (with control and experimental samples) are illustrated as follows: **a.** direct, **b.** reference, **c.** loop. Additionally, the application of these schemes to a time-course experiment is shown as well as follows: **d.** direct time-course, **e.** reference time-course, **f.** loop time-course.

The design choice is heavily influenced by the question or questions being asked in an experiment (Churchill, 2002; Kerr, 2003; Yang & Speed, 2002). For example, consider an experiment where researcher wants to know the effect of several gene targets over several time intervals. Applying the three basic design schemes yields a direct comparison of each experimental time sample to its time-matched control sample (Figure 1 d.), a reference control sample to each experimental time sample (Figure 1 e.), and a loop design that compares the reference control sample to each experimental time sample successively (Figure 1 f.). Here the experimental design determines the number of samples (and arrays)

that need to be used to complete the experiment. The direct scheme will provide the most sensitivity in the degree of change of gene targets over the progression of time. The loop scheme will provide less sensitivity than the direct scheme but will provide better time-course information with respect to particular gene targets. The reference scheme will provide the degree of change in gene targets and the change over the time-course, but also decreases the statistical power for both (Hayes & Bradfield, 2005).

Since the scope of this project was to compare several disinfectants to each other, a direct scheme (see Figure 1 a. and Figure 1 e.) was chosen to maximize the sensitivity and statistical power of the change in gene targets of the sodium hypochlorite-exposed samples, hydrogen peroxide-exposed samples, and peracetic-acid exposed samples compared to the control samples (see Figure 2). In this scheme each control sample is compared to each experimental treatment (e.g. control sample 1 is compared to each sodium hypochlorite sample, each hydrogen peroxide sample, each peracetic acid sample).

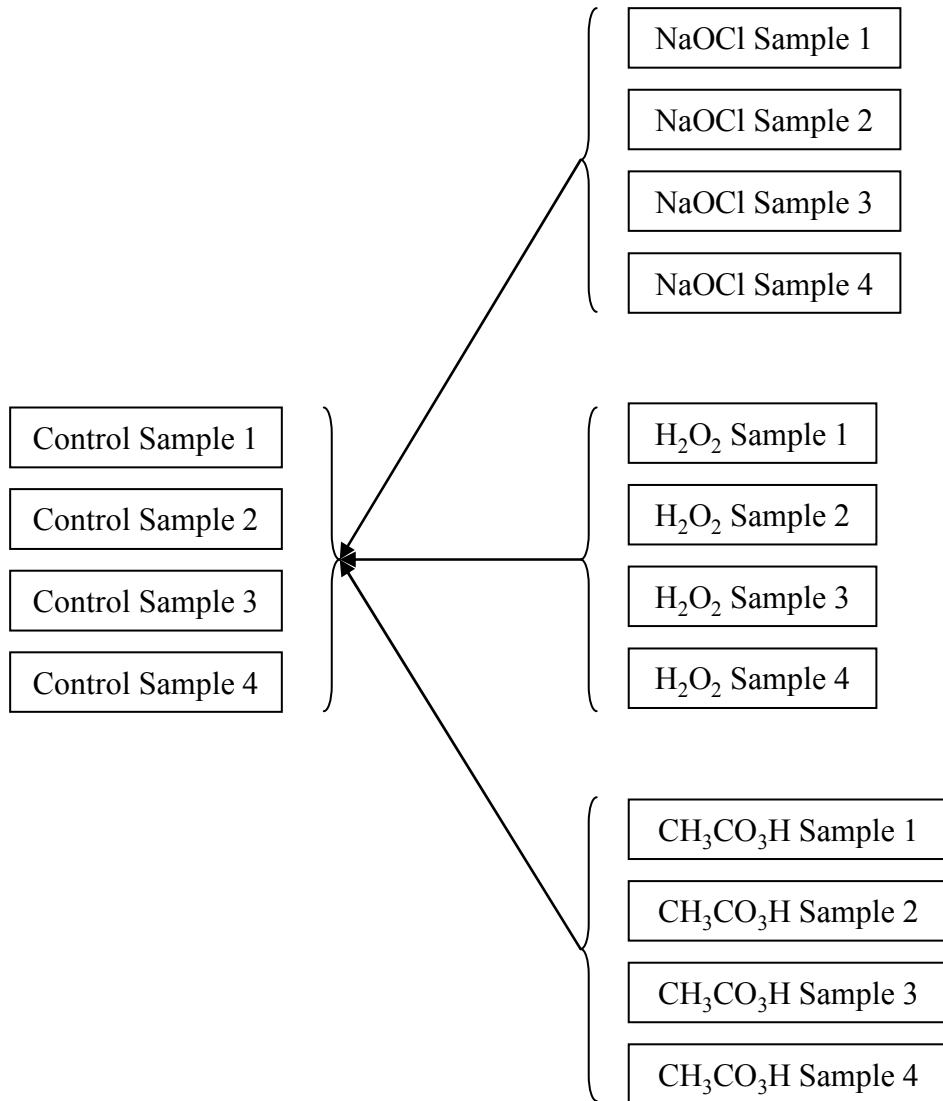


Figure 2: Microarray experimental scheme to compare the effect of oxidative disinfectants on *P. aeruginosa*.

A modified direct design scheme was used to increase sensitivity and statistical power by comparing a set of four control samples to the set of four sodium hypochlorite-exposed, set of four hydrogen peroxide-exposed, and set of four peracetic acid-exposed samples.

1.6. *Pseudomonas aeruginosa*

Pseudomonas aeruginosa is an opportunistic pathogen that frequently causes nosocomial infections (Vincent *et al.*, 1995). *P. aeruginosa* infections are more common in immunosuppressed patients such as those with cystic fibrosis (CF), cancer, or burn wounds (Tummler & Kiewitz, 1999). *P. aeruginosa* can infect the lungs, urinary tract, skin, and in severe infections can even become blood borne (Bodey, Bolivar, Fainstein, & Jadeja, 1983; Campa M., 1993; Stover *et al.*, 2000). Infections caused by *P. aeruginosa* are often difficult to treat due to the organism's prominent resistance to antibiotics (Hancock, 1998). *P. aeruginosa* infections are usually treated with two intravenously or orally administered antibiotics at once. Typical combinations include: ceftazidime (Ceftaz, Fortraz, Tazicef), ciprofloxacin (Cipro), imipenem (Primaxin), gentamicin (Garamycin), tobramycin (Nebcin), ticarcillin-clavulanate (Timentin), or piperacillin-tazobactam (Zosyn) (Stover *et al.*, 2000).



© Dr. Dennis Kunkel / Visuals Unlimited

Figure 3: Picture of *P. aeruginosa*

Pseudomonas aeruginosa is a Gram-negative, aerobic, enteric, rod prokaryote. This bacterium produces a blue-green pigment, pyocyanin, which characterizes the bluish pus produced by the infection. The above image is a SEM X3000 and reprinted with permission from Visuals Unlimited.

1.7. Disinfectants

1.7.1. History

The history of disinfection may easily be traced to the original work of Louis Pasteur. On the behest of Emperor Napoleon III in 1864, Pasteur discovered that briefly heating food products (wine, beer, and milk) at 50°C to 60°C was sufficient to sterilize all the microorganisms within the food (Ackerman, 2004). This procedure, better known as *pasteurization*, is still used for food products today. In 1865, a contemporary of Pasteur, Joseph Lister made the connection of the decay from living organisms in the air to the observation that compound fractures which broke through the skin

resulted in inflammation, infection, and often death; whereas simple fracture wounds that did not break the skin did not result in infection and the patient typically recovered (Brock, 1961). Lister would later discover that the sepsis was not from living organisms in the air, but from the surgeon's dirty hands and instruments (Dormandy, 2004). However, this realization fueled Lister's search for a method of antiseptics that would eliminate these microorganisms. Lister successfully used dilutions of carbolic acid (phenol) in his surgical procedures to heal patients (Lister, 1967). In 1876, Lister came to the United States to lecture before the International Medical Congress. In attendance were a Missouri physician, Joseph Lawrence (who later named his mouthwash, Listerine in honor of Lister) and a New York pharmacist, Robert Johnson (who started the production of gauze-soaked dressings of Lister's phenol mixture which fostered the creation of the surgical products company, Johnson & Johnson) (J. Johnson, 1988).

1.7.2. Differences between disinfectants, sterilants, antiseptics, and biocides

Although the terms disinfectants, sterilants, antiseptics, and biocides are often used interchangeably there are some subtle differences with respect to microorganism destruction. The choice of which term is used frequently depends on the application for the antimicrobial. A list of these terms with their definitions and examples appears in Table 1.

Table 1: Specific definition of antimicrobials

Term	Definition	Example
Disinfectant	Agent applied to non-living materials to destroy microorganisms (usually relatively larger microorganisms)	<ul style="list-style-type: none">• Sodium hypochlorite, acetic acid, potassium peroxydisulfate, sodium carbonate, or sodium hydroxide for use in livestock dwellings• Chlorination in waste water treatment
Sterilant	Agent (usually a gaseous phase chemical) applied to a surface to destroy all organisms	<ul style="list-style-type: none">• Use of chlorine dioxide gas to clear anthrax-exposed rooms in post offices
Antiseptic	Agent (chemical) that may be applied directly to the skin or mucosal membranes that reduces the possibility of bacterial infection on these surfaces	<ul style="list-style-type: none">• Mouthwash• Chlorohexidine gluconate (CHG) for handwashing
Biocide	Agent (chemical) that is capable of killing different forms of living tissue	<ul style="list-style-type: none">• Butylated hydroxyanisole (BHA) and butylated hydroxytoluene (BHT) as a food preservative

(Franklin, 1989)

1.7.3. Mode of action (mechanism of action)

The mode of action is the actual manner in which a physical or chemical agent affects bacteria. Although, biocide exposure elicits bacteriostatic and bactericidal effects; the mode of action caused by these effects may be different. Bacteriostatic effects result from metabolic injuries that are reversed once the biocidal stressor is neutralized or removed from contact with the microorganism (Fitzgerald, Davies, & Russell, 1989). However, prolonged or high-dose exposures to a biocidal stressor result in immediate cell death. A summary of the biocidal effects and the antibacterial

response is listed in Table 2. When a cell is exposed to a biocide, the following sequence of events will occur: (1) absorption of the biocide by the cell, (2) aggregation of the biocide to the target(s), (3) concentration or dose of the biocide at the target(s), (4) the target(s) is injured or destroyed (Denyer, 1991). Thus, successful biocides will be absorbed by the cell, concentrate at the target(s), and damage the target(s) leading to cell death. A summary of antibacterial responses after biocide exposure is listed in Table 3 with increasing degrees of severity to the biocidal effects. However, it should be noted that biocides may or may not have specific targets since the rigorous definition of the term in reference to biological entities includes germicides, antibiotics, antibacterials, antivirals, antifungals, and antiprotozoals.

Table 2: Antibacterial responses after biocide exposure

Biocidal Effect (increasing severity)	Antibacterial Response
Bacteriostatic	Alteration of selective permeability
	Reversible nucleic acid interactions
	Reversible enzyme inhibition
Inability to repair	Structural damage to cell membrane (or cell wall)
	Leakage of cell contents
	Self-destruction of the cell by enzymes (autolysis)
Bacteriocidal	Cell lysis
	Coagulation of the cytoplasm

(Denyer, 1991)

Table 3: Biocidal potential targets

Gram Stain(s)	Structure	Target
Negative	Cell wall	Lipopolysaccharide (LPS)
		Peptidoglycan
		Porins
Negative Positive	Cytoplasmic membrane	Structural molecules
		Respiratory enzymes (membrane-bound)
		Metabolite transport systems
		Energy coupling processes
Negative Positive	Cytoplasm	Anabolic enzymes and associated reactions
		Catabolic enzymes and associated reactions
		Nucleic acids (DNA, RNA)

(Denyer & Stewart, 1998)

If the mode of action affects or interferes with common systems of the pathogen and the host organism, high levels of side effects can be expected. Thus the mode of action of an effective disinfectant should target cellular processes that are unique to the pathogen. For example, oxygen exposure and in particular the elicitation of reactive oxygen species (ROS), can result in DNA, lipid damage, that display antimicrobial effects. Thus, oxidative antimicrobials (sodium hypochlorite, peracetic acid, hydrogen peroxide, etc.) have commonly been used to eliminate pathogenic species such as *P. aeruginosa* (Kitis, 2004; Spoering & Lewis, 2001). A summary of some disinfectants and their modes of action are listed in Table 4.

Table 4: Mode of Action for Various Disinfectants

Target	Disinfectant	Mode of Action
Cell wall or cytoplasmic (outer) membrane	Glutaraldehyde	Protein cross-linking
	EDTA and permeabilizers	Release of lipopolysaccharides (LPS)
Cytoplasmic (inner) membrane	Quaternary ammonia compounds	Damage to phospholipid bilayers
	Diamines	Leakage induction of amino acids
	Phenols	Leakage
Macromolecule cross-linking	Formaldehyde	Protein cross-linking, RNA, and DNA
	Glutaraldehyde	Membrane protein and enzyme cross-linking
DNA intercalation	Acridines	Acridine molecule intercalation between two base pairs in DNA or RNA
Thiol group interaction	Silver compounds	Thiol group interaction of membrane-bound enzymes
DNA effects	Halogens	DNA synthesis inhibition

(McDonnell & Russell, 1999)

1.7.4. Sodium hypochlorite

Sodium hypochlorite (NaOCl) is the most widely used disinfectant (antimicrobial). Presently, sodium hypochlorite is an active ingredient for more than 350 registered by the United States Environmental Protection Agency (EPA) antimicrobial products used in hospitals. Sodium hypochlorite was first produced in 1774, shortly after the discovery of chlorine, by bubbling gaseous chlorine through a potash solution (Hugo, 1995). Today, 233 years later, sodium hypochlorite solutions are still manufactured and sold to be used for disinfection.

Sodium Hypochlorite (NaOCl) is a pale green liquid that is commonly referred to as soda bleach or liquid bleach. It is prepared by reacting dilute caustic soda solution with liquid or gaseous chlorine accompanied by cooling. The stoichiometric reaction for the synthesis of sodium hypochlorite is as follows:

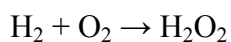


In aqueous solutions sodium hypochlorite ionizes into Na^+ and OCl^- and establishes an equilibrium between these ions and hypochlorous acid (HOCl) (Bloomfield, 1996). The HOCl moiety is dominant in the pH 4 to 7 range, and the OCl^- moiety is dominant above pH 9 (White, 1986). Hypochlorous acid has been shown to disrupt oxidative phosphorylation (McDonnell & Russell, 1999), however the exact mechanism of action by which sodium hypochlorite kills remains to be elucidated (Barrette, Hannum, Wheeler, & Hurst, 1989; Rutala, 1996).

1.7.5. Hydrogen peroxide

Hydrogen peroxide (H_2O_2) is widely used as a disinfectant (antimicrobial) in the concentration ranges of 3 to 90%, and is considered environmentally-friendly because it breaks down into water and oxygen (Block, 2001; McDonnell & Russell, 1999). Hydrogen peroxide is most commonly manufactured by the autoxidation of 2-ethyl-9,10-

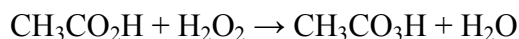
dihydroxyanthracene to 2-ethylanthraquinone and hydrogen peroxide utilizing the oxygen in the air (Hess, 1995). The stoichiometric reaction for the synthesis of hydrogen peroxide is surprisingly simple and is as follows:



Hydrogen peroxide's mechanism of action is believed to be related to the oxidant activity of hydroxyl free radicals ($\cdot\text{OH}$) that attack lipids, proteins, and DNA. Sulfhydryl groups and sulfur double bonds are suspected to be targeted by these free radicals as well (Block, 2001).

1.7.6. Peracetic acid

Peracetic acid ($\text{CH}_3\text{CO}_3\text{H}$) is often considered a more potent disinfectant than hydrogen peroxide since it is effective at concentrations <0.3% (Block, 2001). Peracetic acid is manufactured by reacting acetic acid and hydrogen peroxide in an aqueous reaction medium with a sulfuric acid catalyst (Budavari, 1996). The stoichiometric reaction for the synthesis of peracetic acid is again surprisingly simple and is as follows:



Peracetic acid is also considered environmentally-friendly as it decomposes to acetic acid and oxygen, but has added advantages over

hydrogen peroxide as it is not susceptible to peroxidases and retains its activity in the presence of organic loads (Malchesky, 1993; McDonnell & Russell, 1999). Peracetic acid's mechanism of action is speculated to be the denaturation of proteins and enzymes and increased cell wall permeability by breaking sulfhydryl and disulfide bonds (Baldry, 1983; Block, 2001).

1.8. Overview of methods used

1.8.1. Plate counting for cell viability

Plate counting remains one of the classic methods for viability assessment. Typically, serial dilutions of a sterile liquid are used to dilute a sample of cells growing in culture. These serial dilutions are then spread on an agar plate and incubated for a time interval sufficient to result in cell growth in the form of colonies. The size of the colony that grows on the plate may be highly varied (Tomasino, 2005). The colonies that grow on the plate may also contain one or more cells. Consequently, viable counts are typically expressed as a number of colony-forming units (CFU) (Madigan, Martinko, & Parker, 2003). Plate counts can be highly unreliable to ascertain total number of cells, since the plate counting only accounts for viable or live cells present and not the dead cells that may be present in a culture.

1.8.2. Cell flow cytometry for cell viability

Cell flow cytometric methods, based on intercalating fluorescent dyes, have dramatically increased the speed of measuring live and dead cell

populations (Davey & Kell, 1996; Nebe-von-Caron, Stephens, Hewitt, Powell, & Badley, 2000; Shapiro, 2000). Typically, live cells have intact cell membranes and are impermeable to membrane impermeant dyes such as propidium iodide (PI), whereas SYTO 9 is a cell permeant dye that intercalates into any cell containing nucleic acids (Decker, 2001). When both stains are properly introduced into a mixture of live and dead cells, the PI displaces the SYTO 9 due to PI's higher affinity for nucleic acids (Stocks, 2004). The SYTO 9 dye has an excitation maximum of about 480 nm and an emission maximum of 500 nm, while the PI dye has an excitation maximum of about 490 and an emission maximum of 635 nm. The *BacLight* Live/Dead (Invitrogen) assay system is illustrated in Figure 4.

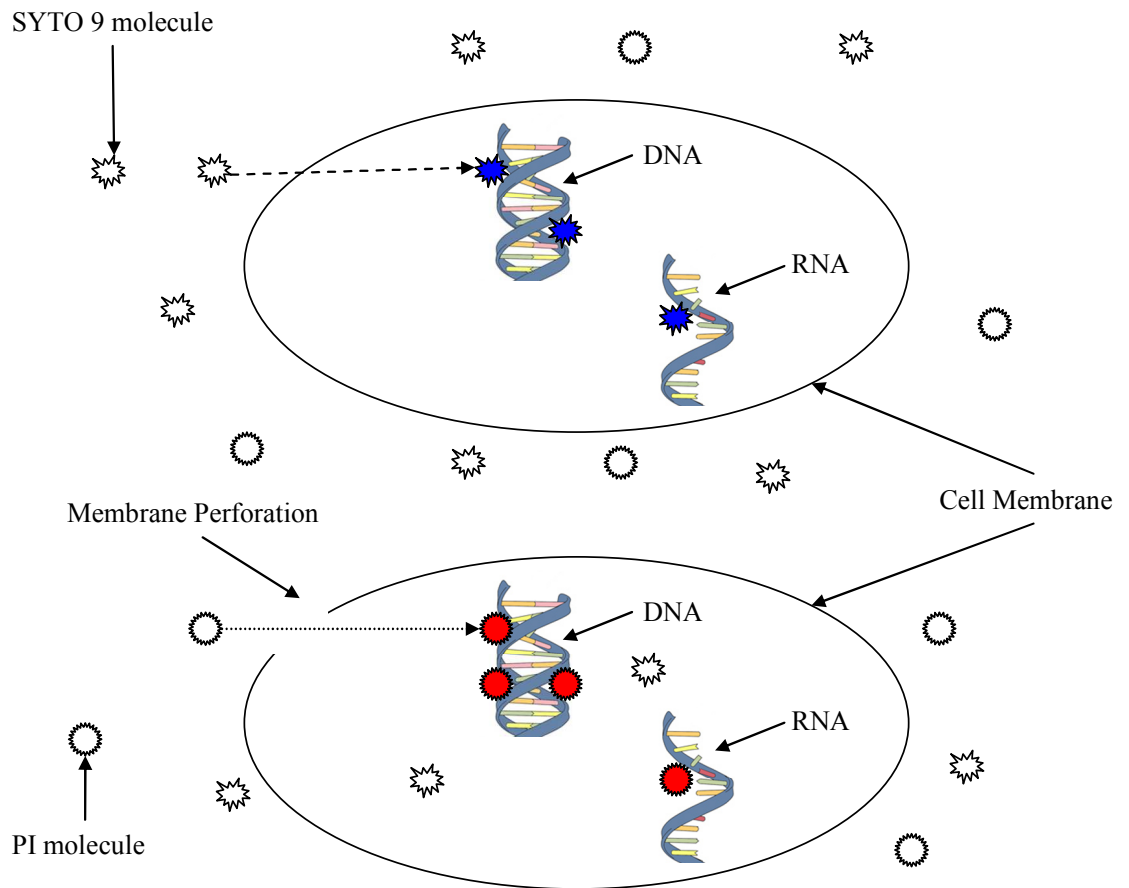


Figure 4: SYTO 9 and propidium iodide (PI) dye viability staining

SYTO 9 is a cell permeant dye that will readily pass through the cell's plasma membrane. Once the SYTO 9 dye comes in contact with a nucleic acid (DNA or RNA), the SYTO 9 will form a stable fluor and emit "blue" fluoresce when the appropriate excitation wavelength is applied. PI is a cell impermeant dye that will only penetrate compromised cell membranes. Once the PI dye comes in contact with a nucleic acid (DNA or RNA), the PI will form a stable fluor and emit "red" fluoresce when the appropriate excitation wavelength is applied. The PI dye has a higher affinity for nucleic acids and will bind much more readily than the SYTO 9 dye.

1.8.3. Adenosine triphosphate (ATP) quantitation for cell viability

Adenosine triphosphate (ATP) is a well-established indicator of metabolically active cells (Stanley, 1986; Thore, Ansehn, Lundin, & Bergman, 1975; Venkateswaran, Hattori, La Duc, & Kern, 2003). Generally, ATP concentration in prokaryotic cells will rapidly decline as the cells die (Hatano et al., 1999; Hattori et al., 2003). ATP assays based on bioluminescence have been on the market for some time now. Recently more specific assays have been created to cater to microbial ATP detection and quantitation, such as the BacTiter-Glo Microbial Cell Viability Assay (see Figure 5).

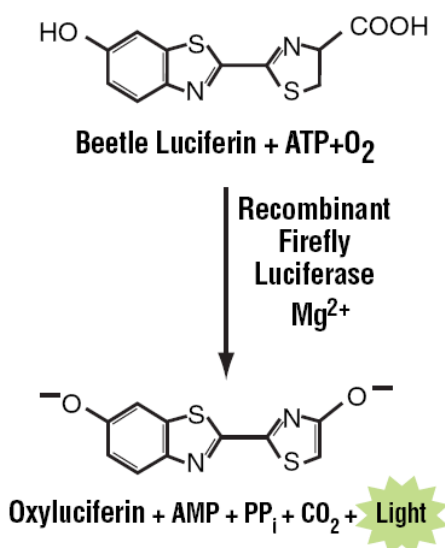


Figure 5: The luciferase reaction for adenosine triphosphate (ATP) quantitation.

Mono-oxygenation of luciferin is catalyzed by luciferase in the presence of magnesium ion (Mg²⁺), ATP, and molecular oxygen (O₂) resulting in oxyluciferin, adenosine monophosphate (AMP), pyrophosphate (PP_i), carbon dioxide (CO₂), and light that can be measured.

1.9. Gene expression measurement

1.9.1. DNA microarray (Affymetrix GeneChip)

Microarray fabrication is in many ways similar to the technology that produces microprocessors for the computer industry from semiconductor materials. A photoresist-based procedure is used to construct cDNA microarrays and is depicted below in Figure 6.

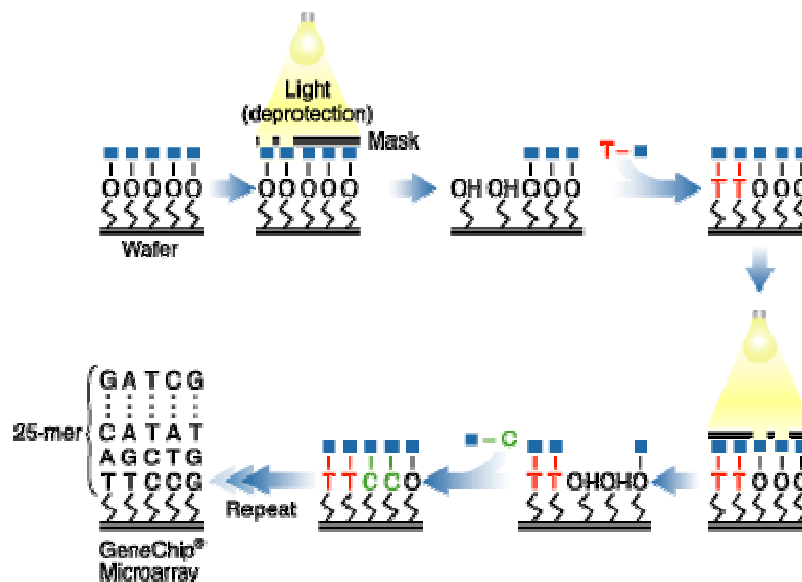


Figure 6: Photolithographic and combinatorial method to construct DNA microarrays.

A glass slide is coated with a photo-resistive material. Adding 4, 4'-dimethoxytrityl (DMT), derivatizes the glass slide. The underlayer is then coated with a soluble polyimide. A photomask is then placed over the array, and the array is exposed to light. This leaves a layer of protection over portions of the glass slide as the next layer of the array is constructed. A detrillate reaction is then performed to leave a hydroxyl (-OH) group to couple a specific nucleotide (either adenine (A), cytosine (C), guanine (G), and thymine (T)). The photoresist is then stripped, and the next set of DMT nucleotides is coupled. The array is effectively painted in these four nucleotides in each pass (DeRisi *et al.*, 1996).

A fluorescently tagged sample will only attach to the oligonucleotide sequence that has the complimentary DNA sequence. This method works well for determining and comparing genes of organisms that have an existing genome map. When a laser beam scans the array, only the tagged sample will fluoresce at the array element that contains the appropriately hybridized complementary DNA (cDNA) or complementary RNA (cRNA) sequence (DeRisi *et al.*, 1996). The intensity of the beam will vary directly with the relative strength of the hybridization. Thus, gene expression may be measured effectively. This DNA chip method is powerful because it can yield a quantitative analysis of gene transcription, the sample preparation requires a short period of time, and analyzing messenger RNA (mRNA) transcript levels requires relatively few reagents. An overview of the method is depicted below in Figure 7.

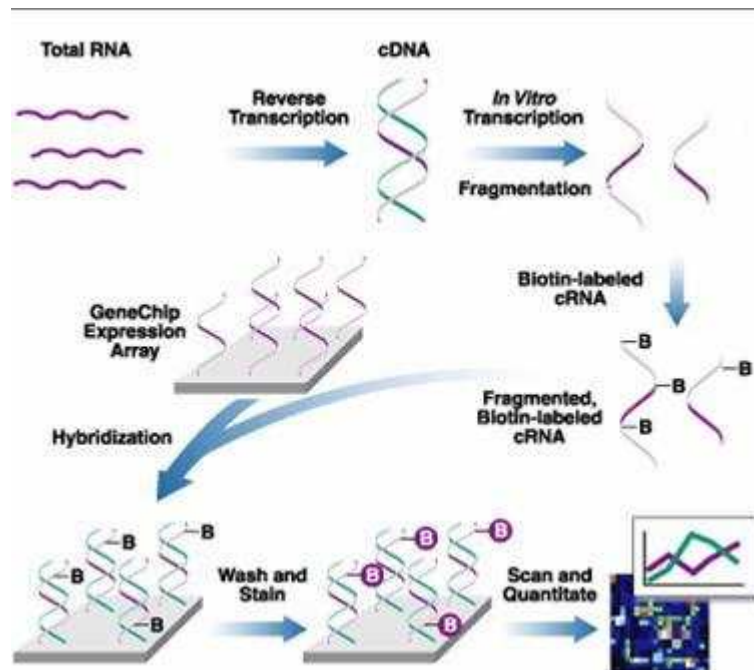


Figure 7: Affymetrix GeneChip system.

Labeled cDNA or cRNA targets derived from the mRNA of an experimental sample are hybridized to nucleic acid probes attached to the solid support. By monitoring the amount of label associated with each DNA location, it is possible to infer the abundance of each mRNA species represented.

1.9.2. Real-time quantitative polymerization chain reaction

The polymerase chain reaction (PCR) is a method to create additional copies of a desired nucleic acid. Conventional PCR reactions are not quantitative, as it is difficult to determine the starting amount of nucleic acid. Additionally, calculation of the subsequent amplification of nucleic acids is exceedingly difficult due to differences in reaction specificity and reaction efficiency. Real-time quantitative PCR solves this problem by attaching a fluorescent reporter molecule to the conventional PCR reaction scheme. The reporter molecule may be specific for a desired amplification product or it

may be nonspecific, intercalating into any double-stranded nucleic acid product (Heid, Stevens, Livak, & Williams, 1996).

The PCR reaction is done in an instrument in which the fluorescence intensity is monitored during each successive amplification cycle of the reaction. Presently, the most widely used systems include the following: Applied Biosystems 7300, 7500, and 7900HT (Applied Biosystems); Chromo4, Opticon, iQ5, and MyiQ (Bio-rad); Smart Cycler 1600, TD, 3200, 4800, 6400, 8000, 9600 (Cepheid); R.A.P.I.D., RapidCycler 2, RAZOR (Idaho Technology Inc.); LightCycler (Roche Applied Science); Mx3000P QPCR, Mx3005P QPCR, Mx4000P QPCR (Stratagene). During the preliminary cycles of amplification, the change in fluorescence is minimal. However, at a specific point the change in fluorescence increases exponentially and can be detected by the system. This point is called the threshold cycle (C_T). The C_T is proportional to the log of the starting amount of nucleic acid (Heid et al., 1996). By concurrently amplifying samples of known and unknown starting material, it is possible to create a standard curve. Correlating the unknown samples to the known samples from the standard curve allows the determination of the starting amount of nucleic acid for the unknown samples. Using individual target genes of interest from the Affymetrix *Pseudomonas* GeneChip array, real-time PCR was used to validate the GeneChip data.

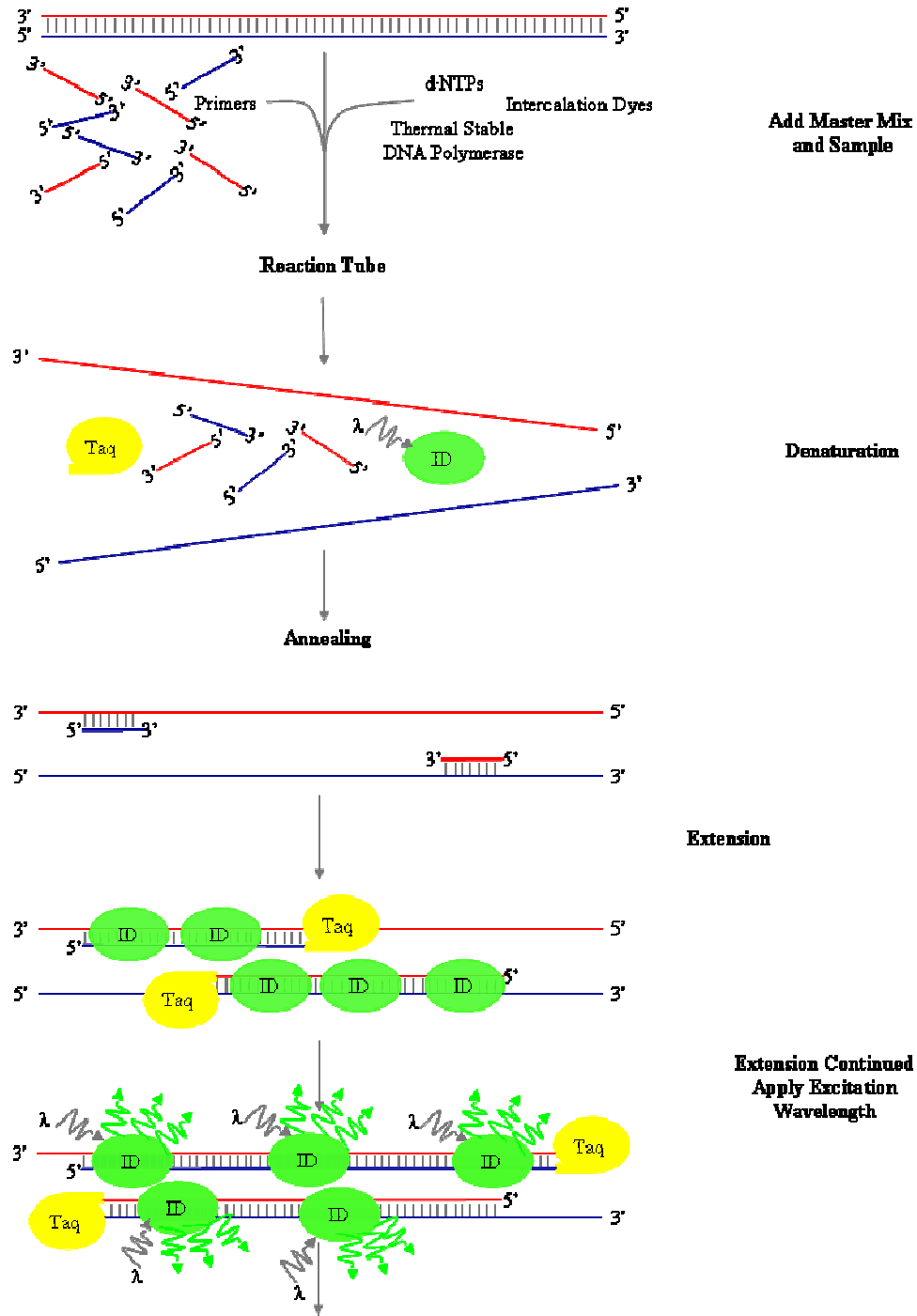


Figure 8: Real-time polymerization chain reaction (PCR)

A master mix containing the template, primers, dNTPs, intercalating dye (ID), and thermally stable DNA Polymerase (Taq) is added in a reaction tube. The reaction continues to include the denaturation, annealing, and extension steps. The extension step allows the intercalating dye to become embedded in the double helix structure of the DNA and be detected with the appropriate wavelength excitation for the dye.

1.10. Statistical analysis of microarray data

DNA microarray data often ranges from hundreds to tens of thousands of data points for each array. In order to interpret this data, statistical methods must be used to analyze this immense amount of biological information. These methods may be as simple as box plots or scatter plots. The following statistical analysis methods were used in this project and are described below: scatter plots and an analysis of variance (ANOVA).

1.10.1. Scatter plots

Scatter plots may be the easiest method to visualize microarray data. Typically, one experimental set of intensities is plotted against a control set of intensities on a log scale. When the reference sample or control sample is placed on the x-axis and the experimental sample is placed on the y-axis, the line $y = x$ forms a diagonal that shows a 1-fold change (no change in expression). Families of diagonal lines, orthogonal to the 1-fold change may now be inserted to show measured increased or decreases in fold-change (see Figure 9). Scatter plots have the advantage of being easy to understand, but are limited by the two (or at most three) dimensions to display the data. Data plotted on scatter plots will often show high variance at low intensities and lower variance at higher intensities. This phenomenon is often proved by showing the scatter plot of a technical or biological replicate and observing the “rocket ship” image (see Figure 9).

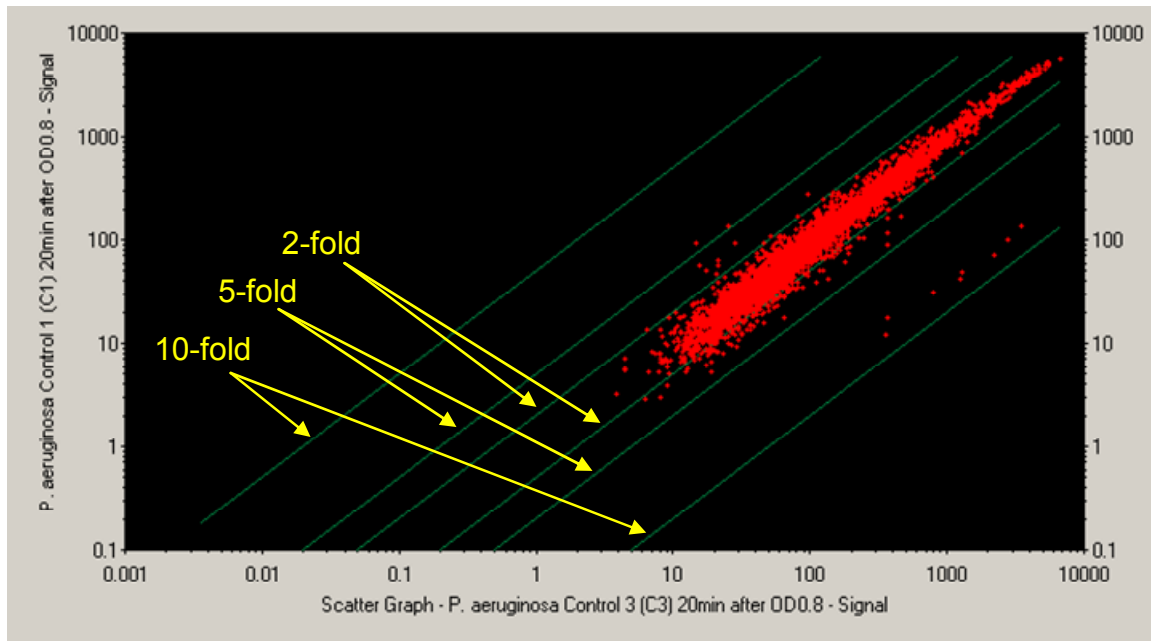


Figure 9: Scatter plot of microarray data.

This is a typical scatter plot of a biological replicate. Notice the “rocket ship” pattern that forms along the line $y = x$, representing a 1-fold change. The diagonal lines represent 2-fold, 5-fold, and 10-fold changes as indicated on the scatter plot.

1.10.2. Analysis of variance (ANOVA)

The analysis of variance (ANOVA) is a statistical procedure for analyzing quantitative responses from experimental measurements. The simplest ANOVA is a single factor or one-way ANOVA. A one-way ANOVA involves the analysis of numerical data sampled by two or more populations, or in the case of the experiments outlined here, the data from experiments in which two or more treatments have been used. The one-way ANOVA algorithm used by GeneSpring GX v. 7.3 incorporated the cross-gene error model and was as follows:

Let i index over the G groups formed by distinct levels of the comparison parameter. For this study, G is initially set at 4 ($G = 4$) for the control group,

sodium hypochlorite-exposed group, hydrogen peroxide-exposed group, and peracetic acid-exposed group.

Let X_{ik} be the expression values, with k running over the replicates for each situation, interpreted according to the log of ratio.

Let:

N_i = the number of non-missing data values for each treatment,

$$\bar{X}_i = \frac{1}{N_i} \sum_{k=1}^{N_i} X_{ik} \quad \text{be the treatment means, and}$$

$$SS_i = \sum_{k=1}^{N_i} (X_{ik} - \bar{X}_i)^2 \quad \text{be the within group sum of squares}$$

Using the computations for a parametric test, where the variances are not assumed equal and all error estimates are utilized (the cross-gene error model), led to the following:

Each group is checked that has $N_i \geq 2$ and $SS_i \geq 0$. If this is not the case, N_i is removed from consideration and G is recomputed. If G is not at least 2, then $p = 1$. This aspect of the cross-gene error model exemplifies the more stringent requirement of not assuming the variances are equal. Since the variances are separately estimated in this calculation, replicates are required for each group. If the variance estimate was

combined in to one group, replicates would only have been required for only one of the four groups.

The following is then computed:

$$w_i = N_i \left(\frac{N_i - 1}{SS_i} \right) \quad \text{for the group weights}$$

$$W = \sum_{i=1}^G w_i \quad \text{the sum of weights}$$

$$\tilde{X} = \frac{\sum_{i=1}^G w_i X_i}{W} \quad \text{the weighted mean}$$

$$BSS = \sum w_i (\bar{X}_i - \tilde{X})^2 \quad \text{the between-groups sum of squares}$$

$$d_1 = G - 1 \quad \text{the numerator degrees of freedom}$$

$$BMS = \frac{BSS}{d_1} \quad \text{the between-groups mean square}$$

$$Z = \frac{1}{G^2 - 1} \sum_{i=1}^G \frac{\left(1 - \frac{w_i}{W}\right)^2}{N_i - 1}$$

$$d_2 = \frac{1}{3Z} \quad \text{the denominator degrees of freedom}$$

If $d_2 > 0$, then $p = 1$

$$WMS = 1 + 2(G - 2)Z \quad \text{the within-group mean square}$$

$$W = \frac{BMS}{WMS} \quad \text{the test statistic}$$

Calculation of the p -value is now completed by looking up W in the upper tail probability of an F distribution with d_1 and d_2 (where d_2 will not generally be an integer) degrees of freedom (Agilent Technologies, 2006).

1.11. Further analysis of microarray data

There are several additional techniques to analyze microarray data that utilize statistically significant data from microarray experiments. The following additional analytical methods were used in this project and are described below: metabolic pathway analysis, hierarchical clustering, functional classification analysis, and principal component analysis.

1.11.1. Metabolic pathway analysis

Metabolic pathway analysis (or functional enrichment) is becoming increasingly popular because it incorporates stringent criteria (the previously listed p -value $p \leq 0.05$ and ≥ 2 -fold change data and the small, subtle, and consistent changes in expression of groups of genes with functional relations (Curtis, Oresic, & Vidal-Puig, 2005). There are three main sources of pathway or functional information as follows: Gene Ontology (GO), the Kyoto Encyclopedia of Genes and Genomes (KEGG), and Gene Microarray Pathway Profiler (GenMAPP). The GO project has three objectives as follows: to develop a regulated vocabulary set or ontology that describes key biological domains, to

apply GO terms in other databases, and to provide a central universally accessible database to the ontologies containing GO data (Harris *et al.*, 2004). GO places genes into a hierarchical listing with similar functioning genes products places near each other (Curtis *et al.*, 2005). KEGG is a daily updated, freely available knowledge-based database that contains searchable graphical diagrams of biochemical, known metabolic, and known regulatory pathways (Ogata *et al.*, 1999). GenMAPP is a free functioning graphical program for displaying and interpreting gene expression data based on biological pathway (Dahlquist, Salomonis, Vranizan, Lawlor, & Conklin, 2002). GenMaPP pathways may contain different accession numbers than KEGGs, but also has the advantage of being user-configurable using additional MAPPbuilder software (Curtis *et al.*, 2005; Doniger *et al.*, 2003).

The *P. aeruginosa* genome (PAO1) is one of the largest prokaryotic genome (5,566 genes) sequenced to date with numerous citings and a formidable research community studying it (Hallin & Ussery, 2004; Stover *et al.*, 2000). A special community-based, continually updated genome annotation is contained in the *P. aeruginosa* Community Annotation Project (PseudoCAP) (Winsor *et al.*, 2005) as well as . PseudoCAP categorizes the *P. aeruginosa* transcriptome into functional classifications listed in Table 5.

Table 5: Functional Classification of *P. aeruginosa* Genes

Functional Class	Number of Genes
Adaptation, protection	168
Amino Acid biosynthesis and metabolism	223
Antibiotic resistance and susceptibility	26
Biosynthesis of cofactors, prosthetic groups and carriers	159
Carbon compound catabolism	172
Cell division	29
Cell wall / LPS / capsule	135
Central intermediary metabolism	99
Chemotaxis	64
Chaperones & heat shock proteins	54
DNA replication, recombination, modification and repair	88
Energy metabolism	207
Fatty acid and phospholipids metabolism	61
Hypothetical, unclassified, unknown	2400
Membrane proteins	684
Motility & Attachment	93
Non-coding RNA gene	35
Nucleotide biosynthesis and metabolism	72
Protein secretion/export apparatus	98
Putative enzymes	476
Related to phage, transposon, or plasmid	58
Secreted Factors (toxins, enzymes, alginate)	76
Transcription, RNA processing and degradation	54
Transcriptional regulators	467
Translational, post-translational modification, degradation	194
Transport of small molecules	593
Two-component regulatory systems	123

1.11.2. Hierarchical clustering

There are several types of cluster analysis, such as K-means clustering, quality threshold (QT) clustering, and hierarchical clustering. However, the one most often utilized in microarray data analysis is hierarchical clustering (Brazma & Vilo, 2001). This entails grouping genes together with experiments in small clusters, grouping these clusters into groups of higher-level clusters, and

continuing this cluster grouping process. The result of this method yields a connectivity tree of observations called a dendrogram when visually displayed. Considering both gene groupings and experiment groupings allows patterns in gene expression profiles to be observed during different experimental conditions (Shams, 2000).

Tables containing primary data have been reordered using cluster analysis. The classes were divided into supervised clustering (where the clusters are vectors described with respect to known vectors) and unsupervised clustering (where the clusters are vectors described without known vectors). This analysis proved that redundant representation of genes would group together, and genes of similar function would cluster together (Eisen, Spellman, Brown, & Botstein, 1998).

S. C. Johnson first defined the basic procedure for hierarchical clustering of a set of N items with an $N \times N$ distance (or similarity matrix) as follows (S. C. Johnson, 1967):

1. Each item is assigned to a cluster, so that if there are N items, there are now N clusters, each containing just one item. Let the distances (similarities) between the clusters be the same as the distances (similarities) between the items they contain.
2. The closest (most similar) pair of clusters is found and merged into a single cluster, so that there is now one cluster less.
3. The distances (similarities) between the new cluster and each of the old clusters are computed.

4. Steps 2 and 3 are repeated until all items are clustered into a single cluster of size N .

Johnson's algorithm for single-linkage clustering is an agglomerative scheme that erases rows and columns in the proximity matrix as old clusters are merged into new ones. The $N \times N$ proximity matrix is $\mathbf{D} = [d(i,j)]$. The clusterings are assigned sequence numbers $0, 1, \dots, (n-1)$, where $L(k)$ is the level of the k^{th} clustering. A cluster is defined by a sequence number (m) and the proximity between clusters (r) and (s) which is denoted by $d[(r),(s)]$. The algorithm is composed of the following steps:

1. Beginning with the disjoint clustering having level $L(0) = 0$ and sequence number $m = 0$.
2. The least dissimilar pair of clusters in the current clustering is found. The pair (r), (s), according to $d[(r),(s)] = \min d[(i),(j)]$, where the minimum is over all pairs of clusters in the current clustering.
3. The sequence number m is incremented as follows: $m = m + 1$. Clusters (r) and (s) are merged into a single cluster to form the next incremental clustering m . The level of this clustering is now set to $L(m) = d[(r),(s)]$.
4. The proximity matrix, \mathbf{D} is updated by deleting the rows and columns corresponding to clusters (r) and (s) and adding a row and column corresponding to the newly formed cluster. The proximity between the new cluster, denoted (r,s) and the old cluster (k) is defined as follows:

$$d[(k), (r,s)] = \min [d[(k),(r)], d[(k),(s)]]$$

5. If all objects are in one cluster, stop. Else, go to step 2.

The following example is provided to illustrate hierarchical clustering. The distances from Boston (Bos), New York (NY), District of Columbia (DC), Los Angeles (LA), and San Francisco (SF) are provided in Table 6 (see Step 1). The nearest cities are Boston and New York at a distance of 206 mi (see Step 2), so these two cities are merged into a single cluster “Boston/New York” with the new sequence number $m = 1$ (Step 3). The distances are now computed from Boston/New York to all other cities in the matrix so as to minimize the distance of the new cluster to all remaining objects in the matrix (see Step 4). The nearest city to the Boston/New York cluster is DC at a distance of 233 mi (see Step 2), so these two cities are merged into a single cluster “Boston/New York/DC” with the new sequence number $m = 2$ (see Step 3). The distances are now computed from Boston/New York/DC to all other cities in the matrix so as to minimize the distance of the new cluster to all remaining objects in the matrix (see Step 4). The process continues until there is only one compound object or cluster. A dendrogram of the clustering from the distance matrix is shown in Figure 10. A typical gene clustering dendrogram or heat map is shown in Figure 11.

Table 6: Distance matrix for hierarchical clustering example

L = 0 (Input distance matrix)					
	Bos	NY	DC	LA	SF
Bos	0	206	429	2,979	3,095
NY	206	0	233	2,786	2,934
DC	429	233	0	2,631	2,799
LA	2,979	2,786	2,631	0	379
SF	3,095	2,934	2,799	379	0

L = 1				
	Bos/NY	DC	LA	SF
Bos/NY	0	233	2,786	2,934
DC	233	0	2,631	2,799
LA	2,786	2,631	0	379
SF	2,934	2,799	379	0

L = 2			
	Bos/NY/DC	LA	SF
Bos/NY/DC	0	2,631	2,799
LA	2,631	0	379
SF	2,799	379	0

L = 3		
	Bos/NY/DC	LA/SF
Bos/NY/DC	0	2,631
LA/SF	2,631	0

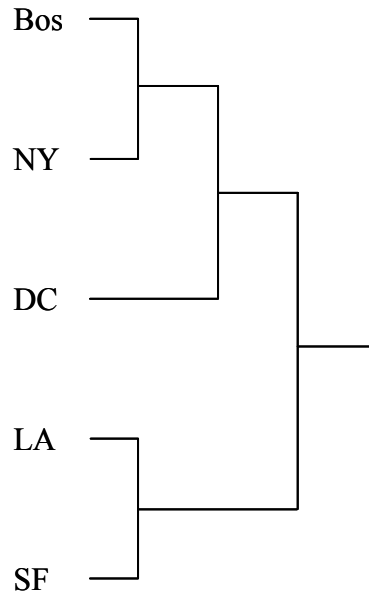


Figure 10: Dendrogram of distance matrix for the hierarchical clustering example
This is illustration is the dendogram or hierarchical tree of the distance matrix example which summarizes the entire process.

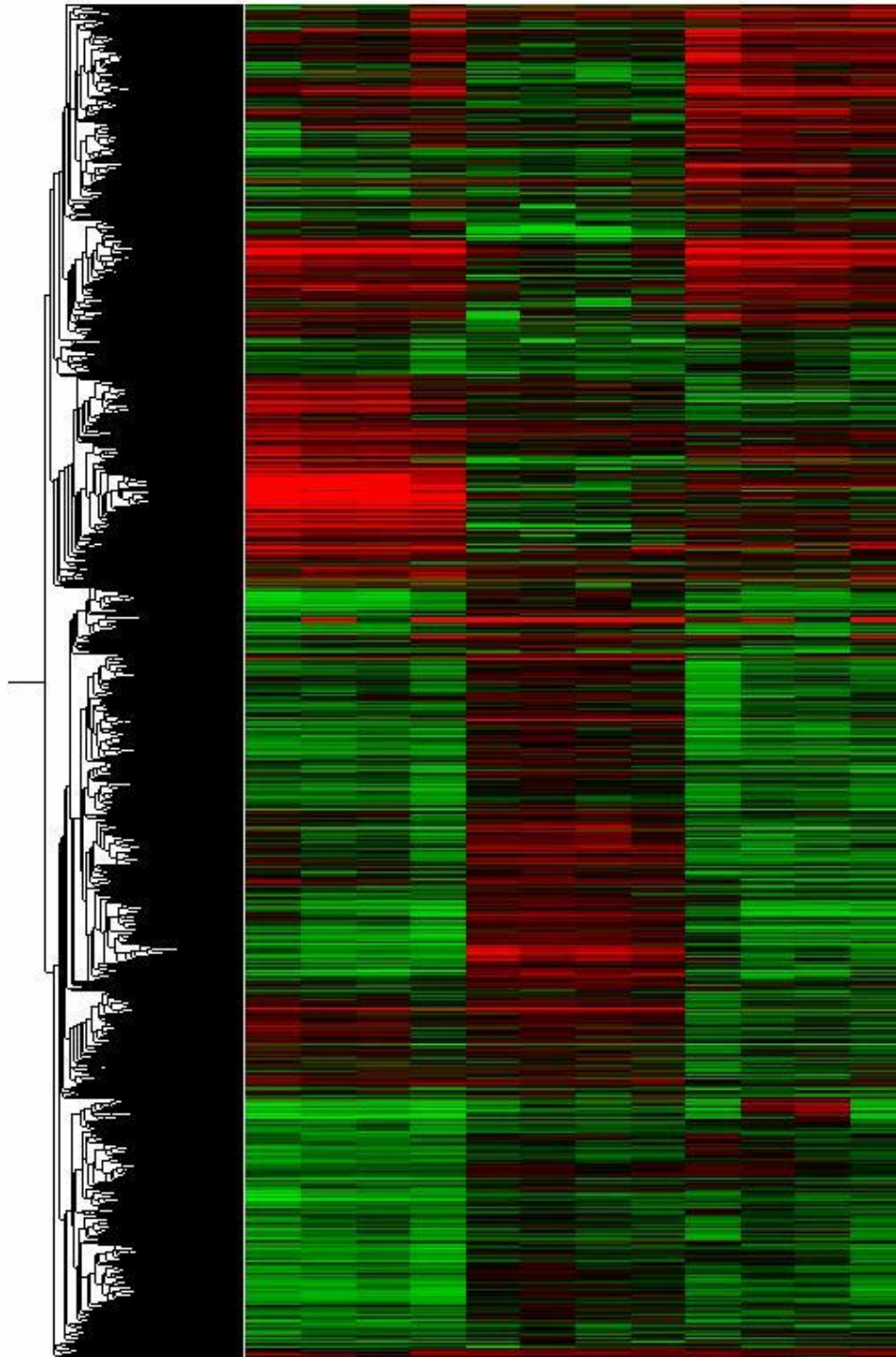


Figure 11: Dendrogram (heat map) illustrating the clustering of microarray data
This is a typical hierarchical clustering of microarray data set. This graphical representation of the data is often referred to as a heat map. The colors of the heat map illustrate expression level as follows: a red color represents an increase in expression level, a green color represents a decrease in expression level, and a black color represents no change in expression level.

1.11.3. Principal component analysis (PCA)

Another method of microarray data analysis is Principal Component Analysis (PCA) which involves mathematically high-dimensional data being reduced to two or three dimensions for easier visualization of the data (Basilevsky, 1994). This deals predominantly with preserving the relative distances of data points in the high dimension and the reduced dimension. PCA is a multivariate technique to illustrate a large data set by finding the axes or principal components of the data variance. The coefficients for the variables are selected so that the first component describes the maximum data variance. The second component will be perpendicular to the first axis and will explain the maximum amount of the remaining variance. The third component is perpendicular to the first and second components and describes the residual amount of the variance in the data. The process continues until all data variances are sufficiently represented (Raychaudhuri, Stuart, & Altman, 2000).

PCA uses a linear combination of the original data to compress the data set. The PCA algorithm used is described here as follows:

The matrix \mathbf{X} is the data set, which is defined as an $m \times n$ matrix, where m is the number of measurement types (for example, signal intensities for each gene in the GeneChip data) and n is the number of samples (or individual treatments used in obtaining the data).

The matrix \mathbf{P} is an orthonormal matrix which has rows that are *principal components* of \mathbf{X} is defined as follows:

$$\mathbf{Y} = \mathbf{P}\mathbf{X} \text{ such that } \mathbf{C}_Y \equiv \frac{1}{n-1} \mathbf{Y}\mathbf{Y}^T \text{ is diagonalized}$$

\mathbf{C}_Y is now rewritten in terms of the variable matrix, \mathbf{P} as follows:

$$\mathbf{C}_Y = \frac{1}{n-1} \mathbf{Y}\mathbf{Y}^T$$

$$\mathbf{C}_Y = \frac{1}{n-1} (\mathbf{P}\mathbf{X})(\mathbf{P}\mathbf{X})^T$$

$$\mathbf{C}_Y = \frac{1}{n-1} \mathbf{P}\mathbf{X}\mathbf{X}^T \mathbf{P}^T$$

$$\mathbf{C}_Y = \frac{1}{n-1} \mathbf{P}(\mathbf{X}\mathbf{X}^T) \mathbf{P}^T$$

$$\mathbf{C}_Y = \frac{1}{n-1} \mathbf{P}\mathbf{A}\mathbf{P}^T, \text{ where } \mathbf{A} \text{ is a new } \textit{symmetric} \text{ matrix } \mathbf{A} \equiv \mathbf{X}\mathbf{X}^T$$

A *symmetric* matrix, \mathbf{A} is now diagonalized by a matrix of its orthonormal eigenvectors as follows:

The matrix \mathbf{A} is a square $n \times n$ symmetrical matrix with associated eigenvectors $[\mathbf{e}_1, \mathbf{e}_2, \dots, \mathbf{e}_n]$. Let the matrix $\mathbf{E} = [\mathbf{e}_1, \mathbf{e}_2, \dots, \mathbf{e}_n]$ where the i^{th} column of \mathbf{E} is the eigenvector, \mathbf{e}_i . Thus, a diagonal matrix \mathbf{D} exists where

$$\mathbf{A} = \mathbf{E}\mathbf{D}\mathbf{E}^T.$$

Since $\mathbf{E}^T = \mathbf{E}^{-1}$, the matrix \mathbf{A} can be rewritten as follows:

$$\mathbf{A} = \mathbf{E}\mathbf{D}\mathbf{E}^T$$

$$\mathbf{A} = \mathbf{E}\mathbf{D}\mathbf{E}^{-1}$$

$$\mathbf{A}\mathbf{E} = \mathbf{E}\mathbf{D}$$

Breaking this equation into parts as follows:

$$\text{Left side of the equation: } \mathbf{A}\mathbf{E} = [\mathbf{A}\mathbf{e}_1, \mathbf{A}\mathbf{e}_2, \dots, \mathbf{A}\mathbf{e}_n]$$

$$\text{Right side of the equation: } \mathbf{E}\mathbf{D} = [\lambda_1\mathbf{e}_1, \lambda_2\mathbf{e}_2, \dots, \lambda_n\mathbf{e}_n]$$

If $\mathbf{A}\mathbf{E} = \mathbf{E}\mathbf{D}$, then $\mathbf{A}\mathbf{e}_i = \lambda_i\mathbf{e}_i$ for all i , which is the definition of the eigenvalue equation.

Thus \mathbf{D} is a diagonal matrix where the i^{th} eigenvalue is placed in the ii^{th} position.

The matrix \mathbf{P} is selected to be a matrix where each row \mathbf{p}_i is an eigenvector or $\mathbf{X}\mathbf{X}^T$, thus $\mathbf{P} \equiv \mathbf{E}^T$ due to this selection.

$$\text{Substituting } \mathbf{P} \text{ into } \mathbf{A} = \mathbf{E}\mathbf{D}\mathbf{E}^T \text{ as follows: } \mathbf{A} = \mathbf{P}^T\mathbf{D}\mathbf{P}$$

\mathbf{C}_Y is now evaluated as follows:

$$\mathbf{C}_Y = \frac{1}{n-1} \mathbf{P}\mathbf{A}\mathbf{P}^T$$

$$\mathbf{C}_Y = \frac{1}{n-1} \mathbf{P}(\mathbf{P}^T\mathbf{D}\mathbf{P})\mathbf{P}^T$$

$$\mathbf{C}_Y = \frac{1}{n-1} (\mathbf{P}\mathbf{P}^T)\mathbf{D}(\mathbf{P}\mathbf{P}^T)$$

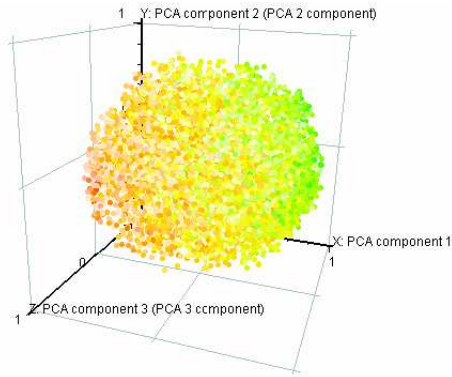
$$\mathbf{C}_Y = \frac{1}{n-1} (\mathbf{P}\mathbf{P}^{-1})\mathbf{D}(\mathbf{P}\mathbf{P}^{-1})$$

$$\mathbf{C}_Y = \frac{1}{n-1} \mathbf{D}$$

The choice of the matrix \mathbf{P} diagonalizes the matrix \mathbf{C}_Y (the entire goal of PCA). The principal components of \mathbf{X} are the eigenvectors of $\mathbf{X}\mathbf{X}^T$ or the rows of \mathbf{P} . Additionally, the i^{th} diagonal value of \mathbf{C}_Y is the variance of \mathbf{X} along \mathbf{p}_i .

In practice, performing the PCA is a bit simpler. The data is organized into an $m \times n$ matrix, where m is the number of measurement types (signal intensities for each gene in the GeneChip data) and n is the number of samples (or individual treatments used in obtaining the data). The mean is then subtracted for each measurement type or row \mathbf{x}_i . The eigenvectors of the covariance is then calculated. Thus, data of high dimension is simplified by removing less pertinent axes revealing the obscure dynamics of the data. The eigenvectors with larger eigenvalues contain more of the information from the data set and represent a higher percentage of the variance of the data (Raychaudhuri *et al.*, 2000).

a.



b.

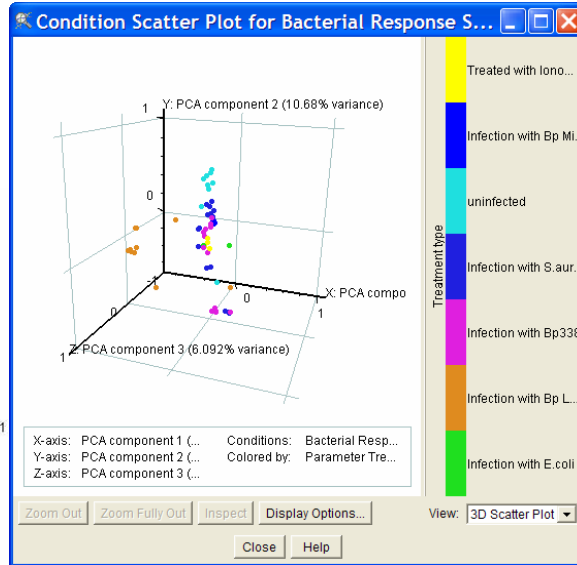


Figure 12: Principial component analysis (PCA) plots

These are typical plots for **a.** a PCA on genes where each point represents a unique gene from a microarray data set generated by GeneSpring GX and **b.** a PCA on conditions where each point represents a sample or microarray from a data set generated by GeneSpring GX.

Chapter 2: Methods and Materials

2.1. Bacterial strains and growth conditions

P. aeruginosa (PA01) was obtained from the laboratory of Dr. E. Peter Greenberg at the University of Iowa. The strain was initially grown in Luria-Bertani (LB) broth (10 g of tryptone, 5 g of yeast extract, and 10 g of sodium chloride per L) at 37°C with shaking at 250 rpm for 17 hr. Overnight cultures were grown from freezer stocks in 100 mL aliquots in 500 mL shaker flasks of LB broth at 37°C with shaking at 250 rpm for 17 hr. The overnight cultures were then diluted 1:100 in 25 mL aliquots (250 mL shaker flasks) of pre-warmed LB broth and incubated at 37°C with shaking at 250 rpm until the optical density at 600 nm (OD_{600}) reached the mid-logarithmic phase (0.8).

A final dilution of 1:10 pre-warmed LB broth in 25 mL aliquots (250 mL shaker flasks) was performed, and the cultures were incubated at 37°C with shaking at 250 rpm until the OD_{600} reached the mid-logarithmic phase (0.8). After reaching the OD_{600} of 0.8, various concentrations of sodium hypochlorite (Aldrich Chemical Co.), peracetic acid (Aldrich Chemical Co.), or hydrogen peroxide (Aldrich Chemical Co.) were added and the cell growth was monitored by measuring the OD_{600} by taking samples at 20 min intervals with a Lambda 25 spectrophotometer. This experiment was repeated three times. An appropriate sodium hypochlorite concentration and time interval for exposure was then selected that resulted in a growth inhibited (but not lethal) condition of growth for the *P. aeruginosa*. Thus, a growth condition was found that had sufficiently inhibited

cellular growth of *P. aeruginosa* without resulting in significant cell death, to allow for the proper extraction of RNA to be assayed on the microarray as discussed later in this chapter.

2.2. Viability verification

Several experimental methods were then performed to verify the viability of the *P. aeruginosa* cells at the selected sodium hypochlorite concentration and exposure time interval. These methods included the following: culture plating, cell flow cytometry, and relative ATP quantitation. The following viability verification procedure was repeated three times:

P. aeruginosa overnight cultures were grown from freezer stocks in 100 mL aliquots (500 mL shaker flasks) of LB broth at 37°C with shaking at 250 rpm for 17 hr. The overnight cultures were diluted 1:100 in 100 mL aliquots (500 mL shaker flasks) of pre-warmed LB broth and incubated at 37°C with shaking at 250 rpm until the OD₆₀₀ reached mid-logarithmic phase (0.8). A final dilution of 1:10 pre-warmed LB broth in 100 mL aliquots (500 mL shaker flasks) was performed, and the cultures were incubated at 37°C with shaking at 250 rpm until the OD₆₀₀ reached mid-logarithmic phase (0.8). Dilutions of sodium hypochlorite, NaOCl (Aldrich Chemical Co.) in 5 mL aliquots were added to 20 mL aliquots of the culture volume immediately after the OD₆₀₀ reached 0.8 and allowed to continue growing for 60 min.

A 1 mL sample was harvested from each culture at 20 min time intervals by centrifugation at 13,000 rcf for 2 min. An additional two 1 mL samples from the water-diluted control (for standard curve generation) were harvested by centrifugation at 13,000

rcf for 2 min. The supernatant was removed via pipette aspiration. The “live cell” standard cell pellet and the sodium hypochlorite-exposed cell pellets were resuspended in 1 mL Agilent Cell Buffer (Agilent Technologies). The “dead cell” standard cell pellet was resuspended in 1 mL of 70% ethanol. After a 45 min incubation of the standard samples at room temperature, the samples were centrifuged at 13,000 rcf for 2 min. The supernatants were removed via pipette aspiration. The cell pellets were then resuspended in 1 mL of Agilent Cell Buffer. The following ratios of live:dead cells were used to make a standard curve: 100% live:0% dead, 75% live:25% dead, 50% live:50% dead, 25% live:75% dead, and 0% live:100% dead.

2.2.1. Culture plating

LB-agar plates were prepared as follows: a solution of 25 g of LB media and 15 g of agar (Fisher Bioscience) in 1 L of DI water was autoclaved; approximately 10 mL was poured into a plate and stored at 4°C until needed. A 100 µL aliquot of each buffer resuspended samples from the viability verification procedure outlined above was serially diluted 7 times by 1:10. A 100 µL aliquot of each serial dilution was then spread on an LB-agar plate and incubated overnight (~10 hr) at 37°C. Photos of the appropriate dilution were taken using a Gel-Doc system (Bio-Rad Laboratories) and colony forming units (CFU) were counted using Quality One v. 4.4.1 software (Bio-Rad Laboratories).

2.2.2. Cell flow cytometry

BacLight Bacterial Viability kit (Molecular Probes) dye staining solution was then mixed consisting of 30 µL of 3.34 mM SYTO 9 in DMSO and 30 µL of

20 mM propidium iodide in DMSO. A 100 μ L aliquot of each Agilent buffer resuspended sample was incubated with 1 μ L of dye staining solution for 15 min at room temperature in the dark. A 10 μ L sample of each cell mixture was loaded onto an Agilent Lab-on-a-Chip Cell Fluorescence LabChip (Agilent Technologies). The Cell Fluorescence LabChip assay was performed using the 2100 Bioanalyzer with the Flow Cytometry Set and 2100 Expert v. B.01.02.SI136 software (Agilent Technologies). The 2100 Expert dot plot data files were then imported in FCS format into FCS Express v. 3.00.0209 Lite Standalone (De Novo Software).

2.2.3. Relative adenosine triphosphate (ATP) quantitation

The BacTiter-Glo Microbial Cell Viability Assay (Promega) was performed as follows: BacTiter-Glo Buffer and BacTiter-Glo substrate were equilibrated to room temperature from -20°C storage. A 100 mL volume of BacTiter Buffer was transferred into the BacTiter Glo substrate bottle and inverted several times to achieve a homogeneous solution. Appropriate wells of a white 96 well plate were loaded with 100 μ L aliquots of the BacTiter Glo reagent. A 100 μ L aliquot of LB media was used for each triplicate blank. At each 20 min time interval, an additional 100 μ L sample in triplicate was withdrawn from the cultures and added to the BacTiter Glo reagent. Luminescence was measured using a LS-55 Fluorescent Spectrophotometer (Perkin-Elmer) with a well-plate reader attachment adapted for luminometry as follows: slits were set to 20 nm, 5 sec read time per well, 0 nm setting emission setting (to allow for all light to be

detected), 16 msec gating, and 20 msec cycle time). The data was exported to MS Excel 2003 (Microsoft) where the averaged blanks were subtracted from the averaged samples to obtain relative luminescence units (RLU) for each sample.

2.3. *P. aeruginosa* RNA isolation

P. aeruginosa RNA was isolated 20 min after the addition of sodium hypochlorite, hydrogen peroxide, or peracetic acid (experimental groups) or water dilution (control group) using RNeasy Mini kit (Qiagen, Inc., Valencia, CA) according to the manufacture's protocol. RNprotect Bacteria Reagent (Qiagen, Inc., Valencia, CA) was also added before the isolation for stabilization. The RNA isolation procedure was as follows: cells were incubated in the RNprotect Bacteria Reagent for 5 min, harvested by centrifugation ($\geq 8,000$ rcf for 10 min), and then incubated in TE buffer (10 mM trishydroxymethylaminomethane and 1 mM ethylenediaminetetraacetic acid at 7.5 pH) with 1mg/mL of lysozyme (Roche Applied Science). Finally, samples were eluted with 50 μ L of nuclease-free water (Ambion Inc.). RNA quality, purity, and integrity were determined using both a Lambda 25 spectrophotometer (PerkinElmer, Inc.) and RNA 6000 Nano LabChips with an Agilent 2100 Bioanalyzer (Agilent Technologies). The results of a typical RNA 6000 Nano LabChip are shown in Figure 13. The A_{260}/A_{280} ratio for all of the samples was between 1.8 and 2.1, which assured removal of DNA and protein contamination and is a requirement to process the samples further according to the Affymetrix protocol.

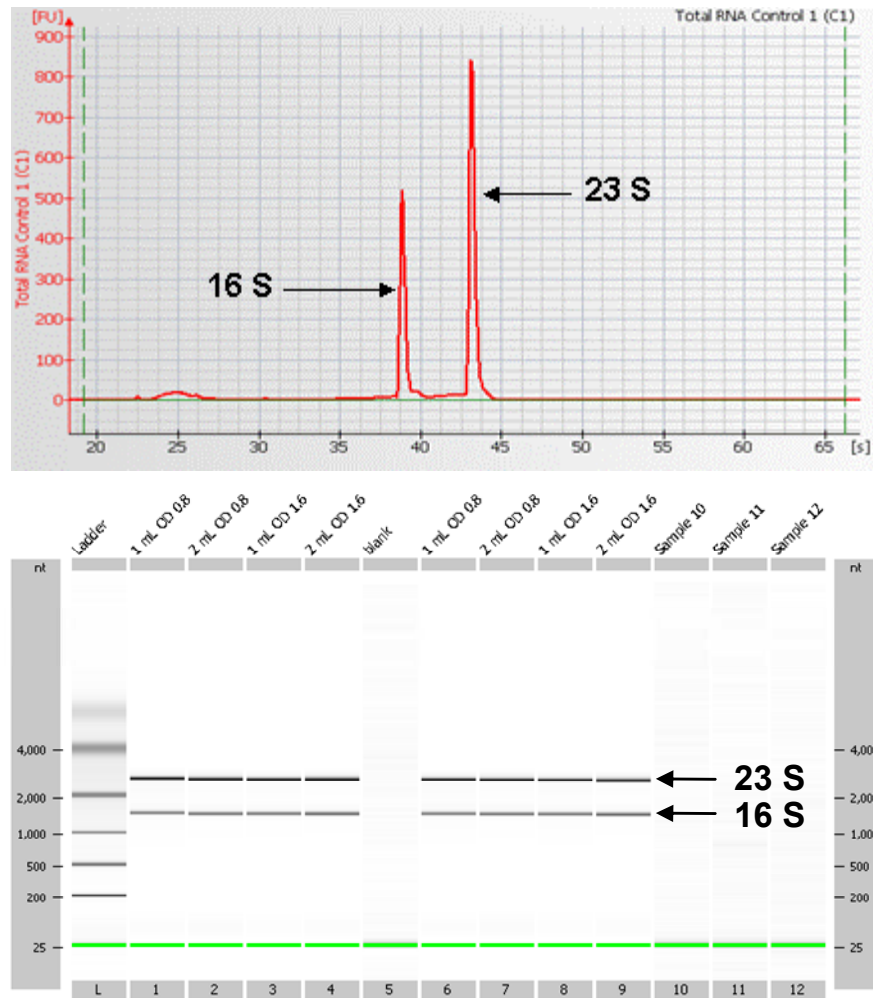


Figure 13: RNA isolation and purification

Shown above are the electrogram (top) and the corresponding gel picture (bottom) of the total RNA isolated from *P. aeruginosa*. The two sharp peaks at the 16S and 23S rRNA locations and the integration of the area underneath the peaks indicates that the total RNA has sufficient purity and quantity to be added to the microarray.

2.4. cDNA synthesis and labeling

Complimentary DNA (cDNA) was synthesized from 12 μ g of RNA with random primers and SuperScript II (both from Invitrogen Corp.) according to the protocol for the Affymetrix *Pseudomonas aeruginosa* GeneChip array (Affymetrix, Inc.). Control transcripts from *Bacillus subtilis* genes *dap*, *thr*, *phe*, and *lys* (Affymetrix, Inc.) were spiked into RNA mixtures to monitor labeling, hybridization, and staining efficiency. The

cDNA purified with a QIAquick PCR purification kit (Qiagen, Inc.) was then fragmented at 37°C for 10 min by addition of DNase I (0.06 U/μg of cDNA) (Roche Applied Science) in One Phor-All buffer (Invitrogen Corp.). The Enzo BioArray Terminal Labeling Kit with Biotin-ddUTP (Enzo Life Sciences, Inc.) was utilized to label 3' termini of the fragmented cDNA.

2.5. Hybridization and scanning

Hybridization cocktail was prepared with fragmented and labeled cDNA and B2 control oligonucleotide (Affymetrix, Inc.). The cocktail was hybridized onto *P. aeruginosa* GeneChip arrays (Affymetrix, Inc.) at 50°C for 16 hr. The arrays were washed and stained with ImmunoPure streptavidin (Pierce Biotechnology), anti-streptavidin goat antibody (Vector Laboratories, Inc.), and R-phycoerythrin streptavidin (Molecular Probes, Inc.) using a GeneChip Fluidics Station 450 (Affymetrix, Inc.). Finally, the arrays were scanned with the GeneChip Scanner 3000 (Affymetrix, Inc.).

2.6. Data analysis

Data analysis was performed with the Affymetrix GeneChip Operating Software (GCOS) v. 1.0 and GeneSpring GX v. 7.3 (Agilent Technologies). The following parameters were utilized for the GCOS expression analysis: *alpha* 1 (α_1), 0.04; *alpha* 2 (α_2), 0.06; *tau* (τ), 0.015; target signal, 150. The data files (.chp files) for all 12 samples (4 water-diluted control samples, 4 sodium hypochlorite-exposed samples, 4 peracetic-acid-exposed samples, and 4 hydrogen-peroxide-exposed samples) from GCOS were then imported into GeneSpring GX. The sodium hypochlorite, peracetic acid, and hydrogen

peroxide exposed sample replicates were then normalized to the water-diluted control sample replicates. A master list of present/marginal call genes was created by merging the lists of genes that received present/marginal calls from 50% or more of the replicates for each sample set (four water-diluted control samples, four sodium hypochlorite treated cultures, four peracetic acid treated cultures, and four hydrogen peroxide treated cultures). Gene expression changes with statistical significance were identified by 1-way ANOVA (p cutoff value, 0.05). Fold changes were calculated as the median ratio between the signal averages of the four water-diluted control samples and to each of the disinfectant-exposed samples.

2.7. Real-time polymerization chain reaction (PCR) validation

The real-time polymerization chain (PCR) technique was used to validate the GeneChip array data using a relative quantitation method ($\Delta\Delta C_T$ method). The $\Delta\Delta C_T$ method examines the relative C_T differences in expression between two sets of samples. This method assumes that the values obtained during the exponential phase of PCR are indeed doubling in product number with each successive cycle. The C_T value is assumed to be reflective of the initial copy number, so that an increase in one cycle corresponds to a two-fold increase in starting copy number (Nigel, 2001).

The following equation was used to show the fold-change of the gene:

$$RE_S = 2^{-(\Delta C_T^S - \Delta C_T^C)}$$

RE_S is the fold-change of the gene

ΔC_T^S is the C_T change of the sample (experimental) gene of interest

ΔC_T^C is the C_T change of the house-keeping gene

The house-keeping gene is a gene that does not show considerable variability when expressed under different experimental conditions (Vandecasteele, Peetermans, Merckx, & Van Eldere, 2001). A house-keeping gene, *rpoD* was confirmed to have no significant changes between the control and experimental groups. This gene was also present in *P. fluorescens* and *E. coli* and has been used as a house-keeping gene for real-time PCR applications in both organisms (Savli *et al.*, 2003; Schnider *et al.*, 1995).

Beacon Designer 3 (Premiere Biosoft International) was used to generate the primer sequences used for the real-time PCR reactions. The gene sequences for the selected genes were taken from the Affymetrix Netaffx database. A summary of the primer sequences used for the real-time PCR reactions is shown in Table 7.

Table 7: Primer sequences for real-time PCR validation

Gene	Sense Primer sequence	Antisense Primer sequence
PA4613 (<i>katB</i>)	5'-GAGCAGAACTTCAAGCAGAC-3'	5'-CTCTCGTCGTCGGTGATC-3'
PA2850 (<i>ohr</i>)	5'-GAGGTCGAACTGCACATC-3'	5'-GGGTAGCGTTGGAGTAGG-3'
PA4763 (<i>recN</i>)	5'-GGAGCAGGAGCAGAAGAC-3'	5'-GTTGAGGCTGGCATTGAG-3'
PA5530	5'-AAGAAGGAAGAGCCGAAGG-3'	5'-ATGTAGGTGGTGTAGGTGTAG-3'
PA0576 (<i>rpoD</i>)	5'-CGTCCTCAGCGGTATATCG-3'	5'-TTCTTCTTCTCGTCGTCCTTC-3'

Chapter 3: Results

3.1. *P. aeruginosa* shaker flask studies

P. aeruginosa cells were grown to an OD₆₀₀ of 0.8 (mid log phase growth) in shaker flasks of 25 mL. After reaching the OD₆₀₀ of 0.8, various concentrations (0.000%, 0.015%, 0.030%, 0.050%, and 0.50%) of sodium hypochlorite were exposed to *P. aeruginosa* and the extent of the inhibitions was monitored for 60 min with samples taken every 20 min. This experiment was repeated three times, and the effects of the various concentrations of sodium hypochlorite are summarized in Figure 14. This data suggested that a 4.4 mM (0.03%) sodium hypochlorite concentration exhibited inhibitory effects on the growth, while still maintaining exponential growth (see Figure 14). Hence, the cell population was viable but with reduced growth capacity; a sub-lethal cellular stress was most likely induced in *P. aeruginosa*. A 20 min time period was selected as a suitable time period for transcription changes based on the growth curve. That is, the response seemed to be immediate and sustained for the first hour post-addition of sodium hypochlorite; a 20 min time period enables careful monitoring of post-addition growth as well as a sufficient time period for repeated and reproducible analysis.

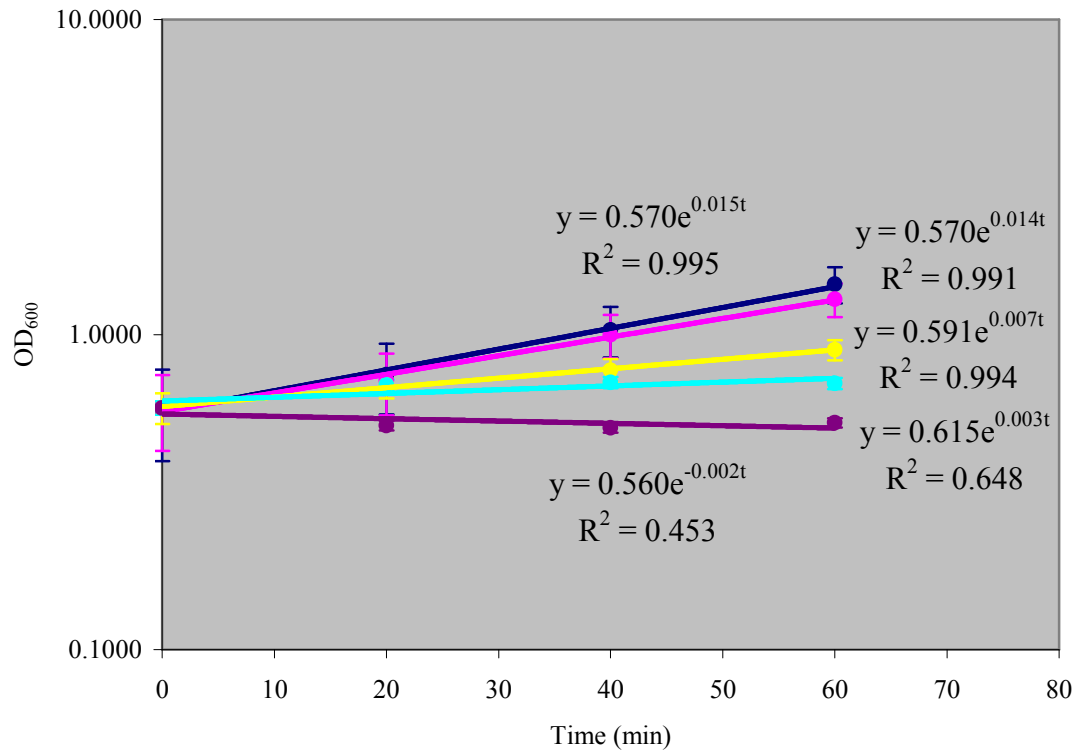


Figure 14: *P. aeruginosa* cell growth after addition of sodium hypochlorite

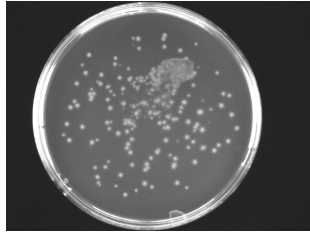
This scatter plot shows the response of *P. aeruginosa* growth with sodium hypochlorite. The control group had deionized water added instead of sodium hypochlorite. The sodium hypochlorite concentrations were as follows: 0.00% as the control (■), 0.015% (■), 0.03% (■), 0.05% (■), and 0.5% (■). Samples were taken at 0 min, 20 min, 40 min, and 60 min. Averages of three biological replicates are reported here. The exponential model regression lines and the coefficient of determination (R^2) are shown for each set of samples.

3.2. *P. aeruginosa* viability studies

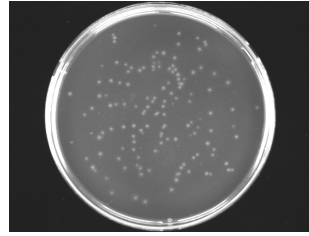
3.2.1. Plating

In order to further confirm the viability of the cells grown at 20 min, plating experiments were performed. *P. aeruginosa* cells were grown to an OD₆₀₀ of 0.8 (mid log phase growth) in shaker flasks of 25 mL. After reaching the OD₆₀₀ of 0.8, *P. aeruginosa* were exposed to various sodium hypochlorite concentrations (0%, 0.015%, 0.030%, 0.05%, and 0.50%) for 20 min. After 20 min, a 100 µL sample was taken, harvested by centrifugation, diluted to an appropriate concentration, and plated on LB-agar plates. After 18 hours of growth, the plates were photographed and the colonies were counted using a Gel Doc XR System (Bio-rad Laboratories, Hercules, CA). A typical series of photographs is shown in Figure 15. This experiment was repeated three times. The data was averaged and appears in Table 8. A t = 0 min sample was also taken, to confirm that the cells were growing. This data confirmed that the cells growing that after a 4.4 mM (0.03%) sodium hypochlorite exposure, the cells remained viable with a sufficiently inhibited growth (~50%) based on the CFU calculations.

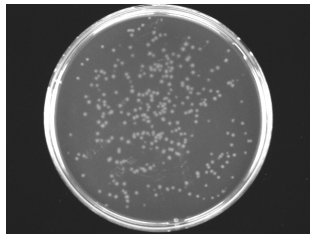
a. 0 min
 1.8×10^9 CFU



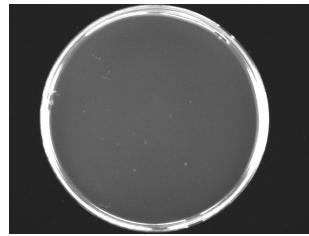
d. 20 min, 0.030% NaOCl
 3.7×10^9 CFU



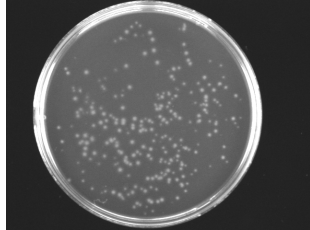
b. 20 min, 0.000% NaOCl
 3.2×10^9 CFU



e. 20 min, 0.050% NaOCl
 2.0×10^9 CFU



c. 20 min, 0.015% NaOCl
 1.6×10^9 CFU



f. 20 min, 0.500% NaOCl
0 CFU

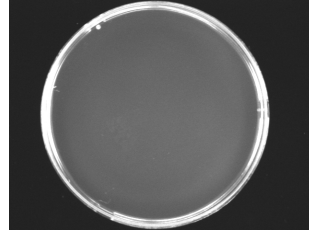


Figure 15: *P. aeruginosa* plating viability after addition of sodium hypochlorite
These images are used to count colony forming units (CFU) of *P. aeruginosa* after 20 min exposures to various concentrations of sodium hypochlorite. The control group had deionized water added instead of sodium hypochlorite. A sample was taken prior to sodium hypochlorite exposure, **a.** at 0 min. The sodium hypochlorite concentrations were as follows: **b.** 0% (0 mM, Control), **c.** 0.015% (2.2 mM), **d.** 0.030% (4.4 mM), **e.** 0.050% (7.4 mM), and **f.** 0.500% (74.0 mM).

Table 8: Summary of plating data for *P. aeruginosa* cell viability

NaOCl Concentration	Colony Forming Units (CFU)	Percentage of Control
(Control) 0.000%	3.7×10^9	100.0%
0.015%	3.2×10^9	85.0%
0.030%	2.0×10^9	53.8%
0.050%	1.6×10^4	0.0%
0.500%	0×10^0	0.0%

3.2.2. Cell flow cytometry

The cell flow cytometry experiments assessed cell viability by examining the cell membrane integrity. A standard curve was generated from the known mixtures of live:dead cells exposed to ethanol for 45 min. The results depicted a very linear standard (see Figure 16). The linearity of the standard curve assured that the regions defined in the dot plots generated in the FCS Express data analysis software method were correct for determining live and dead cells. When these regions were applied to the sodium hypochlorite-exposed samples, the relative percentages of live:dead cells could be determined. The 0.030% sodium hypochlorite exposure did not result in significant perforation of the cell membranes based on this data (see Figure 17). This result further supported the selection of the 0.030% sodium hypochlorite exposure after 20 min as an appropriate antimicrobial concentration and time period since the *P. aeruginosa* cells maintained their plasma membrane integrity.

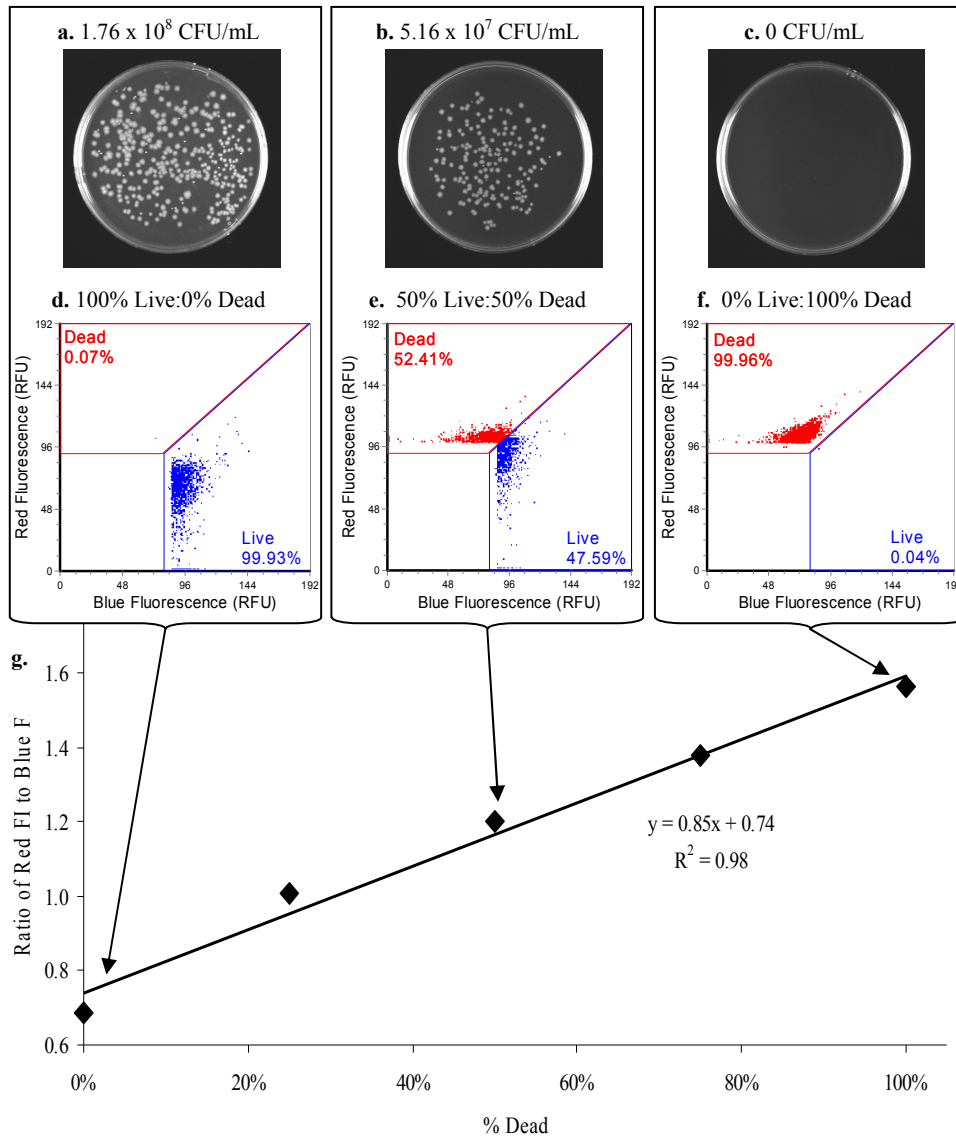
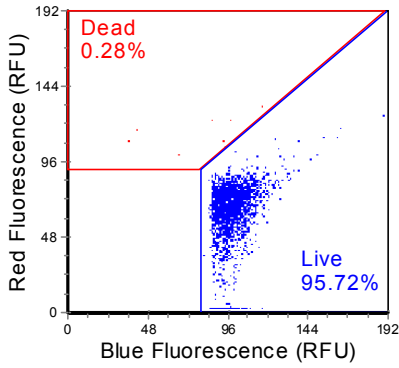


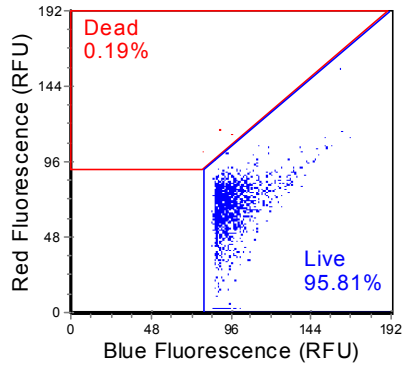
Figure 16: Live/Dead BacLight Bacterial Viability and 2100 Bioanalyzer results with plating confirmation of *P. aeruginosa*

a. Culture plate picture of 100% live:0% dead cell mixture with the adjusted colony forming units (CFU) per mL of culture. **b.** culture plate picture of a 50% live:50% dead cell mixture with the adjusted CFU per mL of culture. **c.** culture plate picture of a 0% live :100% dead cell mixture with the adjusted CFU per mL of culture. Cell fluorescence data imported into FCS Express and formatted for dead and live regions based on the red fluorescence intensity and blue fluorescence intensity for the following corresponding live:dead cell ratio mixtures: **d.** 100% live:0% dead cell mixture, **e.** 50% live:50% dead cell mixture, **f.** 0% live:100% dead cell mixture. **g.** Standard curve of the ratios of the geometric means for the red fluorescence intensity to the blue fluorescence intensity for the various mixtures of live:dead cells.

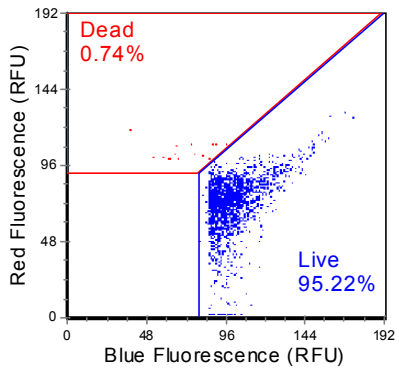
a. 0.000% NaOCl (control)



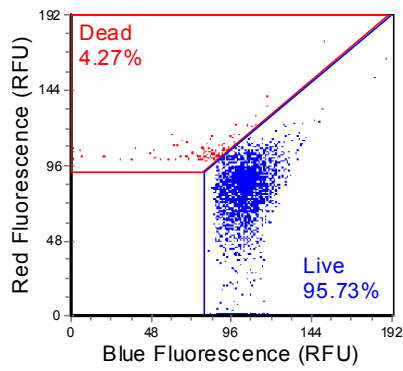
b. 0.015% NaOCl



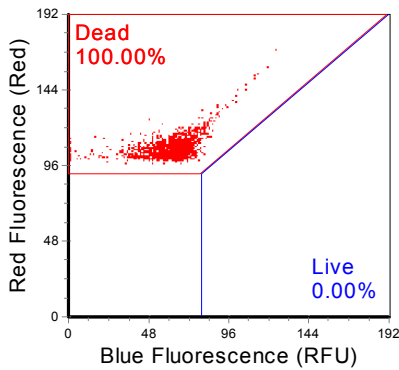
c. 0.030% NaOCl



d. 0.050% NaOCl



e. 0.500% NaOCl



f. 2.000% NaOCl

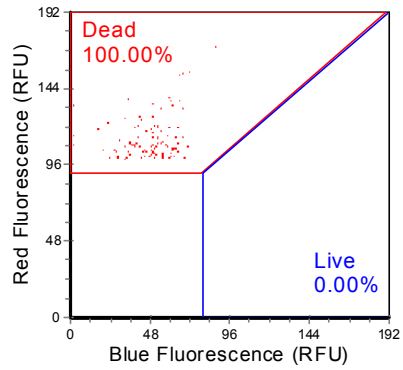


Figure 17: Sodium hypochlorite-exposed cell flow cytometry results

Shown above are live/dead dot plots based on the standard curve regions for the following 20 min exposures to sodium hypochlorite: **a.** 0.000%, **b.** 0.015%, **c.** 0.030%, **d.** 0.050%, **e.** 0.500%, and **f.** 2.000%.

3.2.3. Relative adenosine triphosphate (ATP) quantitation

The relative ATP studies (BacTiter-Glo assay) further assessed cellular metabolic state by quantitating the amount of ATP present in the cells based on the luciferase reaction (see Figure 5). The results suggested that the 0.03% sodium hypochlorite concentration and 20 min exposure time are sufficient to inhibit cell growth with resulting in significant cell death. Sodium hypochlorite exposures of 0.05% and 0.5% resulted in a declining bioluminescence signal (for 0.05%) or a signal below the blank (for 0.5%) which suggested that these cells were dead. The relative ATP quantity in the 0.03% sodium hypochlorite-exposed was between the unexposed control samples (0%) and the dead samples (0.05% and 0.5%) and still increasing exponentially. These results correlated well with the turbidity growth studies, plating studies, and flow cytometry studies.

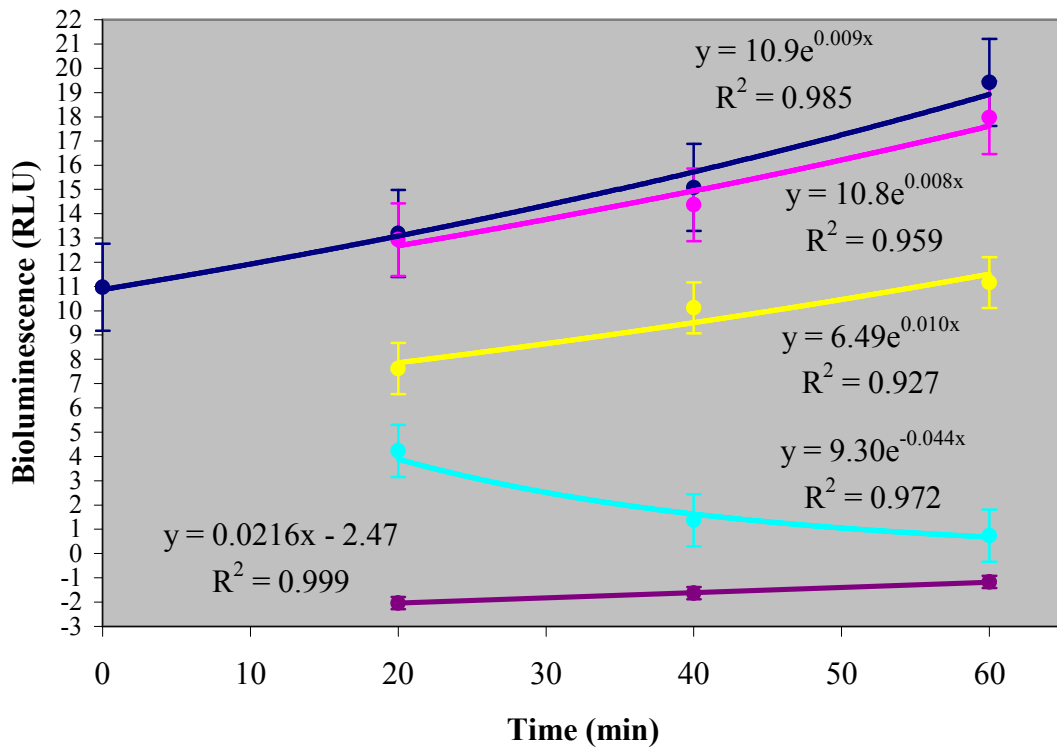


Figure 18: Bioluminescence (relative energy, ATP) results

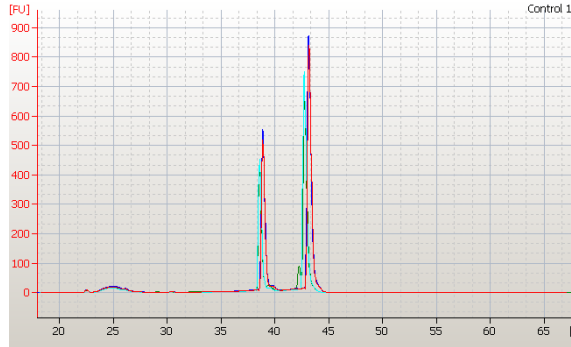
This scatter plot shows the response of *P. aeruginosa* growth with sodium hypochlorite. The control group had deionized water added instead of sodium hypochlorite. The sodium hypochlorite concentrations were as follows: 0.00% as the control (■), 0.015% (■), 0.03% (■), 0.05% (■), and 0.5% (■). Samples were taken at 0 min for the control and 20 min, 40 min, and 60 min for all other samples. Averages of three biological replicates are reported here. The exponential model regression lines and the coefficient of determination (R^2) are shown for each set of samples.

3.3. Ribonucleic acid (RNA) quality control

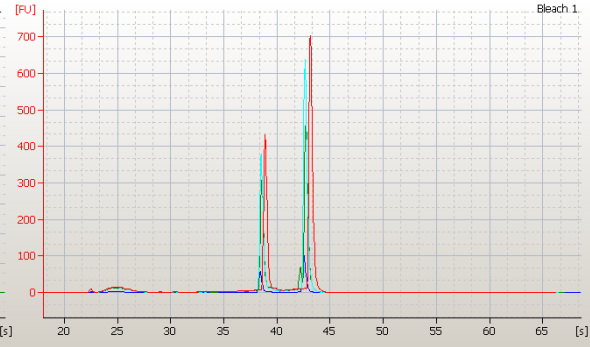
After the RNA was extracted, quality control was performed on the RNA samples to assure that the RNA was of sufficient quantity and quality to proceed with further processing to the microarray. A 1 μ L aliquot from each RNA sample was assayed with the RNA Nano chips on the 2100 Bioanalyzer. The electrograms in Figure 19 show sharp 16S and 23S peaks, indicating good RNA quality. All of the samples exceeded the suggested Affymetrix 23S/16S RNA ratio specification of ≥ 1.2 . The 23S/16S ratios for

all the RNA samples are listed in Table 9. Additionally, integrating the area beneath the 16S and 23S peaks calculated the RNA concentration of the samples. Samples were diluted by a ratio of 1:50 with water, and a UV spectrophotometer was used to measure the absorption at 260 nm (A_{260} , where nucleic acids typically absorb UV light) and the absorption at 280 nm (A_{280} , where proteins typically absorb UV light). The ratio was taken and the A_{320} corrected RNA concentrations were calculated based on the extinction coefficient of RNA. The RNA concentrations from the 2100 Bioanalyzer and UV spectrophotometer are listed in Table 9. All of the samples met the suggested Affymetrix A_{260}/A_{280} ratio of 1.8 to 2.1, which assured the ratio of nucleic acid concentration to protein contaminant concentration was low after the total RNA isolation. Additionally, all of the samples had sufficient total RNA concentrations for the required 12 μg of material required for the cDNA synthesis step.

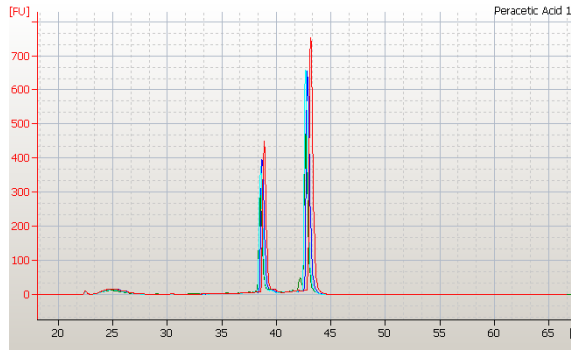
a. control total RNA



b. sodium hypochlorite-exposed total RNA



c. peracetic acid-exposed total RNA



d. hydrogen peroxide-exposed total RNA

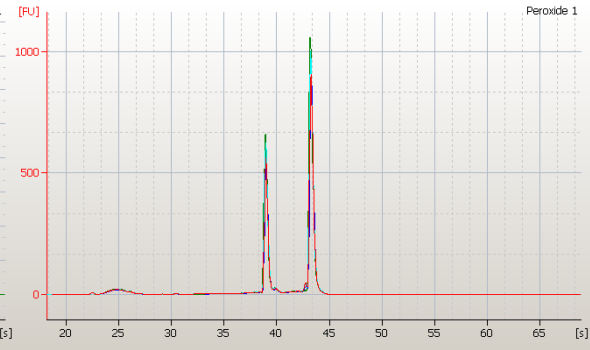


Figure 19: Bioanalyzer 2100 RNA electrograms

These images are used to count colony forming units (CFU) of *P. aeruginosa* after 20 min exposures to various concentrations of sodium hypochlorite. The control group had deionized water added instead of sodium hypochlorite. A sample was taken prior to sodium hypochlorite exposure, **a.** water-diluted control samples (four total) **b.** sodium hypochlorite-exposed samples (four total) **c.** peracetic acid-exposed samples (four total) **d.** hydrogen peroxide-exposed samples (four total).

Table 9: Summary of Bioanalyzer 2100 and Spectrophotometer RNA quality data

Sample	UV Spectrophotometer		Bioanalyzer	
	Corrected Ratio (A ₂₆₀ /A ₂₈₀)	Concentration (µg/mL)	rRNA ratio (23S/16S)	Concentration (µg/mL)
Control #1	1.872	1,450	1.7	2,520
Control #2	1.889	1,598	1.6	2,779
Control #3	1.869	1,377	1.7	2,309
Control #4	1.834	1,111	1.9	2,001
NaOCl #1	1.828	1,122	1.6	2,031
NaOCl #2	1.752	1,007	1.7	1,429
NaOCl #3	1.779	1,038	1.7	1,650
NaOCl #4	1.805	1,118	1.6	1,844
CH ₃ CO ₃ H #1	1.850	1,188	1.6	2,174
CH ₃ CO ₃ H #2	1.798	1,062	1.8	1,601
CH ₃ CO ₃ H #3	1.809	1,044	1.8	1,557
CH ₃ CO ₃ H #4	1.861	1,138	1.7	1,517
H ₂ O ₂ #1	1.882	1,556	1.7	2,178
H ₂ O ₂ #2	1.872	1,503	1.6	2,072
H ₂ O ₂ #3	1.889	1,618	1.7	2,555
H ₂ O ₂ #4	1.887	1,545	1.6	2,462

3.4. GeneChip metrics

A detection algorithm incorporated the 16 probe pair intensities for each of the 5,566 genes in the *Pseudomonas* GeneChip and generated a detection *p*-value that assigned a Present, Marginal, or Absent call for each gene. Each probe set contributed a vote in determining whether the measured transcript was detected (Present call), partially detected (Marginal call), or not detected (Absent call). The vote is described by a Discrimination score (*R*) defined below:

$$R = \frac{PM - MM}{PM + MM}$$

Where the *PM* is the perfect match signal intensity and the *MM* is the mismatch signal intensity. It should be noted that if the *PM* was much larger than the *MM*, the Discrimination score (*R*) for that probe pair was close to 1.0 and the majority of the probe

pairs would have had a calculated Detection p -value which was lower (more significant). A lower p -value was a reliable indicator that the result was valid and that the probability of error in the calculation was small. Conversely, if the MM was larger than or equal to the PM , then the Discrimination score for that probe pair was negative or zero.

The second part to calculating a Detection p -value was the comparison of each Discrimination score to the user-definable threshold, τ , which was a small positive number that could be adjusted to increase or decrease the sensitivity and/or specificity of the analysis. The τ default value of 0.015 was used for the processing of all of the Genechips. A One-Sided Wilcoxon's Signed Rank test was then used to generate the Detection p -value by assigning each probe pair a rank based on how far the probe pair Discrimination score was from τ . Probe pairs with scores higher than τ voted for the *presence* of the transcript. Probe pairs with scores lower than τ voted for the *absence* of the transcript. The voting result was summarized as a p -value. The greater the numbers of discrimination scores calculated for a given probe set that were above τ , the smaller the p -value and the more likely the given transcript was truly *present* in the sample. The p -value associated with this test reflected the confidence of the Detection call.

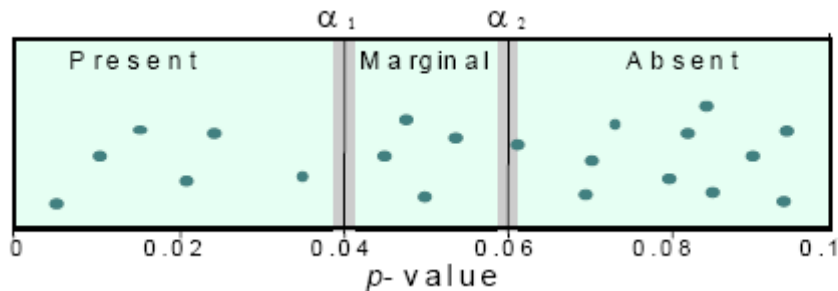


Figure 20: Present, marginal, and absent calls from p -values
Significance levels α_1 and α_2 define cut-offs of p -values for Detection calls.

The user-modifiable Detection p -value cut-offs, α_1 and α_2 shown in Figure 20 provided boundaries for defining Present, Marginal, or Absent calls. The default settings for a 16 probe pair set ($\alpha_1 = 0.04$ and $\alpha_2 = 0.06$) were used to determine if p -values fell below α_1 were assigned Present calls, and above α_2 were assigned Absent calls. Marginal calls were given to probe sets that had p -values between α_1 and α_2 (see Figure 20). These p -value cut-offs were the default values suggested by Affymetrix. A summary of the calls based on number of genes and as a percentage of the 5,570 genes for each GeneChip is provided in Table 10. The considerable detection of present calls (>50%) and relatively low percentage of marginal calls (<5%) suggested that the default values for τ , α_1 , and α_2 were appropriate and did not need to be adjusted.

Table 10: Summary of *P. aeruginosa* GeneChip metrics

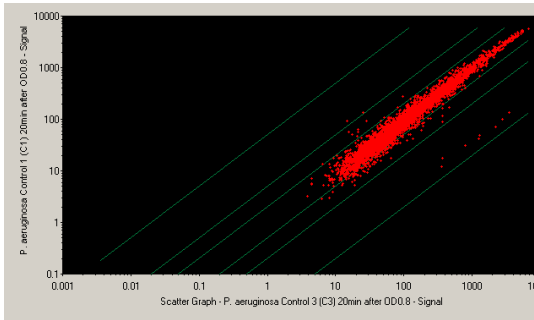
Sample	Genes Present		Genes Marginal		Genes Absent	
	Number	Percent	Number	Percent	Number	Percent
Control #1	4,492	76.2%	169	2.9%	1,235	20.9%
Control #2	4,427	75.1%	210	3.6%	1,259	21.4%
Control #3	4,892	83.0%	179	3.0%	825	14.0%
Control #4	4,304	73.0%	195	3.3%	1,397	23.7%
NaOCl #1	4,512	76.5%	192	3.3%	1,192	20.2%
NaOCl #2	4,919	83.4%	160	2.7%	817	13.9%
NaOCl #3	4,542	77.0%	180	3.1%	1,174	19.9%
NaOCl #4	4,586	77.8%	218	3.7%	1,092	18.5%
CH ₃ CO ₃ H #1	4,692	78.4%	228	3.9%	1,047	17.8%
CH ₃ CO ₃ H #2	4,698	79.7%	176	3.0%	1,022	17.3%
CH ₃ CO ₃ H #3	4,454	75.5%	221	3.7%	1,221	20.7%
CH ₃ CO ₃ H #4	4,419	74.9%	221	3.7%	1,256	21.3%
H ₂ O ₂ #1	3,754	63.7%	187	3.2%	1,955	33.2%
H ₂ O ₂ #2	3,978	67.5%	192	3.3%	1,726	29.3%
H ₂ O ₂ #3	3,769	63.9%	184	3.1%	1,943	33.0%
H ₂ O ₂ #4	4,021	68.2%	238	4.0%	1,637	27.8%

3.5. Scatter plots

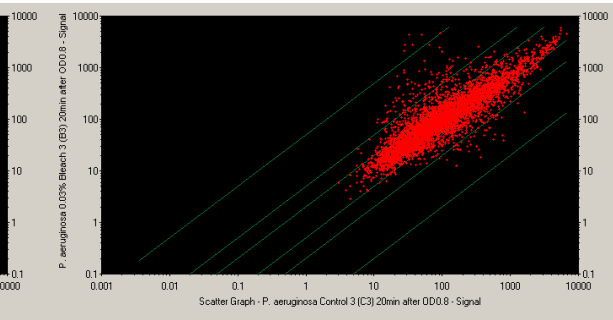
Scatter plots of the fluorescence intensity of each of experimental sample to each control sample were made. An example of each one of these scatter plots is shown below for a control versus control, control versus sodium hypochlorite-exposed sample, control versus hydrogen peroxide-exposed sample, and control versus peracetic acid-exposed sample (see Figure 21). The control samples had fairly good reproducibility as scatter plots of the controls compared to each other always produced the “rocket ship” plot along the 45° line and the majority of the genes were within the ± 2 -fold change line. The “rocket ship” plot was also observed for the sodium-hypochlorite samples, hydrogen peroxide samples, and peracetic acid samples when the samples for each respective treatment were compared to each other which demonstrated the reproducibility of this data as well.

Visual inspection of this data suggested that all three treatments affected the cells differently since the scatter plots look dissimilar from one another. However, these scatter plots cannot be used for much more than a visual comparison, since it is extremely difficult to quantify changes in expression among several treatments with any statistical significance using this method. Consequently, the scatter plots were used to assure that the data was reproducible, but more powerful statistical techniques (ANOVA, hierarchical clustering, metabolic pathway analysis, and principal component analysis) were used to compare the genome-wide effects of the treatments.

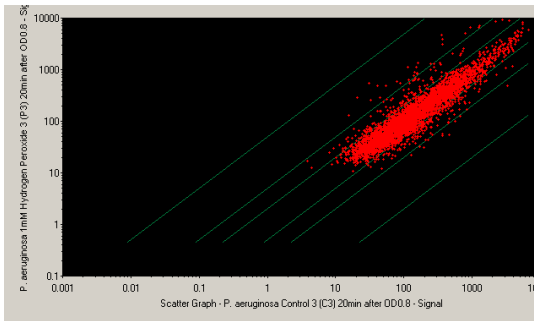
a.



b.



c.



d.

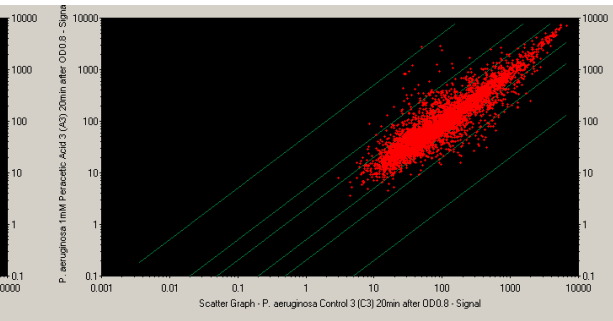


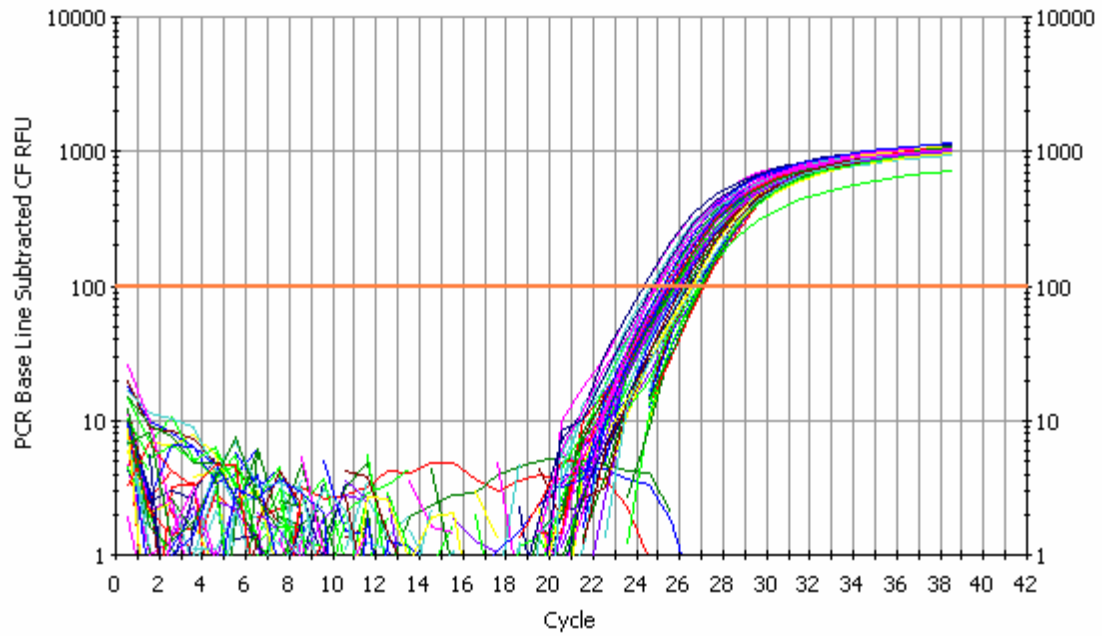
Figure 21: Scatter plots of treatment gene expression data

a. Control sample 3 versus Control sample 1, **b.** Control sample 3 versus Sodium Hypochlorite sample 3, **c.** Control sample 3 versus Hydrogen Peroxide sample 3, **d.** Control sample 3 versus Peracetic Acid sample 3.

3.6. Real-time polymerization chain reaction (PCR) validation

A sample of a real-time PCR comparison between the house-keeping gene, *rpoD* and a gene of interest, *ohr* in this case is shown in Figure 22. The C_T values obtained from these plots for the PA4613 (*katB*), PA2850 (*ohr*), PA4763 (*recN*), and PA5530 were used to calculate the fold-change relative to the house-keeping gene, PA0576 (*rpoD*). The values obtained by real-time PCR have a good correspondence to those obtained by the microarray (Table 11). These values should be expected to have a similar fold change direction (positive for an increase and negative for a decrease). The magnitudes of the change should be similar, but not necessarily the exact same number. The slight differences in fold-change expression correlate very well with prior studies comparing Affymetrix GeneChip expression with real-time quantitative PCR expression (Barnes, Freudenberg, Thompson, Aronow, & Pavlidis, 2005; Dallas *et al.*, 2005; Yauk, Berndt, Williams, & Douglas, 2004). The slight variations are most likely a result of the different natures of the two methodologies.

a.



b.

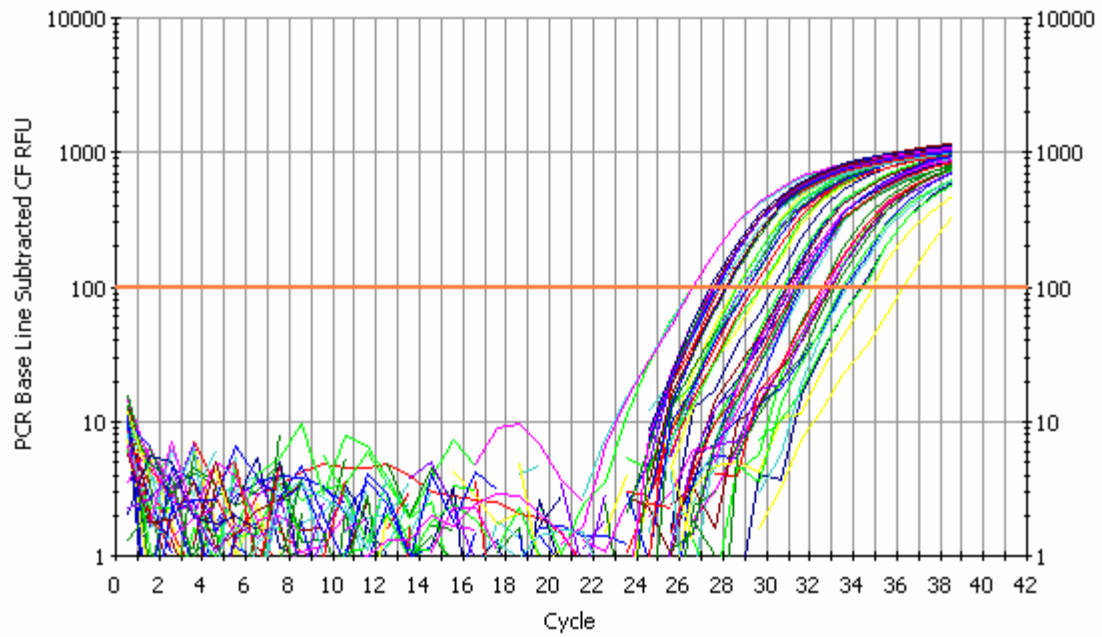


Figure 22: Real-time PCR data

These semi-log plots show the results of a real-time PCR reaction for **a.** house-keeping gene, PA0576 (*rpoD*) and **b.** gene of interest, PA2850 (*ohr*).

Table 11: Summary of real-time PCR data compared to microarray data

Genes (Name)	NaOCl real-time PCR	NaOCl microarray	CH ₃ CO ₃ H real-time PCR	CH ₃ CO ₃ H microarray	H ₂ O ₂ real-time PCR	H ₂ O ₂ microarray
PA4613 (<i>katB</i>)	+3.66 (±0.25)	+7.20	+3.37 (±0.95)	+3.99	+1.69 (±0.44)	+4.08
PA2850 (<i>ohr</i>)	+23.43 (±1.89)	+21.79	+6.72 (±2.01)	+5.32	-1.64 (±0.19)	-1.30
PA4763 (<i>recN</i>)	+1.28 (±0.09)	+2.03	+2.99 (±0.65)	+2.06	+4.24 (±0.17)	+8.78
PA5530	+7.20 (±1.68)	+14.09	+3.52 (±0.88)	+2.22	+34.26 (±7.17)	+26.77
PA0576 (<i>rpoD</i>)*	1.00	1.00	1.00	1.00	1.00	1.00

*PA0576 (*rpoD*) was used as the house-keeping gene.

3.7. Comparison of *P. aeruginosa* transcriptome changes in response to the oxidative stressors: sodium hypochlorite, hydrogen peracetic acid, and hydrogen peroxide

A sub-lethal exposure of 4.4 mM (0.03%) sodium hypochlorite, 0.5 mM peracetic acid (W. Chang et al., 2005b), and 1 mM hydrogen peroxide (W. Chang et al., 2005a) for 20 min showed inhibition of growth without 100% cellular death and enabled mRNA analysis. From the 5,570 genes in the *P. aeruginosa* genome, 3,197 genes showed statistical significance based on the 1-way ANOVA (sodium hypochlorite had 1,245 upregulated and 1,952 downregulated genes, peracetic acid had 1209 upregulated and 1,988 downregulated genes, and hydrogen peroxide had 1,568 upregulated and 1,629 downregulated genes). However, since these groups were being compared to each other a fold change threshold needed to be established. A Venn diagram analysis based on various fold change differences was performed on the statistically significant genes determined by the 1-way ANOVA to further analyze logical relationships (unions and

intersections) of genes between all the disinfectants. A generic Venn diagram is illustrated in Figure 23, and the fold change threshold analysis is summarized in Table 12. Based on these values, a conservative 2-fold or more upregulation or downregulation threshold was selected to differentiate the seven regions of the Venn diagram as follows: sodium hypochlorite in Region 1 (258 upregulated genes and 312 downregulated genes), hydrogen peroxide in Region 2 (107 upregulated and 111 downregulated genes), peracetic acid in Region 3 (175 upregulated and 150 downregulated genes), the intersection of sodium hypochlorite and hydrogen peroxide in Region 4 (26 upregulated and 60 downregulated genes), the intersection of sodium hypochlorite and peracetic acid in Region 5 (133 upregulated and 230 downregulated genes), the intersection of hydrogen peroxide and peracetic acid in Region 6 (14 upregulated and 10 downregulated genes), and the intersection of all three disinfectants in Region 7 (40 upregulated and 23 downregulated genes). Thus, from the 3,197 genes that showed statistical significance based on the 1-way ANOVA, sodium hypochlorite had 457 upregulated and 625 downregulated genes, peracetic acid had 362 upregulated and 413 downregulated genes, and hydrogen peroxide had 187 upregulated and 204 downregulated genes at the 2-fold or more change threshold level.

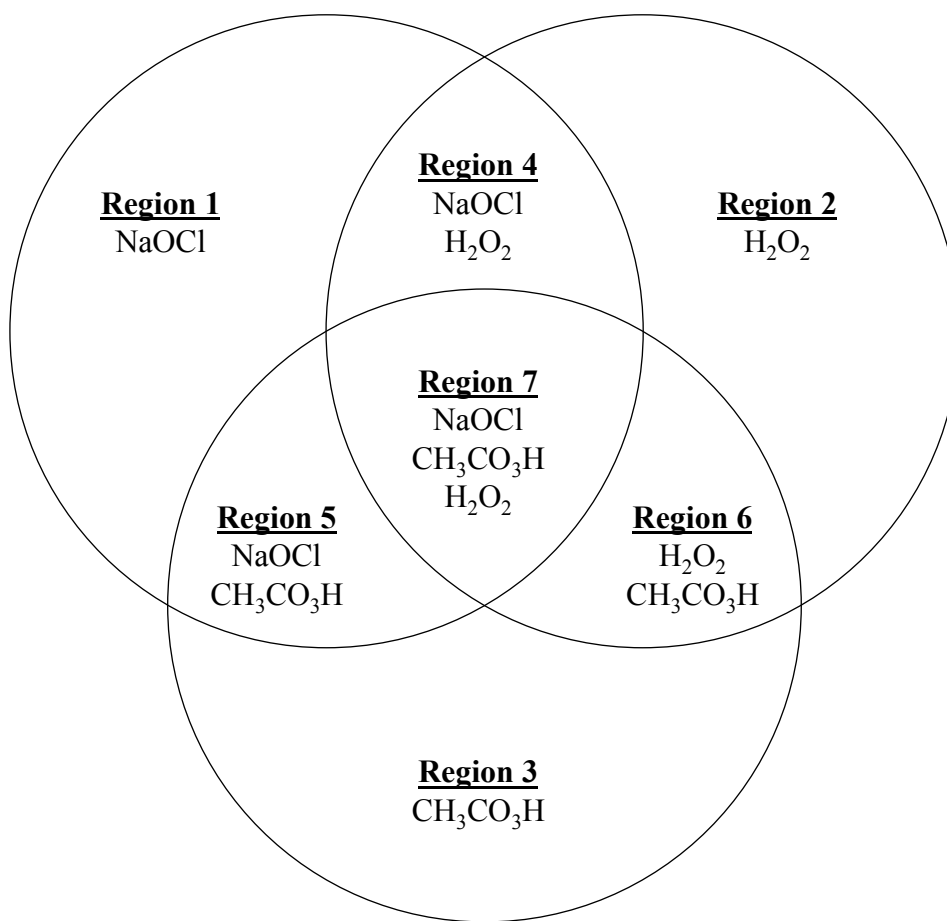


Figure 23: Sodium hypochlorite, peracetic acid, and hydrogen peroxide Venn diagram

This generic Venn diagram shows the unions and intersections of the three disinfectants. Regions are defined as follows: Region 1, hydrogen peroxide in Region 2, peracetic acid in Region 3, the intersection of sodium hypochlorite and hydrogen peroxide in Region 4, the intersection of sodium hypochlorite and peracetic acid in Region 5, and the intersection of all three disinfectants in Region 7. This diagram is referenced in Table 12, Table 13, and Table 14.

Table 12: Venn diagram data for various statistically significant fold changes of upregulated or downregulated genes between sodium hypchlorite, peracetic acid, and hydrogen peroxide.

Region	Region 1	Region 2	Region 3	Region 4	Region 5	Region 6	Region 7
Disinfectant(s)	NaOCl	H ₂ O ₂	CH ₃ CO ₃ H	NaOCl H ₂ O ₂	NaOCl CH ₃ CO ₃ H	H ₂ O ₂ CH ₃ CO ₃ H	NaOCl H ₂ O ₂ CH ₃ CO ₃ H
Fold Change	Number of Genes						
Upregulated ≥ 1-fold	110	648	195	208	302	87	625
Upregulated ≥ 1.25-fold	193	416	194	160	340	35	276
Upregulated ≥ 1.5-fold	281	262	218	95	262	21	117
Upregulated ≥ 1.75-fold	293	170	198	38	181	18	65
Upregulated ≥ 2-fold	258	107	175	26	133	14	40
Upregulated ≥ 3-fold	183	48	98	4	49	4	7
Upregulated ≥ 4-fold	123	28	50	4	29	1	2
Upregulated ≥ 5-fold	96	23	28	2	23	0	0
Upregulated ≥ 10-fold	35	15	9	1	8	0	0
Downregulated ≥ 1-fold	87	302	208	195	648	110	1022
Downregulated ≥ 1.25-fold	232	229	244	204	726	59	469
Downregulated ≥ 1.5-fold	389	173	247	149	547	45	162
Downregulated ≥ 1.75-fold	394	144	185	77	364	27	65
Downregulated ≥ 2-fold	312	111	150	60	230	10	23
Downregulated ≥ 3-fold	142	52	61	8	64	0	1
Downregulated ≥ 4-fold	81	26	28	3	21	0	0
Downregulated ≥ 5-fold	44	18	16	1	7	0	0
Downregulated ≥ 10-fold	8	2	2	0	0	0	0

3.8. Functional classifications analysis

Functional classifications of the responding genes are provided in Figure 24 and Figure 25. Although the “hypothetical, unclassified, unknown” functional class had the most genes significantly upregulated and downregulated for all the disinfectant-exposed samples, this group was omitted in Figure 24 and Figure 25 since the functions of these genes were unknown. Functional classes were taken from the *Pseudomonas aeruginosa* Community Annotation Project and appear in Table 5.

A Venn diagram analysis was performed on the functional classifications marked with asterisks in Figure 24 and Figure 25 to further analyze logical relationships (unions and intersections) of genes in each of these functional classes. The results utilized the generic Venn diagram (Figure 23) and a related table for 2-fold or more increased genes (Table 13) and a related table for 2-fold or more decreasing genes (Table 14).

Functional Classification Summary Genes that are Statistically Significant ($p \leq 0.05$) and Increased by 2-fold or More

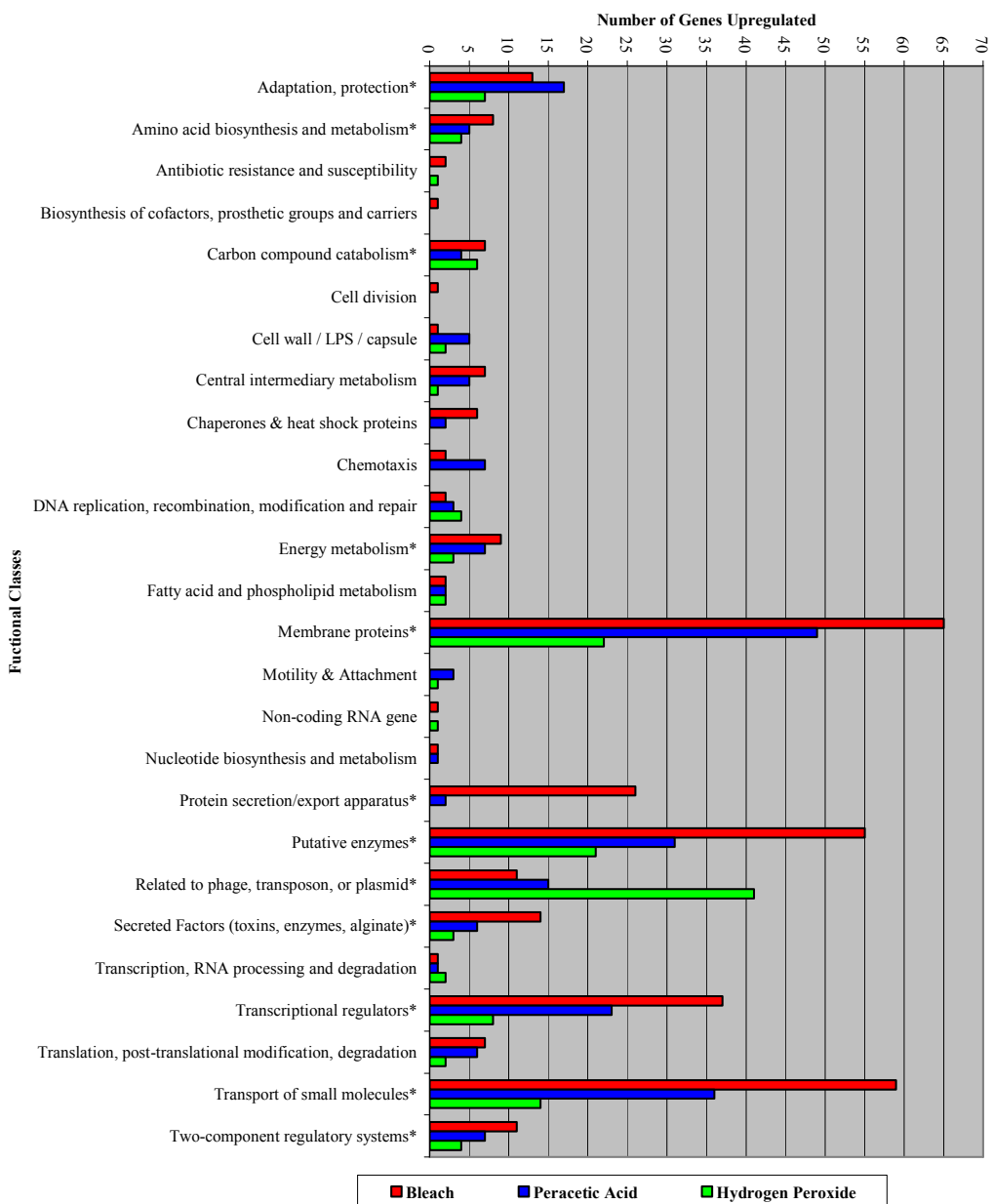


Figure 24: Functional classification of the number of genes with statistically significant increased mRNA levels

The number of genes are shown for each functional classification based on a ≥ 2 -fold increase in mRNA transcript level for 4.4 mM sodium hypochlorite (■), 0.5 mM peracetic acid (■), and 1 mM hydrogen peroxide (■) after a 20 min exposure to each corresponding disinfectant. The unions and intersections of the functional classes marked with an asterisk are further analyzed in Table 13.

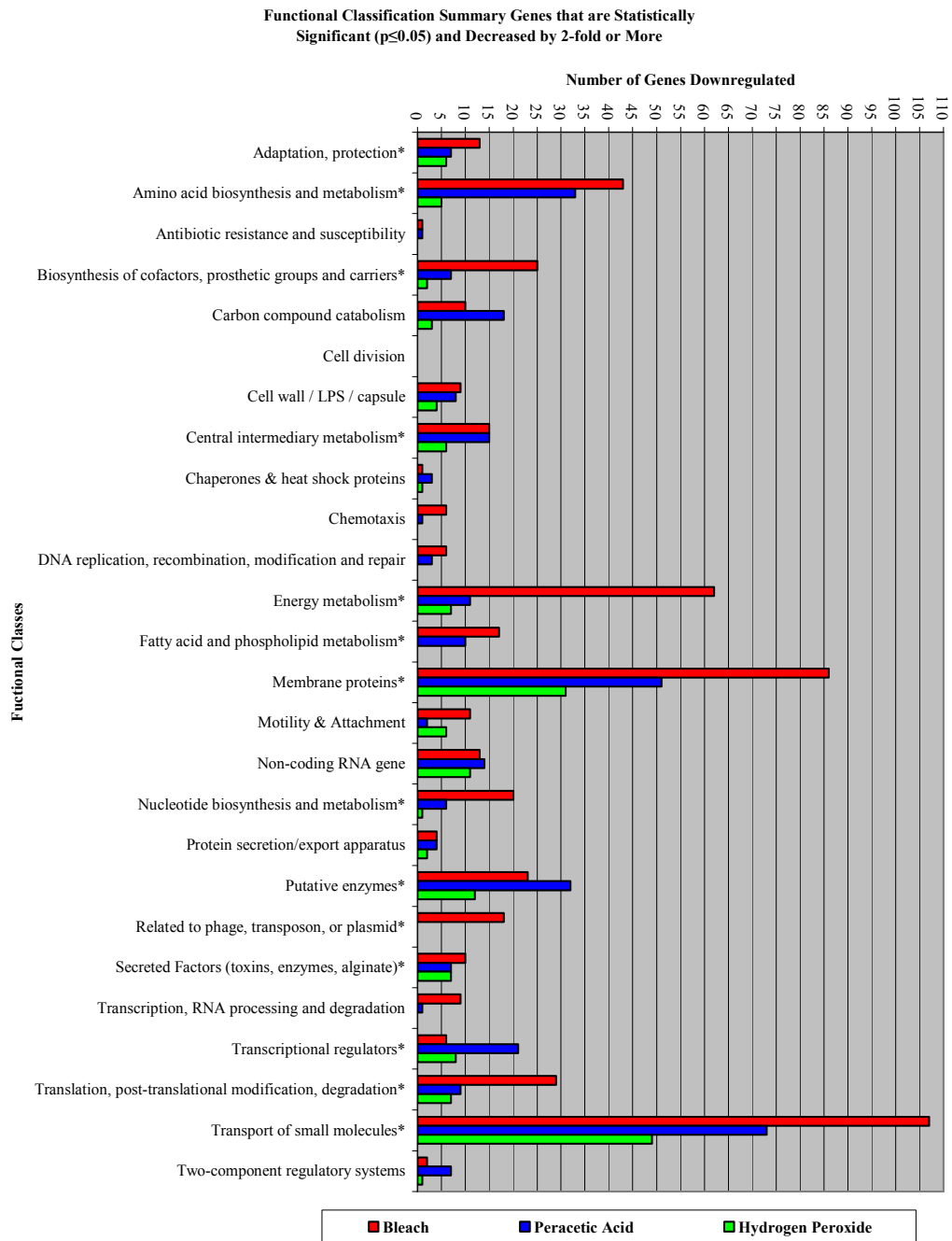


Figure 25: Functional classification of the number of genes with statistically significant decreased mRNA levels

The number of genes are shown for each functional classification based on a 2-fold or more decrease in mRNA transcript level for 4.4 mM sodium hypochlorite (■), 0.5 mM peracetic acid (■), and 1 mM hydrogen peroxide (■) after a 20 min exposure to each corresponding disinfectant. The unions and intersections of the functional classes marked with an asterisk are further analyzed in Table 14.

Table 13: Venn diagram data for functional classifications of statistically significant ≥ 2 -fold genes upregulated between sodium hypochlorite, peracetic acid, and hydrogen peroxide.

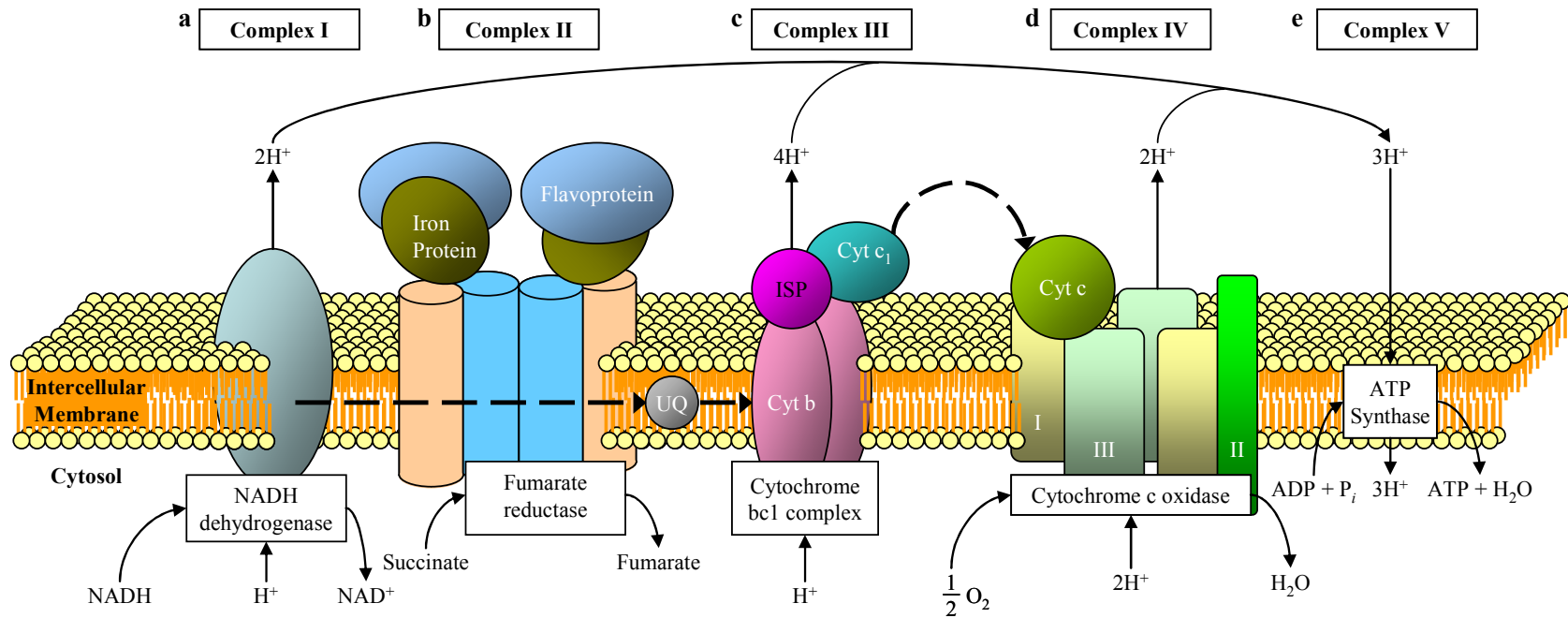
Region	Region 1	Region 2	Region 3	Region 4	Region 5	Region 6	Region 7
Disinfectant(s)	NaOCl	H ₂ O ₂	CH ₃ CO ₃ H	NaOCl H ₂ O ₂	NaOCl CH ₃ CO ₃ H	H ₂ O ₂ CH ₃ CO ₃ H	NaOCl H ₂ O ₂ CH ₃ CO ₃ H
Functional Classification	Number of Genes						
Adaption, protection	4	5	9	1	7	0	1
Amino acid biosynthesis and metabolism	4	3	2	1	3	0	0
Carbon compound catabolism	6	5	4	1	0	0	0
Energy metabolism	6	2	4	0	2	0	1
Membrane proteins	33	8	21	5	19	1	8
Protein secretion and export apparatus	24	0	0	0	2	0	0
Putative enzymes	40	15	18	2	9	0	4
Related to phage, transposon, or plasmid	0	29	3	0	0	1	11
Secreted factors (toxins, enzymes, alginate)	11	3	3	0	3	0	0
Transcriptional regulators	25	6	12	1	10	0	1
Transport of small molecules	36	6	19	6	15	0	2
Two-component systems	8	1	4	1	1	1	1

Table 14: Venn diagram data for functional classifications of statistically significant ≥ 2 -fold genes downregulated between sodium hypchlorite, peracetic acid, and hydrogen peroxide.

Region	Region 1	Region 2	Region 3	Region 4	Region 5	Region 6	Region 7
Disinfectant(s)	NaOCl	H ₂ O ₂	CH ₃ CO ₃ H	NaOCl H ₂ O ₂	NaOCl CH ₃ CO ₃ H	H ₂ O ₂ CH ₃ CO ₃ H	NaOCl H ₂ O ₂ CH ₃ CO ₃ H
Functional Classification	Number of Genes						
Adaption, protection	8	4	4	2	3	0	0
Amino acid biosynthesis and metabolism	20	3	12	2	21	0	0
Biosynthesis of cofactors, prosthetic groups and carriers	21	2	3	0	4	0	0
Central intermediary metabolism	5	5	6	1	9	0	0
Energy metabolism	49	2	2	4	8	0	1
Fatty acid and phospholipid metabolism	11	0	4	0	6	0	0
Membrane proteins	35	11	10	13	34	3	4
Nucleotide biosynthesis and metabolism	16	0	3	1	3	0	0
Putative enzymes	7	6	19	3	10	0	3
Related to phage, transposon, or plasmid	18	0	3	0	0	0	0
Secreted factors (toxins, enzymes, alginate)	2	1	4	5	2	0	1
Transcriptional regulators	2	8	17	1	4	0	0
Translation, post translational modification, degradation	23	4	4	1	3	0	2
Transport of small molecules	31	17	15	21	47	3	8

3.9. Metabolic pathway analysis

P. aeruginosa KEGG pathways were downloaded and imported into the GeneSpring GX genome software and visually inspected for changes based on the 3,197 genes from the 1-way ANOVA analysis. These metabolic pathways were compiled into tables to organize the data based on metabolic functions. The oxidative phosphorylation pathway genes were compiled and organized in Figure 26 and Table 16 based on the KEGG pathways (Ogata et al., 1999). The Entner-Doudoroff (ED) pathway and Embden-Meyerhof-Parnas (EMP) pathway were compiled and organized in to Figure 27 and Table 17 based on prior characterizations and genetic mappings (Roehl, Feary, & Phibbs, 1983; Roehl & Phibbs, 1982). ATP Binding Cassettes (ABC) for organic sulfur transport-related genes were compiled and organized in Table 18 based on the KEGG pathways (Ogata et al., 1999). Additionally, cellular protective mechanism-related genes, iron regulation-related genes and pyocin system-related genes were organized in Table 15, Table 19, Table 20, respectively based on prior studies of peracetic acid and hydrogen peroxide (W. Chang et al., 2005a, 2005b).



82

Figure 26: Oxidative phosphorylation and electron transport Pathways

Genes associated with oxidative phosphorylation and electron transport: **a.** NADH dehydrogenase subunits (Complex I), **b.** fumarate reductase and succinate dehydrogenase and all four subunits (Complex II) **c.** Complex III contains genes encoding iron-sulfur proteins, **d.** cytochrome c oxidases (Complex IV) and associated genes, **e.** Genes responsible for ATP synthase (Complex V).

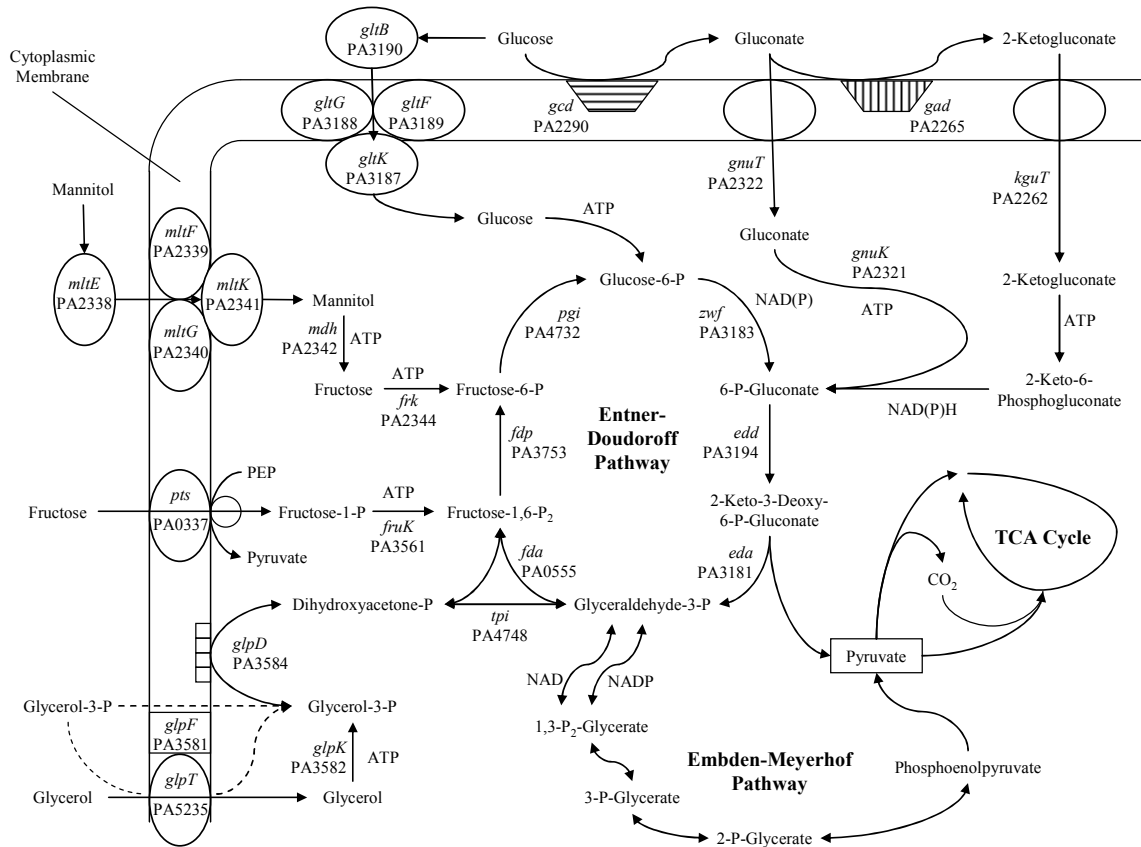


Figure 27: Entner-Doudoroff (ED) and Embden-Meyerhof-Parnas (EMP) pathways
 A compilation of the Entner-Doudoroff (ED) and Embden-Meyerhof-Parnas (EMP) pathways is shown here. The Tri Carboxylic Acid (TCA) pathway is also shown.

3.10. Hierarchical clustering

Hierarchical clustering was performed on the 3,197 genes from the 1-way ANOVA analysis for all of the conditions (four control group replicates, four sodium hypochlorite-exposed group replicates, four peracetic acid-exposed group replicates, and four hydrogen peroxide-exposed group replicates) using Genespring GX. The results of this analysis are shown in Figure 28. Based on these results, additional hierarchical clustering was done on function groups from the functional classifications (see Table 5) as follows: carbon compound catabolism (see Figure 29), energy metabolism (see Figure 30), membrane proteins (see Figure 31), related to phage, transposon, or plasmid (see Figure 32), and transport of small molecules (see Figure 33).

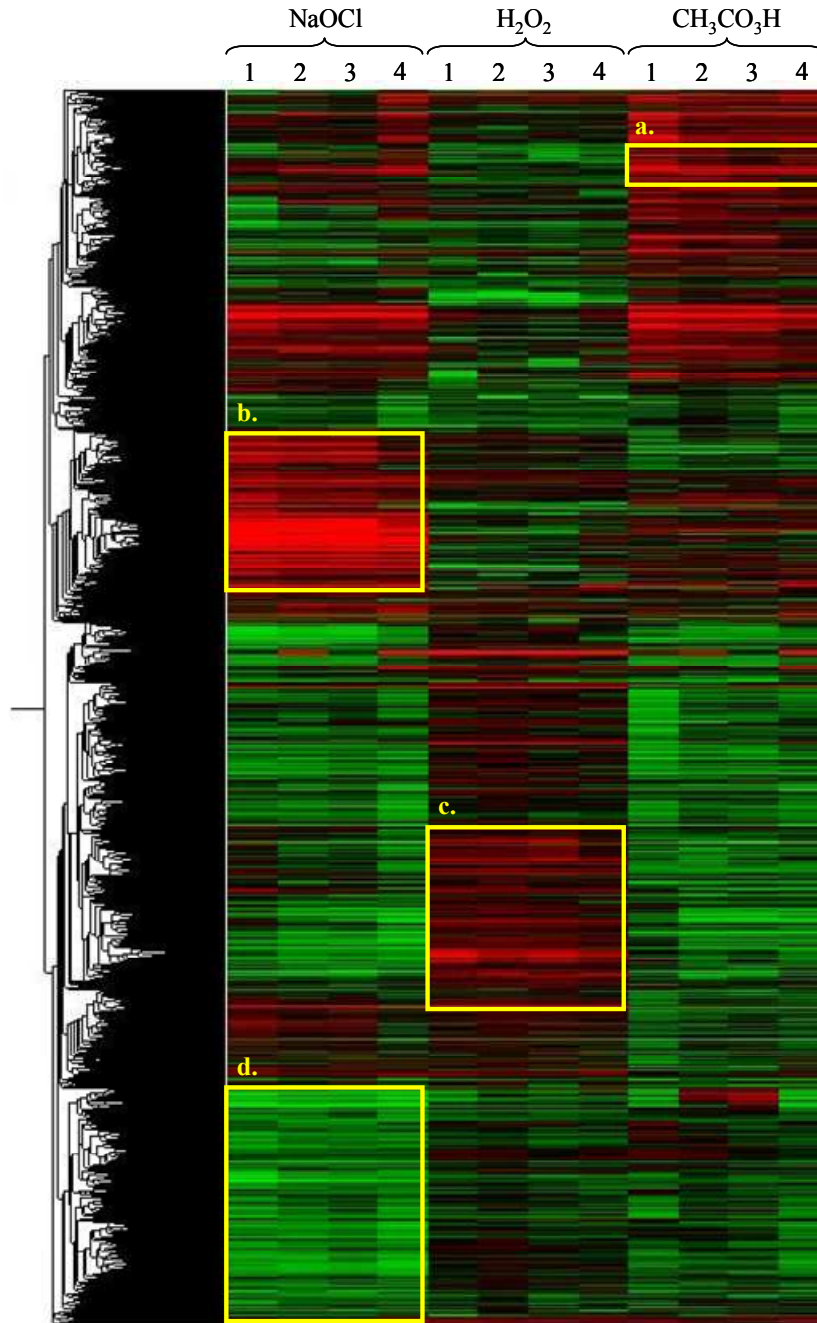


Figure 28: Hierarchical clustering of 1-way ANOVA genes

Hierarchical clustering results of the 3,197 statistically significant genes from the 1-way ANOVA. Four prominent clusters corresponded to results obtained from the metabolic pathway analysis: **a.** upregulation of glycerol transport and catabolism genes for peracetic acid-exposed samples, **b.** upregulation of organic sulfur transport and catabolism genes for sodium hypochlorite-exposed samples, **c.** upregulation of pyocin synthesis genes for the hydrogen peroxide-exposed samples, and **d.** downregulation of oxidative phosphorylation and electron transport genes for sodium hypochlorite-exposed samples.

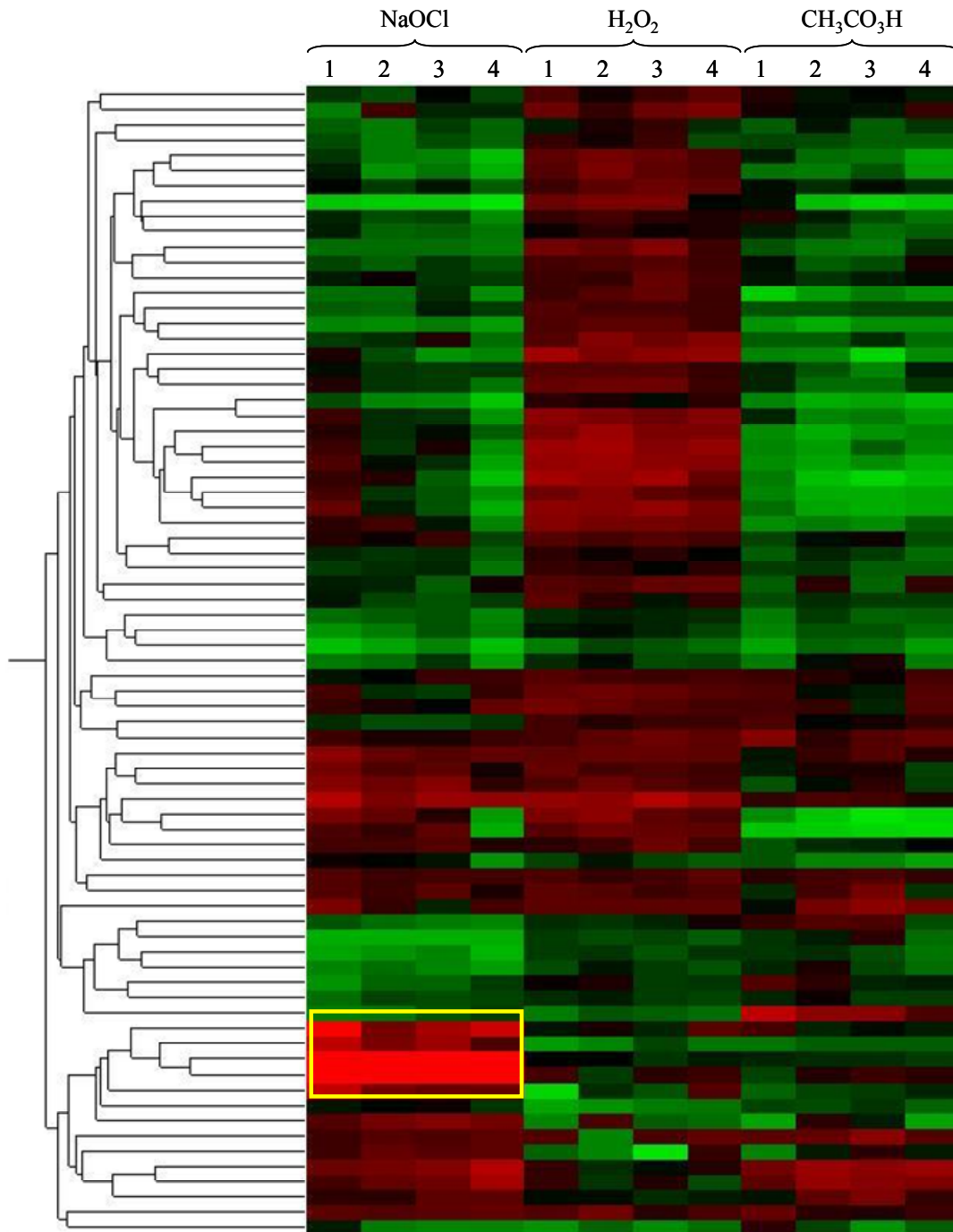


Figure 29: Hierarchical clustering of “carbon compound catabolism” functional class genes

Hierarchical clustering results of the 172 genes in the “carbon compound catabolism” functional class from Table 5. The yellow boxed area highlights the upregulated organic sulfur catabolism genes in the sodium hypochlorite-exposed samples. These genes are not as severely affected in the hydrogen peroxide-exposed or peracetic acid-exposed samples.

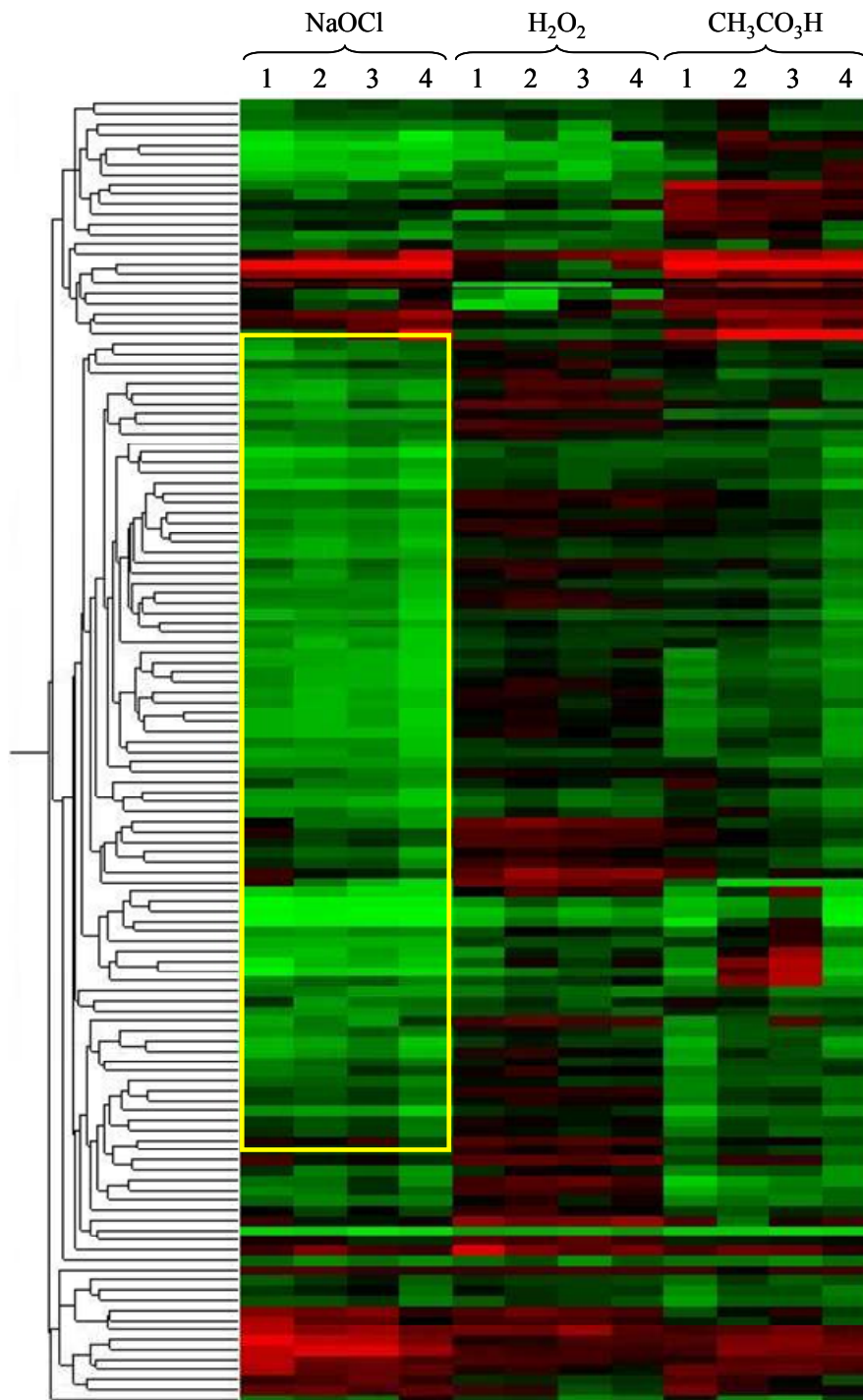


Figure 30: Hierarchical clustering of “energy metabolism” functional class genes
 Hierarchical clustering results of the 207 genes in the “energy metabolism” functional class from Table 5. The yellow boxed area highlights the downregulated oxidative phosphorylation and electron transport genes in the sodium hypochlorite-exposed samples. Most of these genes are not as severely affected in the hydrogen peroxide-exposed or peracetic acid-exposed samples.

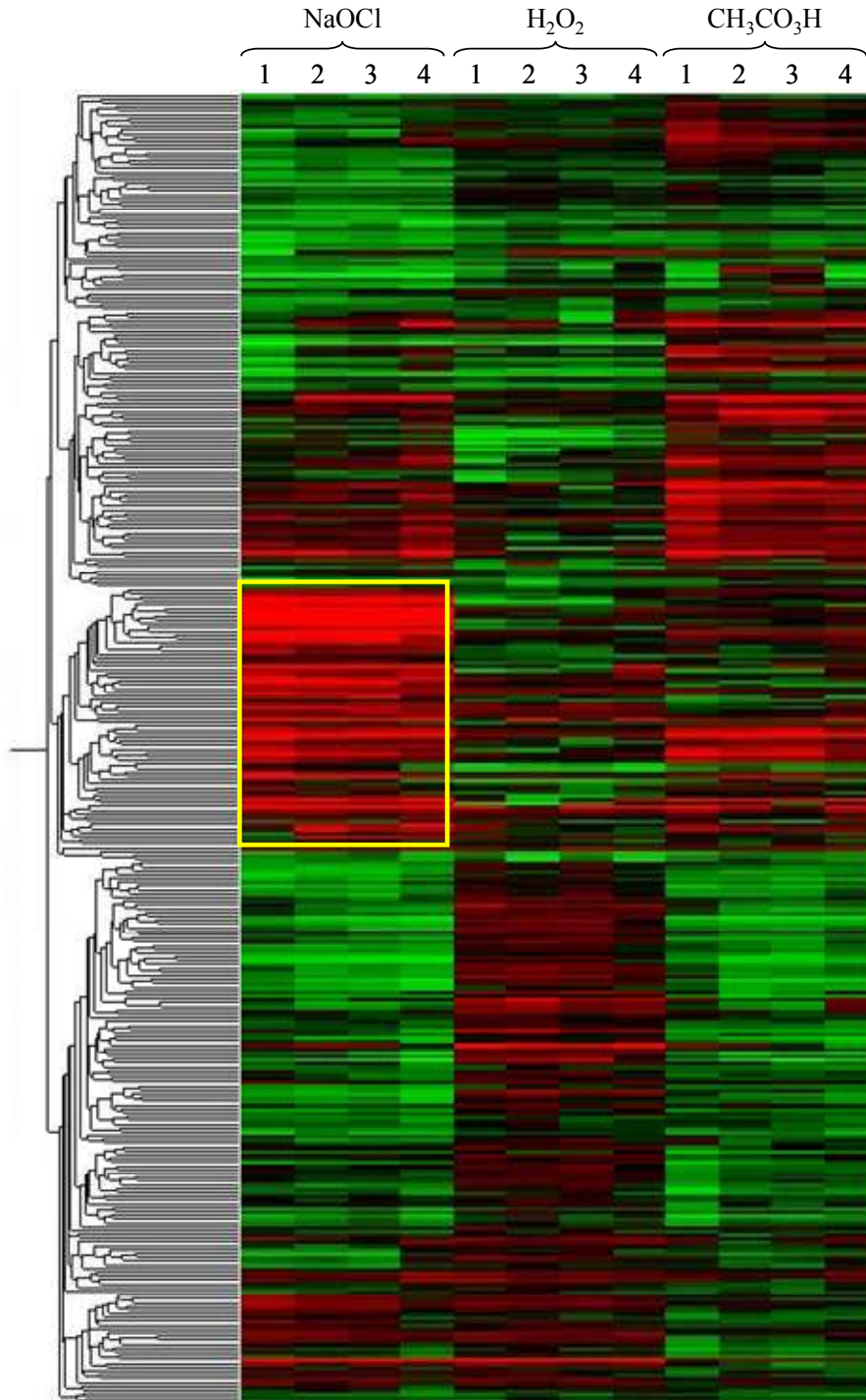


Figure 31: Hierarchical clustering of the “membrane proteins” functional class genes

Hierarchical clustering results of the 684 genes in the “membrane proteins” functional class from Table 5. The yellow boxed area highlights the upregulated organic sulfur transport genes in the sodium hypochlorite-exposed samples. Most of these genes are downregulated in the hydrogen peroxide-exposed or peracetic acid-exposed samples.

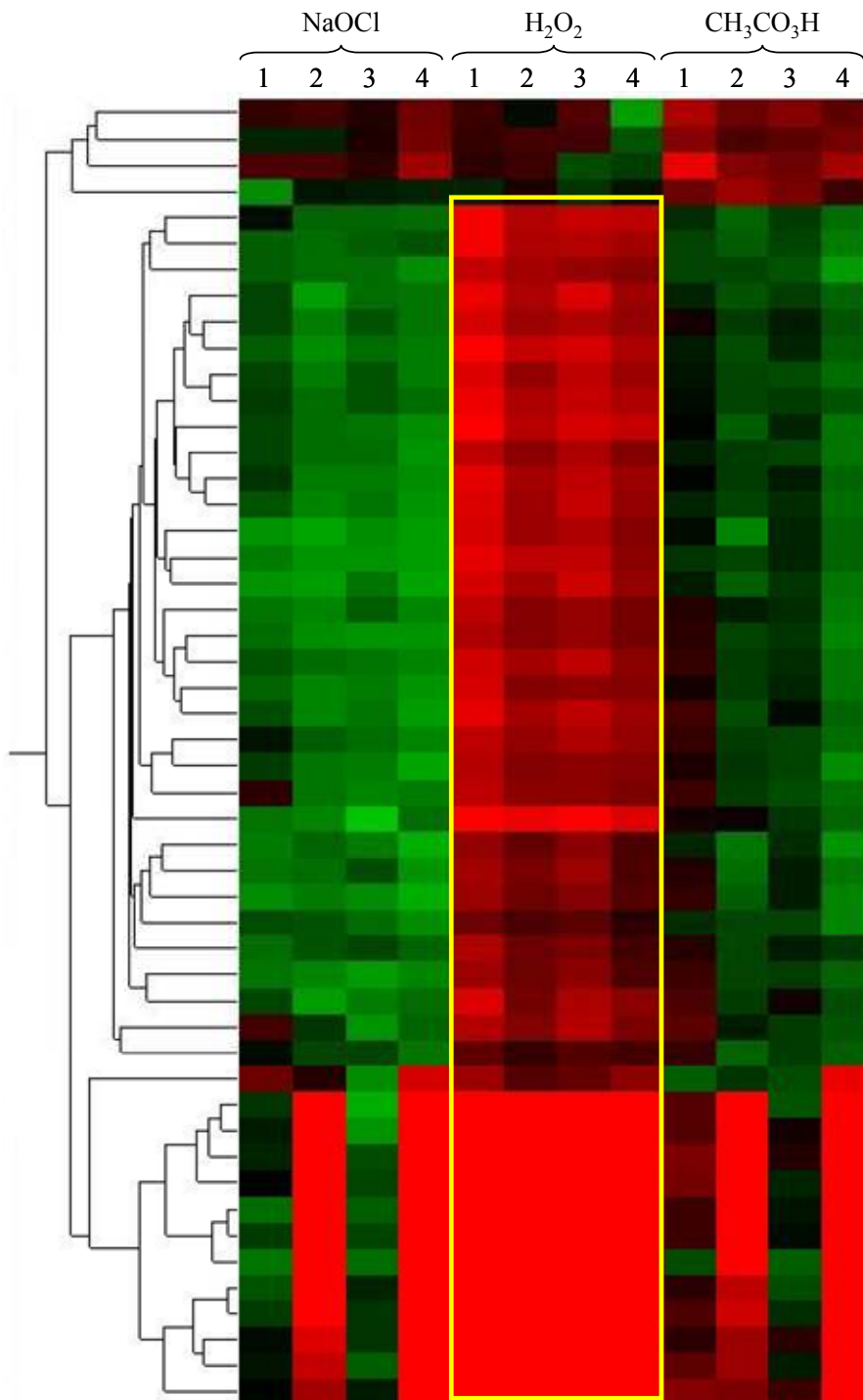


Figure 32: Hierarchical clustering of the “related to phage, transposon, or plasmid” functional class genes

Hierarchical clustering results of the 58 genes in the “related to phage, transposon, or plasmid” functional class from Table 5. The yellow boxed area highlights the upregulated pyocin genes in the hydrogen peroxide-exposed samples. Most of these genes are downregulated in the sodium hypochlorite-exposed or peracetic acid-exposed samples.

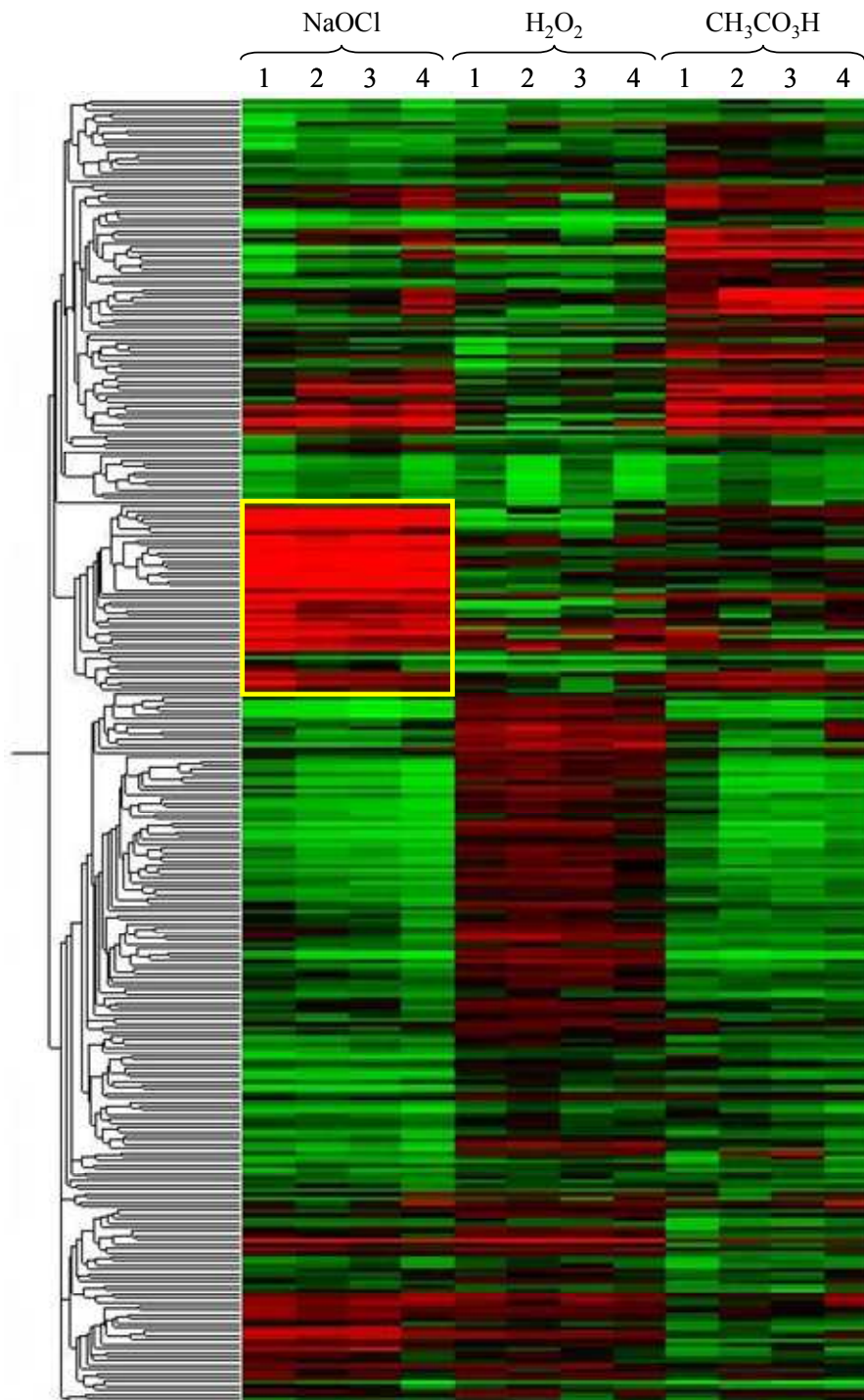


Figure 33: Hierarchical clustering of the “transport of small molecules” functional class genes

Hierarchical clustering results of the 593 genes in the “transport of small molecules” functional class from Table 5. The yellow boxed area highlights the upregulated organic sulfur transport genes in the sodium hypochlorite-exposed samples. These genes are not upregulated in the hydrogen peroxide-exposed or peracetic acid-exposed samples.

3.11. Principal component analysis (PCA)

The PCA was performed on the 3,197 genes from the 1-way ANOVA analysis for all of the conditions (four control group replicates, four sodium hypochlorite-exposed group replicates, four peracetic acid-exposed group replicates, and four hydrogen peroxide-exposed group replicates) using Genespring GX 7.0 centering. The results of this analysis are shown in Figure 34. Based on the 87.28% variance calculated by the PCA analysis, PCA component 1 had an eigenvalue of 770.2 and 56.12% of the variance, PCA component 2 had an eigenvalue of 246.2 and 17.94% of the variance, and PCA component 3 had an eigenvalue of 171.0 and 12.22% of the variance.

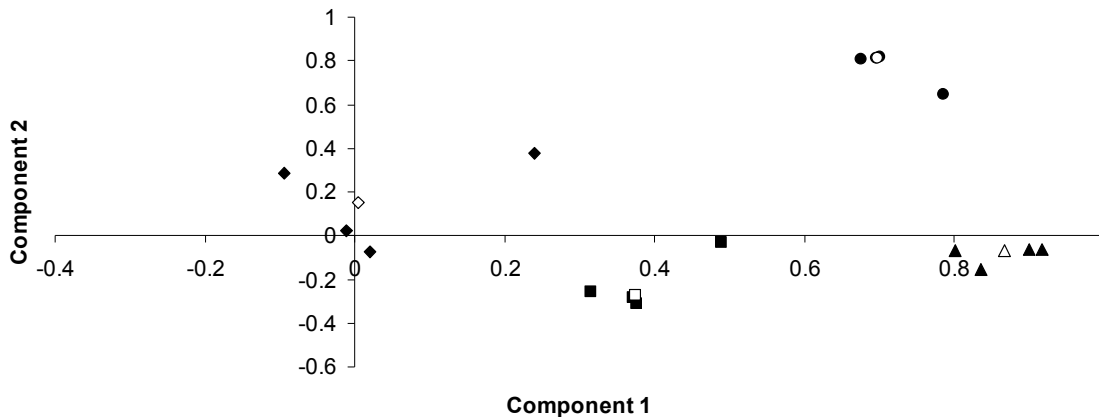


Figure 34: Principal component analysis (PCA) scatter plot of principal component 1 vs. principal component 2.

PCA component analysis on conditions: control group (◆), sodium hypochlorite-exposed samples (▲), peracetic-acid exposed samples (●), and hydrogen peroxide-exposed samples (■) in two dimensions (2-D) based on the 3,197 statistically significant genes from the 1-way ANOVA analysis. The median values of the control group (◇), sodium hypochlorite-exposed samples (△), peracetic-acid exposed samples (○), and hydrogen peroxide-exposed samples (□) are also shown on this scatter plot. All of the respective replicate treatments clearly group in to four distinct areas based on the PCA Component 1 that accounts for 56.12% of the variance between the samples and PCA Component 2 that accounts for the next 17.94% of the variance between the samples.

Chapter 4: Discussion

4.1. Overview

Based on the 1-way ANOVA statistically significant 2-fold or more gene expression changes, sodium hypochlorite had more upregulated or downregulated genes than either hydrogen peroxide-exposed samples or peracetic acid-exposed samples. The hydrogen peroxide-exposed samples had the fewest number of 2-fold or more upregulated and downregulated genes. This same comparative pattern was observed in the functional classification analysis.

All of the treatments showed an increase in the adaptive/protective processes. Sodium hypochlorite exposure resulted in a downregulation in oxidative phosphorylation and electron transport gene expression, while the gene expression for carbon compound catabolism was downregulated and the gene expression for organic sulfur transport was upregulated. Hydrogen peroxide and peracetic acid exposure did not reveal the same patterns of gene expression. However, exposure to peracetic acid resulted in changes in the expression of the glycerol transport and catabolism genes, while exposure to hydrogen peroxide resulted in changes in iron regulation and pyocin synthesis genes.

The hierarchical clustering analysis confirmed the above observations by displaying the data in color-coded dendrograms. The PCA on conditions reduced the dimensionality of the data and effectively characterized the main trends in the data by decomposing the samples into a 2-D or 3-D space. However, both analyses, particularly

the hierarchical clustering analysis, would be even more informative with the addition of more time points (i.e. time-course data).

4.2. Functional classification analysis

Using Venn diagram analysis of the functional classes revealed that sodium hypochlorite indeed does have more uniquely upregulated and downregulated genes for all of the functional classes listed above (see Table 13 and Table 14), except in the “Related to phage, transposon, or plasmid” functional class, where the hydrogen peroxide-exposed samples had more than twice as many gene upregulated than sodium hypochlorite-exposed or peracetic acid-exposed samples. The number of upregulated and downregulated genes for the peracetic acid-exposed samples generally fell in between the highly-affected sodium hypochlorite-exposed and the minimally-affected hydrogen peroxide-exposed samples in either the overall 2-fold or more change analysis and the functional classification analysis. However, peracetic acid-exposed samples had more upregulated genes in the “Adaption, protection” functional class and more downregulated genes in the “Transcriptional regulators” functional classification.

4.3. Adaptive/protective processes

Genes encoding several cellular protective mechanisms were highly upregulated in the hydrogen peroxide-exposed samples (see Table 15). The catalase gene, *katA* (PA4236) did not show a significant upregulation for all three treatments which supports a prior suggestion that *katA* serves as a housekeeping catalase gene (Brown, Howell, Vasil, Anderson, & Hassett, 1995; Elkins, Hassett, Stewart, Schweizer, & McDermott,

1999; Ochsner, Vasil, Alsabbagh, Parvatiyar, & Hassett, 2000). However, the catalase gene, *katB* (PA4613) was upregulated 7-fold in the sodium hypochlorite-exposed samples, 4-fold in the peracetic acid-exposed, and hydrogen-peroxide exposed samples. This result corroborates the necessity of *katB* expression for optimal hydrogen peroxide resistance (Brown et al., 1995; Elkins et al., 1999). The super oxide dismutase enzymes *sodB* (PA4366) and *sodM* (PA4468) did not show a significant upregulation or downregulation in any of the treatments. However the transcript raw signal intensities of *sodM* were among the highest for all of the treatments as well as the control samples (3,524 for sodium hypochlorite, 1,276 for peracetic acid, 1,834 for hydrogen peroxide, and 1923 for the control), thus suggesting that *sodB* gene expression may be considerable during standard aerobic growth conditions (Hassett, Schweizer, & Ohman, 1995). Several DNA repair-related genes were highly induced after hydrogen peroxide-exposure, but were minimally upregulated in the sodium hypochlorite-exposed and peracetic acid-exposed samples. The DNA repair protein, *recN* (PA4763) was the exception since it was upregulated after all three treatments, even though it was upregulated much more so in the hydrogen peroxide-exposed samples. These results again correspond with prior studies establishing DNA damage as a result of hydrogen peroxide exposure (Keyer, Gort, & Imlay, 1995; Martinez & Kolter, 1997; Miller & Britigan, 1997), however sodium hypochlorite and peracetic acid exposure do not seem to result in the same DNA damage.

Table 15: Comparison of cellular protective mechanism-related gene expression for sodium hypochlorite, peracetic acid, and hydrogen peroxide exposed *P. aeruginosa*.

Gene Number	Gene Name	Gene Description	NaOCl	CH ₃ CO ₃ H	H ₂ O ₂
PA0669		probable DNA polymerase alpha chain	+1.21	-1.04	+3.08
PA3007	<i>lexA</i>	repressor protein LexA	+1.62	+1.42	+4.15
PA3008		hypothetical protein	+1.69	+1.27	+5.82
PA3413	<i>yebG</i>	conserved hypothetical protein	+1.42	+1.70	+4.35
PA3414		hypothetical protein	+1.58	+2.26	+9.96
PA3616	<i>recX</i>	conserved hypothetical protein	-1.03	+1.14	+2.84
PA3617	<i>recA</i>	RecA protein	-1.05	-1.08	+2.74
PA4236	<i>katA</i>	catalase	+1.46	+1.51	+1.88
PA4366	<i>sodB</i>	superoxide dismutase	-1.14	-1.81	-1.06
PA4468	<i>sodM</i>	superoxide dismutase	+1.11	+1.62	+1.49
PA4613	<i>katB</i>	catalase	+7.20	+3.99	+4.08
PA4763	<i>recN</i>	DNA repair protein RecN	+2.03	+2.06	+8.78

4.4. Oxidative phosphorylation and electron transport

The oxidative phosphorylation pathway analysis expanded upon the “Energy metabolism”, “Membrane proteins”, and “Putative enzymes” functional classes analysis. The large downregulation of the “Energy metabolism” functional class for sodium hypochlorite-exposed samples correlated with the 2-fold or more decrease in the genes related oxidative phosphorylation (see Figure 26 and Table 16). After sodium hypochlorite exposure, the following downregulations were observed: NADH dehydrogenase genes in Complex I (*nuo* operon) were uniformly downregulated by 3-fold, fumarate reductase genes and all associated genes in Complex II (*sdh* operon) were similarly all downregulated (~2.5-fold), genes in the cytochrome bc₁ complex (Complex III) were downregulated from 2- to 18-fold, and cytochrome c oxidase and associated Complex IV genes (*cyo* operon) were all downregulated 2- to 22-fold. However, the peracetic acid-exposed and hydrogen peroxide-exposed samples did not show the same degree of downregulation of these genes. The transcriptional downregulation of these

genes for the sodium hypochlorite-exposed samples suggested that both oxidative phosphorylation and the electron transport chain were significantly and uniformly downregulated, perhaps resulting in a minimal energy production by these principal metabolic pathways after exposure. This uniform downregulation in the sodium hypochlorite-exposed samples is consistent with prior studies that demonstrated a decrease in respiratory function after hypochlorous acid-exposure (Albrich & Hurst, 1982; Albrich, McCarthy, & Hurst, 1981; Dukan & Touati, 1996). Additionally, sulfhydryls and membrane-bound methionine residues have been shown to be particularly sensitive to oxidation by HOCl (Schraufstatter *et al.*, 1990).

Table 16: Comparison of genes related to oxidative phosphorylation for sodium hypochlorite, peracetic acid, and hydrogen peroxide exposed *P. aeruginosa*.

Complex I, NADH Dehydrogenase I (<i>nuo</i> operon from PA2637 to PA2649)					
Gene Number	Gene Name	Gene Description	NaOCl	CH₃CO₃H	H₂O₂
PA2637	<i>nuoA</i>	NADH Dehydrogenase I chain A	-2.21	-1.69	-1.81
PA2638	<i>nuoB</i>	NADH Dehydrogenase I chain B	-3.08	-2.35	-1.23
PA2639	<i>nuoD</i>	NADH Dehydrogenase I chain C, D	-2.92	-2.02	-1.22
PA2640	<i>nuoE</i>	NADH Dehydrogenase I chain E	-2.70	-1.80	+1.07
PA2641	<i>nuoF</i>	NADH Dehydrogenase I chain F	-2.72	-1.78	-1.20
PA2642	<i>nuoG</i>	NADH Dehydrogenase I chain G	-3.07	-1.69	+1.04
PA2643	<i>nuoH</i>	NADH Dehydrogenase I chain H	-3.08	-1.58	-1.05
PA2644	<i>nuoI</i>	NADH Dehydrogenase I chain I	-3.48	-1.89	1.00
PA2645	<i>nuoJ</i>	NADH Dehydrogenase I chain J	-3.48	-1.93	-1.32
PA2646	<i>nuoK</i>	NADH Dehydrogenase I chain K	-3.39	-1.99	-1.15
PA2647	<i>nuoL</i>	NADH Dehydrogenase I chain L	-3.86	-1.95	-1.11
PA2648	<i>nuoM</i>	NADH Dehydrogenase I chain M	-3.62	-1.96	-1.07
PA2649	<i>nuoN</i>	NADH Dehydrogenase I chain N	-3.75	-1.73	-1.04

Complex II, Fumarate Reductase (<i>sdh</i> operon from PA1581 to PA1584)					
Gene Number	Gene Name	Gene Description	NaOCl	CH₃CO₃H	H₂O₂
PA1581	<i>sdhC</i>	Fumarate Reductase C subunit	-2.56	-1.68	-1.17
PA1582	<i>sdhD</i>	Fumarate Reductase D subunit	-2.40	-1.43	-1.01
PA1583	<i>sdhA</i>	Fumarate Reductase A subunit	-2.44	-1.30	-1.08
PA1584	<i>sdhB</i>	Fumarate Reductase B subunit	-2.44	-1.39	-1.27

Complex III, Cytochrome bc1 Complex					
Gene Number	Gene Name	Gene Description	NaOCl	CH₃CO₃H	H₂O₂
PA4131		probable iron-sulfur protein	-17.79	-8.77	-2.22
PA4429		probable cytochrome c1 precursor	-3.46	-1.73	-1.84
PA4430		probable cytochrome b	-3.44	-1.95	-1.41
PA4431		probable iron-sulfur protein	-2.28	-1.53	1.08

Complex IV, Cytochrome c Oxidase (<i>cyo</i> operon from PA1317 to PA1321)					
Gene Number	Gene Name	Gene Description	NaOCl	CH₃CO₃H	H₂O₂
PA1317	<i>cyoA</i>	ubiquinol oxidase subunit II	-5.59	+1.45	-2.63
PA1318	<i>cyoB</i>	ubiquinol oxidase subunit I	-3.57	+1.03	-2.64
PA1319	<i>cyoC</i>	ubiquinol oxidase subunit III	-4.12	+1.01	-2.09
PA1320	<i>cyoD</i>	ubiquinol oxidase subunit IV	-5.29	+1.13	-2.05
PA1321	<i>cyoE</i>	ubiquinol oxidase protein CyoE	-2.53	+1.08	-1.98
PA1552		probable cytochrome c	-4.85	-1.90	-1.52
PA1553		cytochrome c oxidase subunit	-4.63	-1.88	-1.38
PA1554		subunit (cbb3-type)	-3.85	-2.23	-1.28
PA1555		probable cytochrome c	-12.58	-2.46	-1.36
PA1556		cytochrome c oxidase subunit	-14.47	-2.46	-1.94
PA1557		cytochrome oxidase subunit	-21.65	-3.11	-1.91
PA4133		subunit (cbb3-type)	-5.05	-4.50	-2.12

4.5. Entner-Doudoroff (ED) pathway and Embden-Meyerhof-Parnas (EMP) pathway analysis

The ED pathway and EMP pathway analysis also suggested that genes encoding carbon substrate catabolization during oxidative phosphorylation were affected by the disinfectant treatments (see Figure 27 and Table 17). This pathway analysis also expanded upon the “Carbon compound catabolism”, “Central intermediary metabolism”, “Energy metabolism”, “Membrane protein”, and “Transport of small molecules” functional class analyses. The genes encoding the proteins that actively transport hexose molecules (glucose, maltose, gluconate, 2-ketogluconate, fructose, and glycerol) into the cell were downregulated for sodium hypochlorite-exposed samples. The genes that encode the transport of glucose (PA3186 to PA3190) across the periplasmic and cytoplasmic membranes were highly downregulated, and prior studies have shown glucose uptake to be inhibited after low concentrations of hypochlorous acid-exposure (Schraufstatter et al., 1990). The OprB porin (PA3186) is described more appropriately as a carbohydrate-selective porin since it facilitates the diffusion of a wide range of carbohydrates across the outer membrane in addition to glucose (Wylie & Worobec, 1995).

The genes encoding the same enzymes for these metabolites seemed unaffected by hydrogen peroxide exposure. However, peracetic acid-exposed samples showed a similar but smaller magnitude of downregulation in the glucose transporter genes. The sodium hypochlorite-exposed and hydrogen peroxide-exposed samples did not show a significant upregulation of the glycerol or glycerol-3-phosphate transporter genes which corresponded to studies that showed glyceraldehyde-3-phosphate dehydrogenase was

inactivated by both oxidative stressors (Schraufstatter et al., 1990). Additionally, the genes encoding glycerol and possibly glycerol-3-phosphate (PA3581, PA5235) showed a strong upregulation after peracetic-acid exposure. The genes that code for the enzymes that catabolize glycerol, glycerol kinase (*glpK*, PA3582) and that catabolizes glycerol-3-phosphate, glycerol-3-phosphate dehydrogenase (*glpD*, PA3584) were also strongly upregulated after peracetic acid exposure. This suggested that glycerol and glycerol-3-phosphate may be a preferred substrate for growth as a result of peracetic-acid-exposure. Indeed, prior studies have shown that glycerol and glycerol-3-phosphate are utilized as substrates for *P. aeruginosa* and *E. coli* growth and were regulated by the potent feedback inhibition of fructose-1,6-diphosphate (Lessie & Phibbs, 1984; Lin, 1976; McCowen, Sellers, & Phibbs, 1986). Additionally, *glpK* and *glpD* expression and activity are known to occur only when glycerol is utilized as a substrate for growth (McCowen, Phibbs, & Feary, 1981). Furthermore, the Mg²⁺ transporter genes, *mgtA* (PA4825) was upregulated 6-fold and *mgtC* (PA4635) was upregulated 4-fold, and could very well account for the excess Mg²⁺ ion required for glycerol kinase (*glpk*, PA3582) activity (McCowen et al., 1986; Snavely, Miller, & Maguire, 1991).

Table 17: Comparison of Entner-Doudoroff (ED) pathway and Embden-Meyerhof-Parnas (EMP) pathway gene expression for sodium hypochlorite, peracetic acid, and hydrogen peroxide exposed *P. aeruginosa*.

Gene Number	Gene Name	Gene Description	NaOCl	CH ₃ CO ₃ H	H ₂ O ₂
PA0337	<i>pts</i>	phosphotransferase system	+1.11	-1.39	+1.36
PA0555	<i>fda</i>	fructose-1,6-diphosphate aldolase	NSS	NSS	NSS
PA2262	<i>kguT</i>	probable 2-ketogluconate transporter	-1.92	-1.10	+1.23
PA2265	<i>gad</i>	gluconate dehydrogenase	-1.88	+1.13	-1.16
PA2290	<i>gcd</i>	glucose dehydrogenase	-2.95	-1.12	-1.31
PA2321	<i>gnuK</i>	glucokinase	-1.33	+2.92	-1.41
PA2322	<i>gnuT</i>	gluconate permease	-2.57	+1.74	-1.11
PA2338	<i>mtlE</i>	maltose/mannitol ABC binding protein	Absent	Absent	Absent
PA2339	<i>mtlF</i>	maltose/mannitol ABC permease protein	Absent	Absent	Absent
PA2340	<i>mtlG</i>	maltose/mannitol ABC permease protein	NSS	NSS	NSS
PA2341	<i>mtlK</i>	maltose/mannitol ABC ATP-binding protein	NSS	NSS	NSS
PA2342	<i>mtlD</i>	mannitol dehydrogenase	Absent	Absent	Absent
PA2344	<i>frk</i>	fructokinase	NSS	NSS	NSS
PA3181	<i>eda</i>	2-keto-3-deoxy-6-phosphogluconate adolase	+1.86	+2.04	-1.15
PA3183	<i>zwf</i>	glucose-6-phosphate dehydrogenase	+1.86	+2.07	-1.15
PA3186	<i>oprB</i>	outer membrane porin OprB precursor	-4.08	-1.94	-1.37
PA3187	<i>gltK</i>	glucose ABC ATP-binding protein	-7.25	-3.31	+1.25
PA3188	<i>gltG</i>	glucose ABC permease protein	-12.94	-5.95	+1.10
PA3189	<i>gltF</i>	glucose ABC permease protein	-17.15	-5.21	+1.37
PA3190	<i>gltB</i>	glucose ABC binding protein	-10.56	-4.00	+1.67
PA3194	<i>edd</i>	6-phosphogluconate dehydratase	NSS	NSS	NSS
PA3561	<i>fruK</i>	fructose-1-phosphate kinase	-1.40	+1.23	+1.07
PA3581	<i>glpF</i>	glycerol uptake facilitator protein	+1.14	+7.33	-2.37
PA3582	<i>glpK</i>	glycerol kinase	+1.13	+6.06	-1.96
PA3584	<i>glpD</i>	glycerol-3-phosphate dehydrogenase	+1.36	+13.08	-1.57
PA3753	<i>fdp</i>	fructose-1,6-diphosphate aldolase	NSS	NSS	NSS
PA4732	<i>pgi</i>	phosphoglucoisomerase	-1.26	-1.39	+1.12
PA4748	<i>tpi</i>	triphosphate isomerase	NSS	NSS	NSS
PA5235	<i>glpT</i>	glycerol transport protein	-2.24	+4.40	-3.19

*NNS = not statistically significant

**Absent = gene was not detected on the microarray

4.6. Organic sulfur ATP Binding Cassettes (ABC)

The sodium hypochlorite-exposed samples had a strong upregulation of genes responsible for organic sulfur transport and the associated genes that catabolize these compounds (see Table 18). The genes encoding the alkanesulfonate transport system (PA3441 to PA3446) contained the most highly upregulated genes after sodium hypochlorite-exposure and were not drastically upregulated or downregulated in the peracetic acid-exposed or hydrogen peroxide-exposed samples. *P. aeruginosa* has been known to use *n*-alkanesulfonates or taurine as sources for both carbon and organic sulfur (van der Ploeg *et al.*, 1996). Typically, the *ssuD* (PA3444) and *ssuE* (PA3446) genes are expressed during sulfate or cysteine starvation (Eichhorn, van der Ploeg, & Leisinger, 1999). This result may suggest the following: that the sulfur in these compounds was required due to sulfur starvation caused by the reaction of the HOCl with sulfhydryl groups, that the carbon compound skeletons of the *n*-alkanesulfonates were being used in lieu of the carbon compounds contained in the hexose transporters of the ED pathway, or that the neutrphilic amines and alpha-amino acids formed by catabolization of the *n*-alkanesulfonates may guard the cell against oxidative stress and attack from hypochlorous acid (HOCl).

The genes encoding enzymes responsible for the taurine transport system (PA3935 to PA3938) exhibited the second most highly upregulation after sodium hypochlorite-exposure and again were not drastically upregulated or downregulated in the peracetic acid-exposed or hydrogen peroxide-exposed samples. The *tauD* (PA3935) gene had a 10-fold increase and is required for the catabolization of taurine to sulfite, but has previously been shown to only be expressed under conditions of sulfate starvation

(Eichhorn, van der Ploeg, Kertesz, & Leisinger, 1997; van der Ploeg et al., 1996). Prior studies have demonstrated that taurine alone can be used as a sole source of carbon and sulfur in *P. aeruginosa* (Shimamoto & Berk, 1979, 1980a, 1980b). Taurine has also been known to scavenge HOCl by forming *N*-chlorotaurine which has greater stability and less toxicity than the HOCl moiety (Grisham, Jefferson, Melton, & Thomas, 1984; Harrison, Watson, & Schultz, 1978; Weiss, Klein, Slivka, & Wei, 1982), and the *N*-chlorotaurine molecule has been shown to degrade to sulphaacetaldehyde in response to oxidative stress (Cunningham, Tipton, & Dixon, 1998). This may suggest the following: that the sulfur in the taurine was required due to sulfur starvation caused by the reaction of the HOCl with sulfhydryl groups, that the aldehyde carbon compounds were being utilized instead of the carbon compounds contained in the hexose transporters of the ED pathway, or that the taurine stabilized the highly destructive HOCl by providing a less damaging pathway to degrade this compound.

The genes encoding proteins responsible for sulfate ester transporters (PA0183 to PA0186, PA2307 to PA2310) also had an upregulation after sodium hypochlorite-exposure, and again were not drastically upregulated or downregulated in the peracetic acid-exposed or hydrogen peroxide-exposed samples. The arylsulfatase gene, *atsA* (PA0183) was upregulated almost 4-fold in the sodium hypochlorite-exposed samples. This gene has been associated with the sulfur starvation-induced proteins and has been used as a model system for the sulfate starvation response (Hummerjohann et al., 1998; Hummerjohann, Laudenbach, Retey, Leisinger, & Kertesz, 2000; Quadroni, James, Dainese-Hatt, & Kertesz, 1999). The α -ketoglutarate-dependent dioxygenase gene, *atsK* (PA2310) was upregulated almost 18-fold in the sodium hypochlorite exposed samples.

The *atsK* enzyme catalyzes the oxidative conversion of α -ketoglutarate cofactor into CO₂, succinate, and highly reactive ferryl (IV) species and is known to have a 38% amino acid homology to *tauD* (Kahnert & Kertesz, 2000; Muller, Stuckl, Wakeley, Kertesz, & Uson, 2005). Since these genes were strongly upregulated in the sodium hypochlorite-exposed samples and not the hydrogen-peroxide exposed or peracetic acid-exposed samples, the *atsA* and *atsK* encoded enzymes may have directly reacted with the HOCl or performed side reactions to help mediate the oxidative stress caused by hypochlorous acid-exposure.

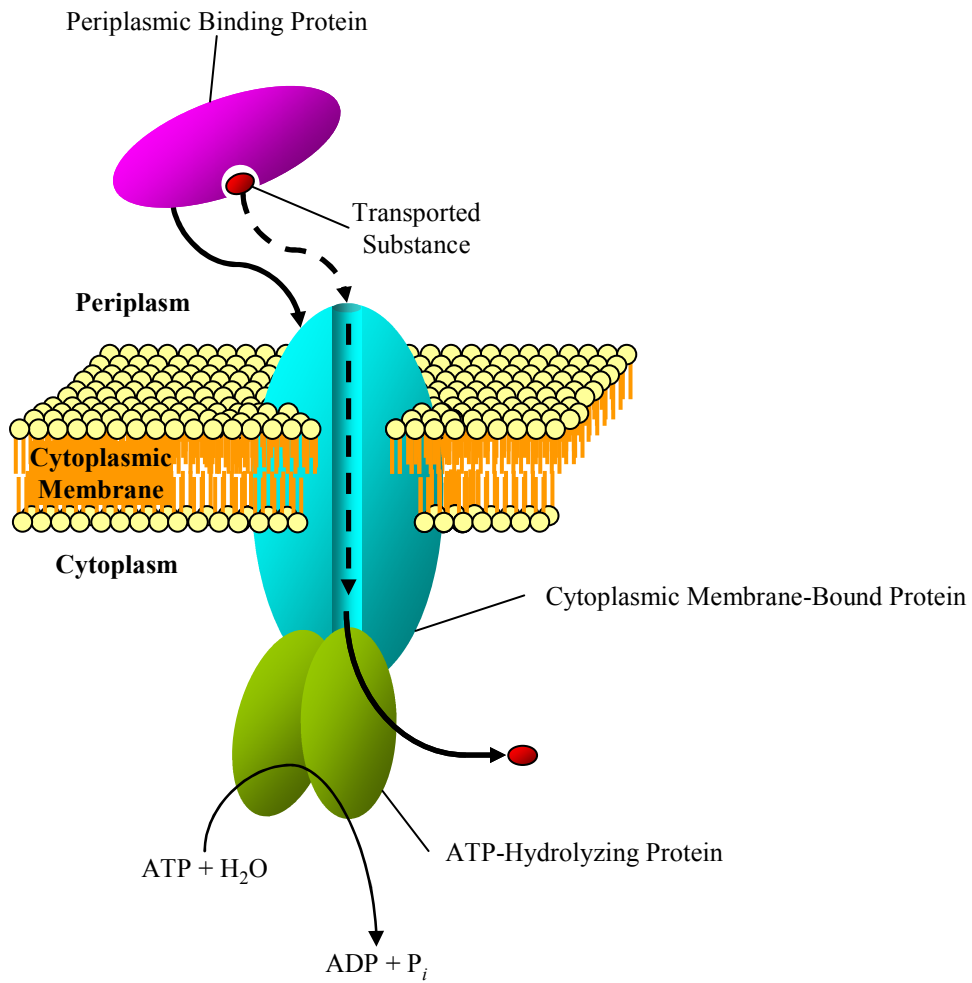


Figure 35: ATP-Binding Cassette

ATP-Binding Cassettes are composed of three types of proteins: substrate binding proteins (green), membrane bound proteins (blue), and ATP-hydrolyzing proteins (pink).

Table 18: Comparison of organic sulfur transport gene expression for sodium hypochlorite, peracetic acid, and hydrogen peroxide exposed *P. aeruginosa*.

Gene Number	Gene Name	Gene Description	NaOCl	CH ₃ CO ₃ H	H ₂ O ₂
PA0183	<i>atsA</i>	arylsulfatase	+3.81	+1.02	+1.11
PA0184	<i>atsC</i>	probable ATP-binding component of ABC sulfate ester transporter	+10.25	+1.73	+1.56
PA0185	<i>atsB</i>	probable permease of ABC sulfate ester transporter	+2.57	1.00	+1.20
PA0186	<i>atsR</i>	probable binding protein component of ABC sulfate ester transporter	+3.15	+1.12	-5.08
PA2307		probable permease of ABC putative sulfonate transporter	+5.01	+1.93	+1.67
PA2308		probable ATP-binding component of ABC putative sulfonate transporter	+5.19	-1.18	-2.41
PA2309		hypothetical protein	+7.51	+1.67	-1.48
PA2310	<i>atsK</i>	alpha-ketoglutarate-dependent dioxygenase	+17.67	-1.18	-2.93
PA3441	<i>ssuF</i>	molybdopterin-binding protein	+21.52	+1.36	-3.21
PA3442	<i>ssuB</i>	probable ATP-binding component of ABC alkanesulfonate transporter	+37.84	+1.88	-2.35
PA3443	<i>ssuC</i>	probable permease of ABC alkanesulfonate transporter	+34.41	+1.84	+1.70
PA3444	<i>ssuD</i>	alkanesulfonate monooxygenase	+107.60	+1.61	+2.10
PA3445	<i>ssuA</i>	conserved hypothetical protein	+103.00	+3.02	+1.24
PA3446	<i>ssuE</i>	NAD(P)H-dependent FMN reductase	+37.69	-1.06	1.00
PA3447		probable ATP-binding component of ABC putative sulfonate transporter	+8.34	-1.39	+1.21
PA3448		probable permease of ABC putative sulfonate transporter	+3.72	-1.38	-1.04
PA3449		conserved hypothetical protein	+9.14	-2.88	-1.25
PA3450	<i>lsfA</i>	peroxidoredoxin (antioxidant protein)	+8.26	-1.53	-1.28
PA3935	<i>tauD</i>	taurine dioxygenase	+10.35	+1.14	+1.22
PA3936	<i>tauC</i>	probable permease of taurine ABC taurine transporter	+14.44	+1.19	+1.04
PA3937	<i>tauB</i>	probable ATP-binding component of ABC taurine transporter	+12.07	+1.24	-1.05
PA3938	<i>tauA</i>	probable periplasmic taurine-binding protein precursor	+22.65	-1.04	-1.04

4.7. Iron regulation

Our previous studies confirmed that Fur-regulated genes were repressed after hydrogen peroxide exposure (W. Chang et al., 2005a; Palma et al., 2003). Comparison of three treatments (see Table 19) to these iron-related genes revealed that sodium hypochlorite-exposed and peracetic acid-exposed samples also showed many of these same repressions in the following: ferri-siderophore or iron-chelating compound receptor genes, *fpvA* (PA2398) and *fptA* (PA4221); siderophore biosynthesis genes, *pchF* (PA4225) and *pchE* (PA4226); pyochelin biosynthesis genes, *pchDCBA* (PA4228 to PA4231); siderophore or pyoverdine system-related genes (PA2403 to PA2410 and PA4156). Interestingly, the hydrogen peroxide responses were much higher than the strikingly similar sodium hypochlorite and peracetic acid responses to these same iron regulation-related genes. These results are understandable, since the *pchABCDREF* operon (PA4225 through PA4231) tends to regulate the same way. Additionally, PA2403 through PA2410 may form one or two operons based on the downregulations shown in Table 19.

Table 19: Comparison of iron regulation-related gene expression for sodium hypochlorite, peracetic acid, and hydrogen peroxide exposed *P. aeruginosa*.

Gene Number	Gene Name	Gene Description	NaOCl	CH ₃ CO ₃ H	H ₂ O ₂
PA2403		hypothetical protein	-1.31	-2.03	-4.29
PA2404		hypothetical protein	-1.23	-2.15	-4.72
PA2405		hypothetical protein	-1.42	-2.08	-5.41
PA2406		hypothetical protein	-1.21	-1.40	-2.08
PA2407		probable adhesion protein	-1.24	-1.65	-4.37
PA2408		probable ATP-binding component of ABC transporter	-1.31	-1.76	-4.22
PA2409		probable permease of ABC transporter	-1.52	-1.83	-5.10
PA2410		hypothetical protein	-1.27	-1.75	-3.37
PA2426	<i>pvdS</i>	sigma factor PvdS	NSS	NSS	NSS
PA2398	<i>fpvA</i>	ferripyoverdine receptor	-4.93	-3.40	-9.90
PA3531	<i>bfrB</i>	bacterioferritin	-1.42	+1.71	-1.81
PA4156		probable TonB-dependent receptor	-1.01	+1.11	-5.95
PA4221	<i>fptA</i>	Fe(III)-pyochelin receptor precursor	-3.42	-2.36	-3.25
PA4225	<i>pchF</i>	pyochelin synthetase	-2.43	-1.85	-3.76
PA4226	<i>pchE</i>	dihydroaeruginic acid synthetase	-2.75	-1.83	-3.25
PA4228	<i>pchD</i>	pyochelin biosynthesis protein PchD	-2.94	-2.16	-2.82
PA4229	<i>pchC</i>	pyochelin biosynthetic protein PchC	-2.35	-1.65	-3.13
PA4230	<i>pchB</i>	salicylate biosynthesis protein PchB	-2.45	-1.96	-5.59
PA4231	<i>pchA</i>	salicylate biosynthesis isochorismate synthase	-2.02	-1.77	-3.08

*NNS = not statistically significant

4.8. Pyocin genes

Perhaps the most striking result of this study was that the F-, R- and S- type pyocins (bacteriocins) of *P. aeruginosa* that were strongly upregulated after hydrogen peroxide exposure, yet these same genes did not reveal the same regulatory patterns after peracetic acid or sodium hypochlorite exposure (see Figure 36 and Table 20). These 41 genes were uniformly upregulated after hydrogen peroxide exposure and 37 of these bacteriocins were uniformly downregulated after sodium hypochlorite or peracetic acid exposure. Pyocins are readily induced by mutagenic agents (i.e. UV radiation and mitomycin C) and are suspected to kill cells by degrading DNA and inhibiting lipid

synthesis (Michel-Briand & Baysse, 2002; Sano, Matsui, Kobayashi, & Kageyama, 1993). Pyocin gene expression is regulated by the enzymes for *recA* (PA3617), *prtR* (PA0610), and *prtN* (PA0611); specifically, UV activated RecA protein cleaves the repressor protein, PrtR allowing the *prtN* gene to be expressed. The PrtN protein then facilitates the expression of various pyocin genes (Matsui, Sano, Ishihara, & Shinomiya, 1993). Thus, the upregulation of the *recA* gene combined with the possible RecA activation by hydroxyl radicals (instead of UV irradiation), may have caused the pyocin gene expression for the hydrogen peroxide-exposed samples. This is quite plausible, since the RecA protein has been shown to cleave single stranded DNA with the aid of the hydroxyl radical (Akaboshi & Howard-Flanders, 1990). However, the lack of *recA* upregulation in sodium hypochlorite-exposed and peracetic acid-exposed samples may have prevented pyocin gene expression as well as the lack of an activator for the RecA protein.

Table 20: Comparison of pyocin system-related gene expression for sodium hypochlorite, peracetic acid, and hydrogen peroxide exposed *P. aeruginosa*.

Gene Number	Gene Name	Gene Description	NaOCl	CH ₃ CO ₃ H	H ₂ O ₂
PA0610	<i>prtN</i>	transcriptional regulator PrtN	+1.90	+4.96	+1.60
PA0611	<i>prtR</i>	transcriptional regulator PrtR	+1.73	+1.93	+1.40
PA0612		hypothetical protein	+1.36	+2.43	+5.51
PA0613		hypothetical protein	+1.47	+2.44	+2.46
PA0614		hypothetical protein, lysis gene cassette	-2.15	-1.77	+2.98
PA0615		hypothetical protein, R2-specific region	-1.98	-1.93	+4.18
PA0616		hypothetical protein, R2-specific region	-1.76	-1.73	+3.56
PA0617		probable bacteriophage protein, R2-specific region	-2.18	-1.64	+3.33
PA0618		probable bacteriophage protein, R2-specific region	-1.99	-1.95	+3.05
PA0619		probable bacteriophage protein, R2-specific region	-1.89	-1.56	+3.04
PA0620		probable bacteriophage protein, R2-specific region	-1.91	-1.48	+4.31

Table 20 (continued): Comparison of pyocin system-related gene expression for sodium hypochlorite, peracetic acid, and hydrogen peroxide exposed *P. aeruginosa*.

Gene Number	Gene Name	Gene Description	NaOCl	CH ₃ CO ₃ H	H ₂ O ₂
PA0621		conserved hypothetical protein, R2-specific region	-1.85	-1.48	+2.68
PA0622		probable bacteriophage protein, R2-specific region	-1.79	-1.31	+3.08
PA0623		probable bacteriophage protein, R2-specific region	-1.92	-1.47	+2.77
PA0624		hypothetical protein, R2-specific region	-2.05	-1.87	+2.65
PA0625		hypothetical protein, R2-specific region	-2.42	-1.38	+3.32
PA0626		hypothetical protein, R2-specific region	-2.17	-1.43	+2.36
PA0627		conserved hypothetical protein, R2-specific region	-2.16	-1.52	+2.45
PA0628		conserved hypothetical protein, R2-specific region	-2.49	-1.51	+2.26
PA0629		conserved hypothetical protein, lysis gene cassette	-2.25	-1.40	+2.59
PA0630		hypothetical protein, lysis gene cassette	-2.38	-1.38	+1.91
PA0631		hypothetical protein, lysis gene cassette	-1.90	-1.48	+2.29
PA0632		hypothetical protein, lysis gene cassette	-2.39	-1.75	+1.87
PA0633		hypothetical protein, F2-specific region	-1.81	-1.50	+3.38
PA0634		hypothetical protein, F2-specific region	-2.56	-1.45	+3.48
PA0635		hypothetical protein, F2-specific region	-2.19	-1.52	+3.76
PA0636		hypothetical protein, F2-specific region	-1.96	-1.34	+3.37
PA0637		conserved hypothetical protein, F2-specific region	-2.54	-1.53	+3.36
PA0638		probable bacteriophage protein, F2-specific region	-2.10	-1.47	+3.26
PA0639		conserved hypothetical protein, F2-specific region	-2.31	-1.39	+3.01
PA0640		probable bacteriophage protein, F2-specific region	-2.21	-1.54	+2.72
PA0640		probable bacteriophage protein, F2-specific region	-2.94	-1.45	+5.14
PA0641		hypothetical protein, F2-specific region	-2.10	-1.16	+2.76
PA0642		hypothetical protein, F2-specific region	-1.53	-1.14	+2.11
PA0643		hypothetical protein, F2-specific region	-2.78	-1.55	+1.83
PA0644		hypothetical protein, F2-specific region	-1.69	-1.24	+2.55
PA0645		hypothetical protein, F2-specific region	-1.60	-1.22	+2.50
PA0646		hypothetical protein, F2-specific region	-1.46	-1.36	+1.38
PA0647		hypothetical protein, F2-specific region	-1.67	-1.45	+1.53
PA0648		hypothetical protein, F2-specific region	+1.36	+2.43	+5.51
PA0985		pyocin S5, probable colicin-like toxin	-1.95	-1.75	+2.08
PA1150	<i>psy2</i>	pyocin S2	-1.38	-1.24	+3.02
PA1151	<i>imm2</i>	pyocin S2 immunity protein	-1.49	-1.07	-1.97
PA3866		pyocin S3, pyocin protein	-2.12	-1.96	+2.37

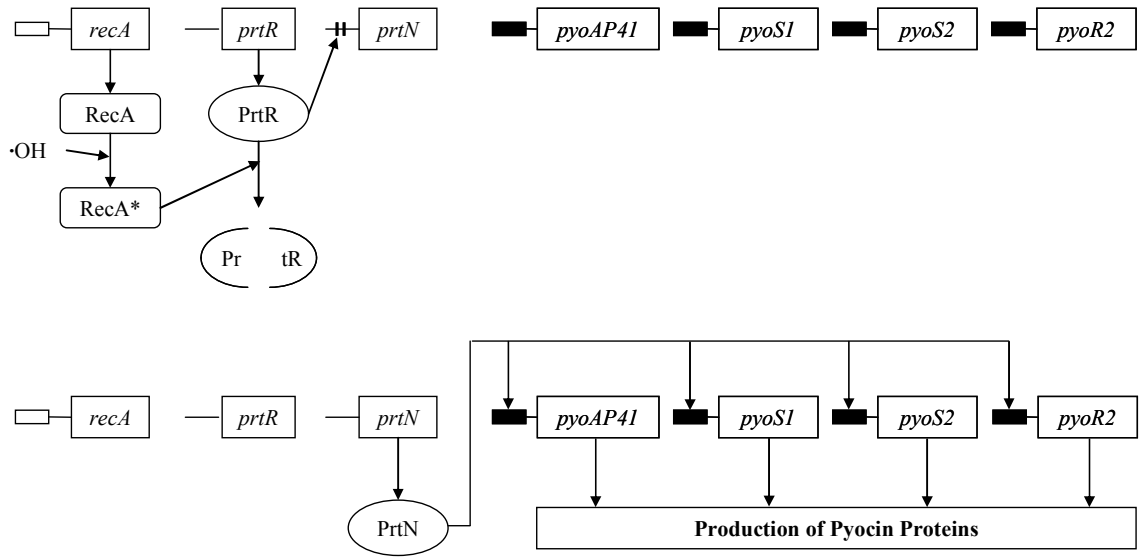


Figure 36: Production of pyocin

The pyocin expression system in *P. aeruginosa* is shown here. Cleavage of the PrtR protein by a hydroxyl radical activated RecA protein (designated RecA*) allows the PrtN protein to foster expression of the pyocin proteins (bacteriocins).

4.9. Hierarchical clustering

The 1-way ANOVA hierarchical clustering of the 3,197 statistically significant genes clearly shows that there are similarities and differences between all three treatments (see Figure 28). Further examination of the 1-way ANOVA hierarchical clustering visibly depicted the following: upregulation of the glycerol transport and catabolism genes after peracetic acid exposure, upregulation of the organic sulfur transport and catabolism genes and downregulation of the oxidative phosphorylation and electron transport genes after sodium hypochlorite exposure, and the upregulation of the pyocin synthesis genes after hydrogen-peroxide exposure. The hierarchical clustering of the 1-way ANOVA genes generally supported the results of the metabolic pathway analysis as well.

Further hierarchical clusterings of the following functional classes: “carbon compound catabolism” (see Figure 29), “energy metabolism” (see Figure 30), “membrane proteins” (see Figure 31), “related to phage, transposon, or plasmid” (see Figure 32), and “transport of small molecules” (see Figure 33) again generally supported the results of the metabolic pathway analysis. In particular, the upregulated organic sulfur transport and catabolism genes formed distinct clusters that were clearly upregulated in the “carbon compound catabolism”, “membrane proteins”, and “transport of small molecules” functional classes for the sodium hypochlorite-exposed samples, while these same genes were unchanged in the peracetic acid-exposed samples and the hydrogen peroxide-exposed samples. The downregulated oxidative phosphorylation and electron transport genes clearly formed a distinct cluster in “energy metabolism” functional class for the sodium hypochlorite-exposed samples. The upregulated pyocin synthesis genes unmistakably formed a distinct cluster in the “related to phage, transposon, or plasmid” functional class for the hydrogen peroxide-exposed samples. Hierarchical clustering of the functional classes above, again generally supported the results of the metabolic pathway analysis.

The hierarchical clustering was useful in displaying the data to see similarities and differences among the samples. However, the hierarchical clustering was only able to better illustrate the results obtained from the metabolic pathway analysis. Hierarchical clustering is often used to assign the putative function of proteins on the basis of a “guilt-by-association” in comparison to genes of known biological functions (Clare & King, 2002). Typically, hierarchical clustering is performed on time-course data (Waite *et al.*, 2006). Thus, with only one time point used for all of the treatments (the 20 min time

point), any inference to the function of unknown proteins within the *P. aeruginosa* genome from the microarray data using hierarchical clustering would be highly speculative at best and most likely inappropriate. The 1-way ANOVA removed 42.6% of the genes (2,373 genes) resulting in a data restriction which affected the stability of the microarray data used in the hierarchical clustering (de Brevern, Hazout, & Malpertuy, 2004). Additionally, hierarchical clustering, as well as self organizing maps (SOM), has been shown to be somewhat ineffective in analyzing simulated data sets as well as publicly available data sets (Datta & Datta, 2003; Kim, Lee, & Lee, 2005; Thalamuthu, Mukhopadhyay, Zheng, & Tseng, 2006).

4.10. Principal component analysis (PCA) on conditions

The PCA on conditions analysis assessed how the samples were related to each other (see Figure 21). Each set of samples for the three oxidative stressor treatments and the control samples are grouped into four small clusters in a simplistic 2-D space. This grouping pattern is also seen when the samples are viewed in a more complex 3-D space. The closeness of the clusters was representative of the precision of the biological replicates for each sample set. The control samples groups around the origin since all samples were normalized to the control samples. Clearly, all three treatments did not function the same way since all the treatment samples do not appear in the same area of space compared to the control samples (in a 2-D space), which suggests that these three oxidative stressors did not affect the cells the same way.

The hydrogen peroxide-exposed samples are very far away from the sodium hypochlorite-exposed and peracetic acid-exposed samples (in the newly defined PCA

space), which populate the lower right quadrant when viewed in 2-D (and even seem to reside in the same plane when viewed in 3-D). This result highlighted that there were some similarity between the sodium hypochlorite-exposed and peracetic acid-exposed samples. This result was surprising, since hydrogen peroxide and peracetic acid were thought to have similar effects, and a close grouping of these samples should have been expected. Based on this result, the effects of hydrogen peroxide and sodium hypochlorite should have resulted in the most extreme gene expression changes. This aspect of the PCA was illustrated in Table 21 by examining the five most drastically affected genes for each oxidative stressor. Generally, the magnitudes of change (in this extreme sample of genes) were largest for sodium hypochlorite and much less so for peracetic acid.

Perhaps the most intriguing aspect of the PCA was the appearance of all samples in the positive x-axis (positive direction of principal component 1). This result suggested that there may be a general trend in response to oxidative stressors, since more than half of the variance in the data was accounted for by principal component 1 (56.12%). However, in order to definitively prove this, more data would be required with different stressors other than oxidative stressors. Perhaps, even a direct comparison between strong oxidative stressors and strong reducing agents using the PCA would show two different trends using a PCA.

Table 21: Comparison of the five extreme upregulated and downregulated gene expression for sodium hypochlorite, peracetic acid, and hydrogen peroxide exposed *P. aeruginosa*.

Gene Number	Gene Name	Gene Description	NaOCl	CH ₃ CO ₃ H	H ₂ O ₂
Sodium Hypochlorite Extreme Upregulated Genes					
PA0565		Conserved hypothetical protein	+182.10	+4.45	+1.08
PA3444		Conserved hypothetical protein	+107.60	+1.61	+2.10
PA3445		Conserved hypothetical protein	+103.00	+3.02	+1.24
PA3281		Hypothetical membrane protein	+85.48	+29.13	+2.23
PA3282		Hypothetical protein	+61.83	+26.97	+2.40
Sodium Hypochlorite Extreme Downregulated Genes					
PA1557		Probable cytochrome oxidase subunit (cbb3-type)	-21.65	-3.11	-1.91
PA4134		Probable iron-sulfur protein	-17.79	-8.77	-2.22
PA3189		Probable permease of ABC sugar transporter	-17.15	-5.21	+1.37
PA1556		Probable cytochrome c oxidase subunit	-14.47	-2.46	-1.94
PA4067	<i>oprG</i>	Outer membrane protein OprG precursor	-14.41	-2.71	-1.31
Peracetic Acid Extreme Upegulated Genes					
PA3283		Conserved hypothetical protein	+52.49	+31.76	+3.17
PA3281		Hypothetical protein	+85.48	+29.13	+2.23
PA2664	<i>fhp</i>	Flavoheomprotein	+29.31	+27.00	+1.27
PA3282		Hypothetical protein	+61.83	+26.97	+2.40
PA2827		Conserved hypothetical protein	+23.17	+23.20	+1.20
Peracetic Acid Extreme Downregulated Genes					
PA3329		Hypothetical protein	-1.15	-23.47	+1.70
PA3330		Probable short chain dehydrogenase	+1.06	-10.45	+2.01
PA5024		Conserved hypothetical protein	+2.88	-9.90	-2.60
PA2079		Probable amino acid permease	-3.15	-9.71	-2.00
PA1869		Probable acyl carrier protein	-2.65	-9.17	-1.13
Hydrogen Peroxide Extreme Upegulated Genes					
PA0724		Probable coat protein A of bacteriophage Pfl	+2.89	+2.46	+118.90
PA0721		Hypothetical protein of bacteriophage Pfl	+2.51	+3.33	+84.56
PA0726		Hypothetical protein of bacteriophage Pfl	+2.45	+2.59	+83.99
PA0719		Hypothetical protein of bacteriophage Pfl	+2.79	+3.25	+77.22
PA30725		Hypothetical protein of bacteriophage Pfl	+2.59	+2.66	+67.97
Hydrogen Peroxide Extreme Downregulated Genes					
PA2412		Conserved hypothetical protein	-1.73	-1.40	-13.77
PA2411		Probable thioesterase	-1.52	-1.36	-13.72
PA2398	<i>fpvA</i>	Ferripyoverdine receptor	-4.93	-3.40	-9.90
PA4179		Probable porin	-8.77	-1.05	-9.43
PA5385		Hypothetical protein	-1.49	+1.38	-8.20

Chapter 5: Conclusions

5.1. Overview

The DNA microarrays (Affymetrix GeneChips) were able to successfully distinguish the gene expression changes after exposure to the oxidative disinfectants used in this study (sodium hypochlorite, peracetic acid, and hydrogen peroxide). Some modes of actions were suggested for further study, particularly the oxidative phosphorylation and electron transport mechanisms after sodium hypochlorite exposure. Additionally, the glycerol uptake and metabolism system after peracetic acid exposure and the pyocin synthesis genes after hydrogen peroxide exposure warrant further study based on the gene expression results. The gene expression profiles from this study revealed an increase in the adaptive/protective processes for all three disinfectants. However, despite some overlaps in gene expression, these oxidative stressors seem to cause remarkably different upregulations and downregulations in gene expression, suggesting that the modes of action by which each of these disinfectants actually kill bacteria are unique.

5.2. Oxidative stressor comparison

The results suggested the well-documented unparalleled effectiveness of sodium hypochlorite as a disinfectant may be due to the greater number of statistically significant genome-wide changes after sodium hypochlorite exposure compared to peracetic acid or hydrogen peroxide exposures. The synergistic effect previously shown on cells exposed

to mixtures of peracetic acid and hydrogen peroxide (Alasri, Roques, Michel, Cabassud, & Aptel, 1992; Alasri *et al.*, 1993) may be due to the lack of overlap between the genome-wide changes of these two antimicrobials. Additionally, this synergistic effect may in part be due to the striking similarity of a notably large portion of genes that are similarly expressed between peracetic acid-exposed and sodium hypochlorite-exposed *P. aeruginosa* cells.

5.3. Cell viability

The assessment of viable cells was critical since dead cells yield little to no mRNA to be hybridized to the microarray. Turbidity measurements allowed for a simple estimation of the growth rate to insure that the cells were indeed growth inhibited. Several techniques to assess cell viability were implemented as well, including the following: culture plating, cell flow cytometry, and relative ATP measurement. However, it should be noted that the successful hybridization of bacterial mRNA to the microarray was an even better metric for cell viability. Generally, eukaryotic mRNA composes roughly 1 to 5% of the total RNA, however, prokaryotic mRNA composes roughly 3% of the total RNA. Prokaryotic mRNA typically has an extremely short half life of approximately 3 min (Alifano, Bruni, & Carlomagno, 1994; Belasco, Nilsson, von Gabain, & Cohen, 1986; von Gabain, Belasco, Schottel, Chang, & Cohen, 1983). Concentrations of sodium hypochlorite above 0.5% resulted in no cell growth from turbidity measurements, no CFU from the plating studies, heavily perforated cell membranes from flow cytometry studies, and no relative ATP detection from the luciferase assays. Additionally, total RNA could not be detected with the methods used in

this study to ascertain RNA quality. The 20 min exposure time to the sodium hypochlorite, peracetic acid, and hydrogen peroxide (in addition to the 5 min incubation with RNA stabilizing compounds prior to RNA extraction) yielded mRNA that was further processed into cDNA and successfully hybridized to the GeneChips.

5.4. Eukaryotic implications

The myeloperoxidase (MPO) system of eukaryotes is considered to play a key role in the destruction of microbes by phagocytes (Klebanoff, 2005). The MPO enzyme catalyzes the conversion of H_2O_2 and Cl^- to HOCl during the respiratory burst (Klebanoff, 1999). Thus, studies that examine the effects of reactive oxygen species (ROS) inherently apply to how neutrophilic polymorphonuclear leukocytes (neutrophils) destroy foreign bodies in more complex organisms. The MPO system is present in the phagocytes of eukaryotes, yet it does not kill the phagocytes or the tissues surrounding these cells. Human leukocytes were shown to have high concentrations of taurine and hypotaurine (Learn, Fried, & Thomas, 1990), which would both mediate the hypochlorous acid that would be exposed to these cells. Additionally, the formation of the Tau-Cl system has been shown to downregulate the production of inflammatory mediators (Quinn, Barua, Liu, & Serban, 2003; Quinn, Liu, Barua, & Serban, 2003; G. Schuller-Levis, Mehta, Rudelli, & Sturman, 1990; G. Schuller-Levis, Quinn, Wright, & Park, 1994; G. B. Schuller-Levis, Gordon, Wang, & Park, 2003; G. B. Schuller-Levis & Park, 2003; Suzuki, Suzuki, Wada, Saigo, & Watanabe, 2002). These findings correlate with the upregulation of the taurine transport genes as well as the alkanesulfonate transport genes in the *P. aeruginosa* from this study, and may suggest that this was an

evolutionary conserved reaction to ROS that was evolutionarily incorporated into eukaryotic species over time.

5.5. Future directions

5.5.1. Disinfectant time-course studies

This study provides several directions for future experimentation. Due to financial limitations, only one time point (exposure time) could be assessed using the techniques outlined in this study. A more complete and comprehensive understanding could be attained by using more time points, particularly in the early to late exposure range. A time span of 5 to 15 min is sufficient to detect mRNA level changes induced by ROS in *P. aeruginosa*, *E. coli*, and other bacteria. (Baichoo, Wang, Ye, & Helmann, 2002; Bals, Weiner, & Wilson, 1999; Prieto-Alamo et al., 2000). Thus, a compelling time course experiment could consist of 5, 10, and 20 min exposure times to gauge the early, middle, and late responses of *P. aeruginosa* to ROS. As this study already contains the 20 min time points, the experimental procedures described in the methods section could be repeated with 5 and 10 min exposure times. Again, the same data analysis methods (1-way ANOVA, hierarchical clustering, PCA) used for the 20 min exposure time point could be applied to the 5 and 10 min exposure time points. Clustering techniques and PCA should prove to be even more effective in describing and characterizing this time-course data compared to a 20 min exposure time point.

5.5.2. Sodium hypochlorite and organic sulfur compounds

5.5.2.1. Real-time PCR studies after sodium hypochlorite exposure

Further investigation to discover the metabolism of organic sulfur compounds after sodium hypochlorite-exposure would also be another avenue of future study. This could be done on the genetic level by selecting several of the organic sulfur transport and metabolism genes (the 22 genes that appear in Table 18) and performing real-time PCR to see the time-course response of the gene expression. As stated above in the time-course design, RNA could be extracted at several time points for a set of sodium hypochlorite-exposed cultures and water-diluted (control) cultures. RNA could be then be extracted at several times points from all of the cultures. The RNA could then be subjected to the real-time PCR methods used in this study for the validation of the microarray data but using primers designed from the genes in Table 18 instead of the randomly selected gene for microarray validation. Analysis of this data would give a much more comprehensive understanding of the effect of sodium hypochlorite on the gene expression of these organic sulfur compounds.

5.5.2.2. Media studies after sodium hypochlorite exposure

P. aeruginosa could be cultured in different media preparations that are enriched or devoid of the organic sulfur compounds that were shown to be highly upregulated in this study. The cells could then be exposed to various sodium hypochlorite concentrations and the cell

growth, membrane integrity, and ATP concentrations could also be simultaneously measured with the same techniques described in the methods section of this study. Using this type of experimental design, changes in media before and after exposure to sodium hypochlorite could also help determine how the organic sulfur transport and metabolism genes are regulated after sodium hypochlorite exposure.

For example, the *P. aeruginosa* cells could be cultured in LB media, and then exposed to sub-lethal concentrations of sodium hypochlorite for a set time period. These cells could then be pelleted using centrifugation and resuspended in a media rich in organic sulfur compounds (taurine, alkanesulfonates, sulfate esters, etc.). Monitoring the cell growth by turbidity measurements, membrane integrity via cell flow cytometry, and ATP concentrations via bioluminescence would provide a growth-based response of *P. aeruginosa* sensitivity to these organic sulfur compounds after sodium hypochlorite exposure. The cell growth turbidity measurements, membrane integrity cell flow cytometry measurements, and bioluminescence measurements to determine ATP concentration would be performed like the viability methods of this study. Instead of using time points after exposure to the sodium hypochlorite, time points would be used after the cells begin to grow in the organic sulfur-rich media. Similar experiments could be performed with peracetic acid-exposed cells with respect to a glycerol-rich substrate for growth.

5.5.3. Signature genes in different bacteria

Yet another course of study would be to repeat the methods of this study in different bacterial species. The US EPA presently uses four unique bacterial species to register disinfectants: *Pseudomonas. aeruginosa*, *Staphylococcus aureus*, *Bacillus subtilis*, and *Mycobacterium bovis*. This study used *P. aeruginosa* as the test organism; however, microarrays (GeneChips) are now available for the other three bacterial species that the EPA uses to test disinfectant efficacies. The exact same methods used in this study could be repeated with these other bacterial species. After the data is imported into GeneSpring GX as described in the data analysis portion of this study, the “Gene Ontology” function could be used to interpret the data and identify signature genes that are affected after the exposure of sodium hypochlorite, peracetic acid, and hydrogen peroxide. Gene ontology divides gene products into three structured, controlled vocabularies or ontologies based on the (1) associated biological processes of a gene product, (2) cellular components of a gene product, and (3) molecular functions of a gene product in a species-independent manner (Ashburner *et al.*, 2000). The gene ontologies could then be used as a basis for the hierarchical clustering or PCA to interpret the data and find signature genes that are affected after exposure to oxidative compounds.

5.6. Further applications of this study

Applications of disinfectants are not limited to hospitals and healthcare facilities. These compounds are also used as germicides in locker rooms and sports-related

facilities, swimming pools, and lavatory water sources. Cystic Fibrosis (CF) patients, particularly young ones, are extremely susceptible to contracting lung infections from *P. aeruginosa* growing in public swimming pools and tainted water supplies (Barben, Hafen, & Schmid, 2005). Additionally, antimicrobial solutions are used in almost all aspects of the food industry (sterilization of the harvest equipment, disinfection of surfaces used in food processing, etc.). The resulting global transcription profile of the disinfectants in this comparison can help identify commonly activated genes between these oxidative disinfectants. Furthermore, this information will help researchers better understand the mechanisms by which oxidative disinfectants kill bacteria.

REFERENCES

- Ackerman, J. (2004). *Louis Pasteur and the Founding of Microbiology*. Greensboro, NC: Morgan Reynolds Publishing, Inc.
- Agilent Technologies, I. (2006). GeneSpring GX (Version 7.3). Santa Clara: Agilent Technologies, Inc.
- Akaboshi, E., & Howard-Flanders, P. (1990). RecA-ssDNA interaction: induced strand cleavage by hydroxyl radical at a defined distance from the 5' end. *Mol Gen Genet*, 220(3), 456-460.
- Alasri, A., Roques, C., Michel, G., Cabassud, C., & Aptel, P. (1992). Bactericidal properties of peracetic acid and hydrogen peroxide, alone and in combination, and chlorine and formaldehyde against bacterial water strains. *Can J Microbiol*, 38(7), 635-642.
- Alasri, A., Valverde, M., Roques, C., Michel, G., Cabassud, C., & Aptel, P. (1993). Sporocidal properties of peracetic acid and hydrogen peroxide, alone and in combination, in comparison with chlorine and formaldehyde for ultrafiltration membrane disinfection. *Can J Microbiol*, 39(1), 52-60.
- Albrich, J. M., & Hurst, J. K. (1982). Oxidative inactivation of *Escherichia coli* by hypochlorous acid. Rates and differentiation of respiratory from other reaction sites. *FEBS Lett*, 144(1), 157-161.
- Albrich, J. M., McCarthy, C. A., & Hurst, J. K. (1981). Biological reactivity of hypochlorous acid: implications for microbicidal mechanisms of leukocyte myeloperoxidase. *Proc Natl Acad Sci U S A*, 78(1), 210-214.
- Alifano, P., Bruni, C. B., & Carlomagno, M. S. (1994). Control of mRNA processing and decay in prokaryotes. *Genetica*, 94(2-3), 157-172.
- Ashburner, M., Ball, C. A., Blake, J. A., Botstein, D., Butler, H., Cherry, J. M., et al. (2000). Gene ontology: tool for the unification of biology. The Gene Ontology Consortium. *Nat Genet*, 25(1), 25-29.
- Baichoo, N., Wang, T., Ye, R., & Helmann, J. D. (2002). Global analysis of the *Bacillus subtilis* Fur regulon and the iron starvation stimulon. *Mol Microbiol*, 45(6), 1613-1629.
- Baker, R. (1959). Types and significance of chlorine residuals. *Journal of the American Water Works Association*(59), 1185-1190.
- Baldry, M. G. (1983). The bactericidal, fungicidal and sporicidal properties of hydrogen peroxide and peracetic acid. *J Appl Bacteriol*, 54(3), 417-423.
- Bals, R., Weiner, D. J., & Wilson, J. M. (1999). The innate immune system in cystic fibrosis lung disease. *J Clin Invest*, 103(3), 303-307.
- Barben, J., Hafen, G., & Schmid, J. (2005). *Pseudomonas aeruginosa* in public swimming pools and bathroom water of patients with cystic fibrosis. *J Cyst Fibros*, 4(4), 227-231.

- Barnes, M., Freudenberg, J., Thompson, S., Aronow, B., & Pavlidis, P. (2005). Experimental comparison and cross-validation of the Affymetrix and Illumina gene expression analysis platforms. *Nucleic Acids Res*, 33(18), 5914-5923.
- Barrette, W. C., Jr., Hannum, D. M., Wheeler, W. D., & Hurst, J. K. (1989). General mechanism for the bacterial toxicity of hypochlorous acid: abolition of ATP production. *Biochemistry*, 28(23), 9172-9178.
- Basilevsky, A. (1994). *Statistical Factor Analysis and Related Methods: Theory and Applications*. New York, NY: John Wiley & Sons.
- Belasco, J. G., Nilsson, G., von Gabain, A., & Cohen, S. N. (1986). The stability of *E. coli* gene transcripts is dependent on determinants localized to specific mRNA segments. *Cell*, 46(2), 245-251.
- Block, S. S. (2001). *Disinfection, sterilization, and preservation*. Philadelphia: Lippincott Williams & Wilkins Publishers.
- Bloomfield, S. (1996). *Chlorine and iodine formulations*. New York, N.Y: Marcel Dekker, Inc.
- Bodey, G. P., Bolivar, R., Fainstein, V., & Jadeja, L. (1983). Infections caused by *Pseudomonas aeruginosa*. *Rev Infect Dis*, 5(2), 279-313.
- Brazma, A., & Vilo, J. (2001). Gene expression data analysis. *Microbes Infect*, 3(10), 823-829.
- Brock, T. D. (1961). *Milestones in Microbiology*. London: Prentice Hall.
- Brown, S. M., Howell, M. L., Vasil, M. L., Anderson, A. J., & Hassett, D. J. (1995). Cloning and characterization of the *katB* gene of *Pseudomonas aeruginosa* encoding a hydrogen peroxide-inducible catalase: purification of KatB, cellular localization, and demonstration that it is essential for optimal resistance to hydrogen peroxide. *J Bacteriol*, 177(22), 6536-6544.
- Budavari, S. (1996). *Merck Index 12th Ed*. Whitehouse Station, NJ: Merck & Co., Inc.
- Campa M., B. M., Fiedman H. (1993). *Pseudomonas aeruginosa as an opportunistic pathogen*. New York: Plenum Press.
- Chang, W., Small, D. A., Toghrol, F., & Bentley, W. E. (2005a). Microarray analysis of *Pseudomonas aeruginosa* reveals induction of pyocin genes in response to hydrogen peroxide. *BMC Genomics*, 6(1), 115.
- Chang, W., Small, D. A., Toghrol, F., & Bentley, W. E. (2005b). Microarray analysis of toxicogenomic effects of peracetic acid on *Pseudomonas aeruginosa*. *Environ Sci Technol*, 39(15), 5893-5899.
- Chang, W., Small, D. A., Toghrol, F., & Bentley, W. E. (2006). Global Transcriptome Analysis of *Staphylococcus aureus* Response to Hydrogen Peroxide. *J. Bacteriol.*, 188(4), 1648-1659.
- Churchill, G. A. (2002). Fundamentals of experimental design for cDNA microarrays. *Nat Genet*, 32 Suppl, 490-495.
- Clare, A., & King, R. D. (2002). How well do we understand the clusters found in microarray data? *In Silico Biol*, 2(4), 511-522.
- Cunningham, C., Tipton, K. F., & Dixon, H. B. (1998). Conversion of taurine into N-chlorotaurine (taurine chloramine) and sulphoacetaldehyde in response to oxidative stress. *Biochem J*, 330 (Pt 2), 939-945.
- Curtis, R. K., Oresic, M., & Vidal-Puig, A. (2005). Pathways to the analysis of microarray data. *Trends Biotechnol*, 23(8), 429-435.

- Dahlquist, K. D., Salomonis, N., Vranizan, K., Lawlor, S. C., & Conklin, B. R. (2002). GenMAPP, a new tool for viewing and analyzing microarray data on biological pathways. *Nat Genet*, *31*(1), 19-20.
- Dallas, P. B., Gottardo, N. G., Firth, M. J., Beesley, A. H., Hoffmann, K., Terry, P. A., et al. (2005). Gene expression levels assessed by oligonucleotide microarray analysis and quantitative real-time RT-PCR -- how well do they correlate? *BMC Genomics*, *6*(1), 59.
- Datta, S., & Datta, S. (2003). Comparisons and validation of statistical clustering techniques for microarray gene expression data. *Bioinformatics*, *19*(4), 459-466.
- Davey, H. M., & Kell, D. B. (1996). Flow cytometry and cell sorting of heterogeneous microbial populations: the importance of single-cell analyses. *Microbiol Rev*, *60*(4), 641-696.
- de Brevern, A. G., Hazout, S., & Malpertuy, A. (2004). Influence of microarrays experiments missing values on the stability of gene groups by hierarchical clustering. *BMC Bioinformatics*, *5*, 114.
- Decker, E. M. (2001). The ability of direct fluorescence-based, two-colour assays to detect different physiological states of oral streptococci. *Lett Appl Microbiol*, *33*(3), 188-192.
- Denyer, S. P. (1991). *Mechanisms of Action of Chemical Biocides : Their Study and Exploitation*. Oxford: Blackwell Science Inc.
- Denyer, S. P., & Stewart, G. S. A. B. (1998). Mechanisms of action of disinfectants. *International Biodeterioration & Biodegradation*, *41*(3-4), 261.
- DeRisi, J., Penland, L., Brown, P. O., Bittner, M. L., Meltzer, P. S., Ray, M., et al. (1996). Use of a cDNA microarray to analyse gene expression patterns in human cancer. *Nat Genet*, *14*(4), 457-460.
- Doniger, S. W., Salomonis, N., Dahlquist, K. D., Vranizan, K., Lawlor, S. C., & Conklin, B. R. (2003). MAPPFinder: using Gene Ontology and GenMAPP to create a global gene-expression profile from microarray data. *Genome Biol*, *4*(1), R7.
- Dormandy, T. (2004). *Moments of Truth: Four Creators of Modern Medicine* West Sussex, England: Wiley, John & Sons, Inc.
- Dukan, S., & Touati, D. (1996). Hypochlorous acid stress in *Escherichia coli*: resistance, DNA damage, and comparison with hydrogen peroxide stress. *J Bacteriol*, *178*(21), 6145-6150.
- Eichhorn, E., van der Ploeg, J. R., Kertesz, M. A., & Leisinger, T. (1997). Characterization of alpha-ketoglutarate-dependent taurine dioxygenase from *Escherichia coli*. *J Biol Chem*, *272*(37), 23031-23036.
- Eichhorn, E., van der Ploeg, J. R., & Leisinger, T. (1999). Characterization of a two-component alkanesulfonate monooxygenase from *Escherichia coli*. *J Biol Chem*, *274*(38), 26639-26646.
- Eisen, M. B., Spellman, P. T., Brown, P. O., & Botstein, D. (1998). Cluster analysis and display of genome-wide expression patterns. *Proc Natl Acad Sci U S A*, *95*(25), 14863-14868.
- Elkins, J. G., Hassett, D. J., Stewart, P. S., Schweizer, H. P., & McDermott, T. R. (1999). Protective role of catalase in *Pseudomonas aeruginosa* biofilm resistance to hydrogen peroxide. *Appl Environ Microbiol*, *65*(10), 4594-4600.

- Fair, G. M., Morris, J. C., & Chang, S. L. (1948). The behavior of chlorine as a water disinfectant. *Journal of the American Water Works Association*, 40, 1051-1061.
- Fitzgerald, K. A., Davies, A., & Russell, A. D. (1989). Uptake of ¹⁴C-chlorhexidine diacetate to *Escherichia coli* and *Pseudomonas aeruginosa* and its release by azolectin. *FEMS Microbiol Lett*, 51(3), 327-332.
- Franklin, T. J. a. S., G.A. (1989). *Biochemistry of antimicrobial action* Chapman and Hall: New York.
- Fridovich, I. (1975). Oxygen: boon and bane. *Am Sci*, 63(1), 54-59.
- Fridovich, I. (1978). The biology of oxygen radicals. *Science*, 201(4359), 875-880.
- Fukuzaki, S. (2006). Mechanisms of actions of sodium hypochlorite in cleaning and disinfection processes. *Biocontrol Sci*, 11(4), 147-157.
- Grisham, M. B., Jefferson, M. M., Melton, D. F., & Thomas, E. L. (1984). Chlorination of endogenous amines by isolated neutrophils. Ammonia-dependent bactericidal, cytotoxic, and cytolytic activities of the chloramines. *J Biol Chem*, 259(16), 10404-10413.
- Hallin, P. F., & Ussery, D. W. (2004). CBS Genome Atlas Database: a dynamic storage for bioinformatic results and sequence data. *Bioinformatics*, 20(18), 3682-3686.
- Hancock, R. E. (1998). Resistance mechanisms in *Pseudomonas aeruginosa* and other nonfermentative gram-negative bacteria. *Clin Infect Dis*, 27 Suppl 1, S93-99.
- Harris, M. A., Clark, J., Ireland, A., Lomax, J., Ashburner, M., Foulger, R., et al. (2004). The Gene Ontology (GO) database and informatics resource. *Nucleic Acids Res*, 32(Database issue), D258-261.
- Harrison, J. E., Watson, B. D., & Schultz, J. (1978). Myeloperoxidase and singlet oxygen: a reappraisal. *FEBS Lett*, 92(2), 327-332.
- Hassett, D. J., Schweizer, H. P., & Ohman, D. E. (1995). *Pseudomonas aeruginosa* *sodA* and *sodB* mutants defective in manganese- and iron-cofactored superoxide dismutase activity demonstrate the importance of the iron-cofactored form in aerobic metabolism. *J Bacteriol*, 177(22), 6330-6337.
- Hatano, T., Uebayashi, H., Ito, H., Shiota, S., Tsuchiya, T., & Yoshida, T. (1999). Phenolic constituents of Cassia seeds and antibacterial effect of some naphthalenes and anthraquinones on methicillin-resistant *Staphylococcus aureus*. *Chem Pharm Bull (Tokyo)*, 47(8), 1121-1127.
- Hattori, N., Sakakibara, T., Kajiyama, N., Igarashi, T., Maeda, M., & Murakami, S. (2003). Enhanced microbial biomass assay using mutant luciferase resistant to benzalkonium chloride. *Anal Biochem*, 319(2), 287-295.
- Hayes, K. R., & Bradfield, C. A. (2005). Advances in toxicogenomics. *Chem Res Toxicol*, 18(3), 403-414.
- Heid, C. A., Stevens, J., Livak, K. J., & Williams, P. M. (1996). Real time quantitative PCR. *Genome Res*, 6(10), 986-994.
- Hess, W. T. (1995). *Hydrogen Peroxide* (Vol. 13). New York: Wiley.
- Hugo, W. B. (1995). A brief history of heat, chemical and radiation preservation and disinfection. *International Biodeterioration & Biodegradation*, 36(3-4), 197.
- Hummerjohann, J., Kuttel, E., Quadroni, M., Ragaller, J., Leisinger, T., & Kertesz, M. A. (1998). Regulation of the sulfate starvation response in *Pseudomonas aeruginosa*: role of cysteine biosynthetic intermediates. *Microbiology*, 144 (Pt 5), 1375-1386.

- Hummerjohann, J., Laudenbach, S., Retey, J., Leisinger, T., & Kertesz, M. A. (2000). The sulfur-regulated arylsulfatase gene cluster of *Pseudomonas aeruginosa*, a new member of the *cys* regulon. *J Bacteriol*, *182*(7), 2055-2058.
- Johnson, J. (1988). *History of medical product sterilization*. New York: Johnson & Johnson.
- Johnson, S. C. (1967). Hierarchical clustering schemes. *Psychometrika*, *32*(3), 241-254.
- Kahnert, A., & Kertesz, M. A. (2000). Characterization of a sulfur-regulated oxygenative alkylsulfatase from *Pseudomonas putida* S-313. *J Biol Chem*, *275*(41), 31661-31667.
- Kerr, M. K. (2003). Design considerations for efficient and effective microarray studies. *Biometrics*, *59*(4), 822-828.
- Keyer, K., Gort, A. S., & Imlay, J. A. (1995). Superoxide and the production of oxidative DNA damage. *J Bacteriol*, *177*(23), 6782-6790.
- Kim, D. W., Lee, K. H., & Lee, D. (2005). Detecting clusters of different geometrical shapes in microarray gene expression data. *Bioinformatics*, *21*(9), 1927-1934.
- Kitagawa, E., Takahashi, J., Momose, Y., & Iwahashi, H. (2002). Effects of the pesticide thiuram: genome-wide screening of indicator genes by yeast DNA microarray. *Environ Sci Technol*, *36*(18), 3908-3915.
- Kitis, M. (2004). Disinfection of wastewater with peracetic acid: a review. *Environ Int*, *30*(1), 47-55.
- Klebanoff, S. J. (1999). Myeloperoxidase. *Proc Assoc Am Physicians*, *111*(5), 383-389.
- Klebanoff, S. J. (2005). Myeloperoxidase: friend and foe. *J Leukoc Biol*, *77*(5), 598-625.
- Learn, D. B., Fried, V. A., & Thomas, E. L. (1990). Taurine and hypotaurine content of human leukocytes. *J Leukoc Biol*, *48*(2), 174-182.
- Lessie, T. G., & Phibbs, P. V. (1984). Alternative Pathways of Carbohydrate Utilization in Pseudomonads. *Annual Review of Microbiology*, *38*(1), 359-388.
- Lin, E. C. (1976). Glycerol dissimilation and its regulation in bacteria. *Annu Rev Microbiol*, *30*, 535-578.
- Lister, J. (1967). Antiseptic principle in the practice of surgery. *Br Med J*, *2*(543), 9-12.
- Madigan, M. T., Martinko, J. M., & Parker, J. (2003). *Brock Biology of Microorganisms* (10th ed.). Upper Saddle River, NJ: Pearson Education, Inc.
- Malchesky, P. S. (1993). Peracetic acid and its application to medical instrument sterilization. *Artif Organs*, *17*(3), 147-152.
- Marquis, R. E., Rutherford, G. C., Faraci, M. M., & Shin, S. Y. (1995). Sporicidal action of peracetic acid and protective effects of transition metal ions. *J Ind Microbiol*, *15*(6), 486-492.
- Martinez, A., & Kolter, R. (1997). Protection of DNA during oxidative stress by the nonspecific DNA-binding protein Dps. *J Bacteriol*, *179*(16), 5188-5194.
- Matsui, H., Sano, Y., Ishihara, H., & Shinomiya, T. (1993). Regulation of pyocin genes in *Pseudomonas aeruginosa* by positive (*priN*) and negative (*priR*) regulatory genes. *J Bacteriol*, *175*(5), 1257-1263.
- McCowen, S. M., Phibbs, P. V., & Feary, T. W. (1981). Glycerol catabolism in wild-type and mutant strains of *Pseudomonas aeruginosa*. *Current Microbiology*, *5*(3), 191.
- McCowen, S. M., Sellers, J. R., & Phibbs, P. V. (1986). Characterization of fructose-1,6-diphosphate-insensitive catabolic glycerol kinase of *Pseudomonas aeruginosa*. *Current Microbiology*, *14*(6), 323.

- McDonnell, G., & Russell, A. D. (1999). Antiseptics and Disinfectants: Activity, Action, and Resistance. *Clin. Microbiol. Rev.*, *12*(1), 147-179.
- Michel-Briand, Y., & Baysse, C. (2002). The pyocins of *Pseudomonas aeruginosa*. *Biochimie*, *84*(5-6), 499-510.
- Miller, R. A., & Britigan, B. E. (1997). Role of oxidants in microbial pathophysiology. *Clin Microbiol Rev*, *10*(1), 1-18.
- Morris, J. C. (1966). Future of chlorination. *Journal of the American Water Works Association*, *58*, 1475-1482.
- Muller, I., Stuckl, C., Wakeley, J., Kertesz, M., & Uson, I. (2005). Succinate complex crystal structures of the alpha-ketoglutarate-dependent dioxygenase AtsK: steric aspects of enzyme self-hydroxylation. *J Biol Chem*, *280*(7), 5716-5723.
- Nebe-von-Caron, G., Stephens, P. J., Hewitt, C. J., Powell, J. R., & Badley, R. A. (2000). Analysis of bacterial function by multi-colour fluorescence flow cytometry and single cell sorting. *J Microbiol Methods*, *42*(1), 97-114.
- Nigel, J. W. (2001). Real-time and quantitative PCR: applications to mechanism-based toxicology. *Journal of Biochemical and Molecular Toxicology*, *15*(3), 121-127.
- Ochsner, U. A., Vasil, M. L., Alsabbagh, E., Parvatiyar, K., & Hassett, D. J. (2000). Role of the *Pseudomonas aeruginosa oxyR-recG* operon in oxidative stress defense and DNA repair: OxyR-dependent regulation of *katB-ankB*, *ahpB*, and *ahpC-ahpF*. *J Bacteriol*, *182*(16), 4533-4544.
- Ogata, H., Goto, S., Sato, K., Fujibuchi, W., Bono, H., & Kanehisa, M. (1999). KEGG: Kyoto Encyclopedia of Genes and Genomes. *Nucleic Acids Res*, *27*(1), 29-34.
- Palma, M., Worgall, S., & Quadri, L. E. (2003). Transcriptome analysis of the *Pseudomonas aeruginosa* response to iron. *Arch Microbiol*, *180*(5), 374-379.
- Prieto-Alamo, M. J., Jurado, J., Gallardo-Madueno, R., Monje-Casas, F., Holmgren, A., & Pueyo, C. (2000). Transcriptional regulation of glutaredoxin and thioredoxin pathways and related enzymes in response to oxidative stress. *J Biol Chem*, *275*(18), 13398-13405.
- Quadroni, M., James, P., Dainese-Hatt, P., & Kertesz, M. A. (1999). Proteome mapping, mass spectrometric sequencing and reverse transcription-PCR for characterization of the sulfate starvation-induced response in *Pseudomonas aeruginosa* PAO1. *Eur J Biochem*, *266*(3), 986-996.
- Quinn, M. R., Barua, M., Liu, Y., & Serban, V. (2003). Taurine chloramine inhibits production of inflammatory mediators and iNOS gene expression in alveolar macrophages; a tale of two pathways: part I, NF-kappaB signaling. *Adv Exp Med Biol*, *526*, 341-348.
- Quinn, M. R., Liu, Y., Barua, M., & Serban, V. (2003). Taurine chloramine inhibits production of inflammatory mediators and iNOS gene expression in alveolar macrophages; a tale of two pathways: part II, IFN-gamma signaling through JAK/Stat. *Adv Exp Med Biol*, *526*, 349-356.
- Raychaudhuri, S., Stuart, J. M., & Altman, R. B. (2000). Principal components analysis to summarize microarray experiments: application to sporulation time series. *Pac Symp Biocomput*, 455-466.
- Roehl, R. A., Feary, T. W., & Phibbs, P. V., Jr. (1983). Clustering of mutations affecting central pathway enzymes of carbohydrate catabolism in *Pseudomonas aeruginosa*. *J Bacteriol*, *156*(3), 1123-1129.

- Roehl, R. A., & Phibbs, P. V., Jr. (1982). Characterization and genetic mapping of fructose phosphotransferase mutations in *Pseudomonas aeruginosa*. *J Bacteriol*, *149*(3), 897-905.
- Rutala, W. A. (1996). APIC guideline for selection and use of disinfectants. 1994, 1995, and 1996 APIC Guidelines Committee. Association for Professionals in Infection Control and Epidemiology, Inc. *Am J Infect Control*, *24*(4), 313-342.
- Salunkhe, P., von Götz, F., Wiehlmann, L., Lauber, J., Buer, J., & Tümmler, B. (2002). GeneChip Expression Analysis of the Response of *Pseudomonas aeruginosa* to Paraquat-Induced Superoxide Stress *Genome Lett.*, *1*(4), 165-174.
- Sano, Y., Matsui, H., Kobayashi, M., & Kageyama, M. (1993). Molecular structures and functions of pyocins S1 and S2 in *Pseudomonas aeruginosa*. *J Bacteriol*, *175*(10), 2907-2916.
- Savli, H., Karadenizli, A., Kolayli, F., Gundes, S., Ozbek, U., & Vahaboglu, H. (2003). Expression stability of six housekeeping genes: A proposal for resistance gene quantification studies of *Pseudomonas aeruginosa* by real-time quantitative RT-PCR. *J Med Microbiol*, *52*(Pt 5), 403-408.
- Schnider, U., Keel, C., Blumer, C., Troxler, J., Defago, G., & Haas, D. (1995). Amplification of the housekeeping sigma factor in *Pseudomonas fluorescens* CHA0 enhances antibiotic production and improves biocontrol abilities. *J Bacteriol*, *177*(18), 5387-5392.
- Schraufstatter, I. U., Browne, K., Harris, A., Hyslop, P. A., Jackson, J. H., Quehenberger, O., et al. (1990). Mechanisms of hypochlorite injury of target cells. *J Clin Invest*, *85*(2), 554-562.
- Schuller-Levis, G., Mehta, P. D., Rudelli, R., & Sturman, J. (1990). Immunologic consequences of taurine deficiency in cats. *J Leukoc Biol*, *47*(4), 321-331.
- Schuller-Levis, G., Quinn, M. R., Wright, C., & Park, E. (1994). Taurine protects against oxidant-induced lung injury: possible mechanism(s) of action. *Adv Exp Med Biol*, *359*, 31-39.
- Schuller-Levis, G. B., Gordon, R. E., Wang, C., & Park, E. (2003). Taurine reduces lung inflammation and fibrosis caused by bleomycin. *Adv Exp Med Biol*, *526*, 395-402.
- Schuller-Levis, G. B., & Park, E. (2003). Taurine: new implications for an old amino acid. *FEMS Microbiol Lett*, *226*(2), 195-202.
- Shams, S. (2000). *Information Processing Issues and Solutions Associated with Microarray Technology*: Eaton Publisher.
- Shapiro, H. M. (2000). Microbial analysis at the single-cell level: tasks and techniques. *J Microbiol Methods*, *42*(1), 3-16.
- Shimamoto, G., & Berk, R. S. (1979). Catabolism of taurine in *Pseudomonas aeruginosa*. *Biochim Biophys Acta*, *569*(2), 287-292.
- Shimamoto, G., & Berk, R. S. (1980a). Taurine catabolism. II. biochemical and genetic evidence for sulfoacetaldehyde sulfo-lyase involvement. *Biochim Biophys Acta*, *632*(1), 121-130.
- Shimamoto, G., & Berk, R. S. (1980b). Taurine catabolism. III. Evidence for the participation of the glyoxylate cycle. *Biochim Biophys Acta*, *632*(3), 399-407.
- Shin, S. Y., Calvisi, E. G., Beaman, T. C., Pankratz, H. S., Gerhardt, P., & Marquis, R. E. (1994). Microscopic and Thermal Characterization of Hydrogen Peroxide Killing

- and Lysis of Spores and Protection by Transition Metal Ions, Chelators, and Antioxidants. *Appl Environ Microbiol*, 60(9), 3192-3197.
- Snavely, M. D., Miller, C. G., & Maguire, M. E. (1991). The *mgtB* Mg²⁺ transport locus of *Salmonella typhimurium* encodes a P- type ATPase. *J. Biol. Chem.*, 266(2), 815-823.
- Spoering, A. L., & Lewis, K. (2001). Biofilms and planktonic cells of *Pseudomonas aeruginosa* have similar resistance to killing by antimicrobials. *J Bacteriol*, 183(23), 6746-6751.
- Stanley, P. E. (1986). Extraction of adenosine triphosphate from microbial and somatic cells. *Methods Enzymol*, 133, 14-22.
- Stocks, S. M. (2004). Mechanism and use of the commercially available viability stain, BacLight. *Cytometry A*, 61(2), 189-195.
- Stover, C. K., Pham, X. Q., Erwin, A. L., Mizoguchi, S. D., Warrener, P., Hickey, M. J., et al. (2000). Complete genome sequence of *Pseudomonas aeruginosa* PA01, an opportunistic pathogen. *Nature*, 406(6799), 959-964.
- Suzuki, T., Suzuki, T., Wada, T., Saigo, K., & Watanabe, K. (2002). Taurine as a constituent of mitochondrial tRNAs: new insights into the functions of taurine and human mitochondrial diseases. *Embo J*, 21(23), 6581-6589.
- Thalamuthu, A., Mukhopadhyay, I., Zheng, X., & Tseng, G. C. (2006). Evaluation and comparison of gene clustering methods in microarray analysis. *Bioinformatics*, 22(19), 2405-2412.
- Thore, A., Ansehn, S., Lundin, A., & Bergman, S. (1975). Detection of bacteriuria by luciferase assay of adenosine triphosphate. *J Clin Microbiol*, 1(1), 1-8.
- Tomasino, S. F. (2005). Efficacy testing of disinfectants. *JAOAC Int*, 88(1), 355-358.
- Tummler, B., & Kiewitz, C. (1999). Cystic fibrosis: an inherited susceptibility to bacterial respiratory infections. *Mol Med Today*, 5(8), 351-358.
- van der Ploeg, J. R., Weiss, M. A., Saller, E., Nashimoto, H., Saito, N., Kertesz, M. A., et al. (1996). Identification of sulfate starvation-regulated genes in *Escherichia coli*: a gene cluster involved in the utilization of taurine as a sulfur source. *J Bacteriol*, 178(18), 5438-5446.
- Vandecasteele, S. J., Peetermans, W. E., Merckx, R., & Van Eldere, J. (2001). Quantification of expression of *Staphylococcus epidermidis* housekeeping genes with Taqman quantitative PCR during in vitro growth and under different conditions. *J Bacteriol*, 183(24), 7094-7101.
- Venkateswaran, K., Hattori, N., La Duc, M. T., & Kern, R. (2003). ATP as a biomarker of viable microorganisms in clean-room facilities. *J Microbiol Methods*, 52(3), 367-377.
- Vincent, J. L., Bihari, D. J., Suter, P. M., Bruining, H. A., White, J., Nicolas-Chanoin, M. H., et al. (1995). The prevalence of nosocomial infection in intensive care units in Europe. Results of the European Prevalence of Infection in Intensive Care (EPIC) Study. EPIC International Advisory Committee. *Jama*, 274(8), 639-644.
- von Gabain, A., Belasco, J. G., Schottel, J. L., Chang, A. C., & Cohen, S. N. (1983). Decay of mRNA in *Escherichia coli*: investigation of the fate of specific segments of transcripts. *Proc Natl Acad Sci U S A*, 80(3), 653-657.
- Waite, R. D., Paccanaro, A., Papakonstantinou, A., Hurst, J. M., Saqi, M., Littler, E., et al. (2006). Clustering of *Pseudomonas aeruginosa* transcriptomes from

- planktonic cultures, developing and mature biofilms reveals distinct expression profiles. *BMC Genomics*, 7, 162.
- Weiss, S. J., Klein, R., Slivka, A., & Wei, M. (1982). Chlorination of taurine by human neutrophils. Evidence for hypochlorous acid generation. *J Clin Invest*, 70(3), 598-607.
- White, G. C. (1986). *Handbook of Chlorination, 2nd ed.* New York, NY: Van Nostrand Reinhold.
- Winsor, G. L., Lo, R., Sui, S. J., Ung, K. S., Huang, S., Cheng, D., et al. (2005). *Pseudomonas aeruginosa* Genome Database and PseudoCAP: facilitating community-based, continually updated, genome annotation. *Nucleic Acids Res*, 33(Database issue), D338-343.
- Wylie, J. L., & Worobec, E. A. (1995). The OprB porin plays a central role in carbohydrate uptake in *Pseudomonas aeruginosa*. *J Bacteriol*, 177(11), 3021-3026.
- Yang, Y. H., & Speed, T. (2002). Design issues for cDNA microarray experiments. *Nat Rev Genet*, 3(8), 579-588.
- Yauk, C. L., Berndt, M. L., Williams, A., & Douglas, G. R. (2004). Comprehensive comparison of six microarray technologies. *Nucleic Acids Res*, 32(15), e124.
- Zheng, M., Wang, X., Templeton, L. J., Smulski, D. R., LaRossa, R. A., & Storz, G. (2001). DNA microarray-mediated transcriptional profiling of the *Escherichia coli* response to hydrogen peroxide. *J Bacteriol*, 183(15), 4562-4570.